UNIVERSITY OF TURKU

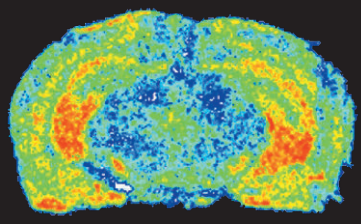

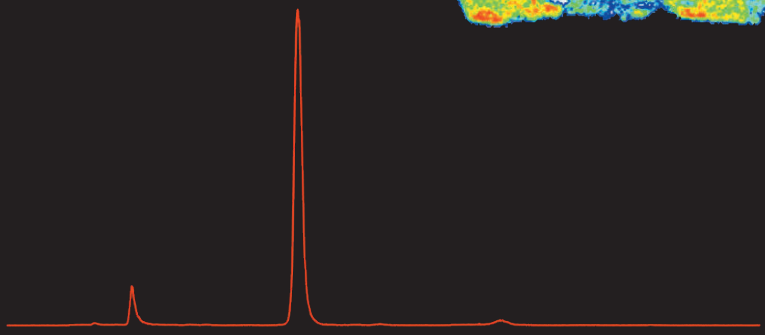

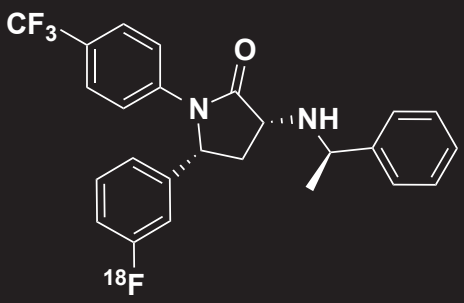

SYNTHESIS OF ^{18}F-LABELLED RADIOPHARMACEUTICALS FOR CNS IMAGING

From Radiosynthesis Development to GMP Production

Salla Lahdenpohja

TURUN YLIOPISTON JULKAISUJA – ANNALES UNIVERSITATIS TURKUENSIS
SARJA – SER. AI OSA – TOM. 641 | ASTRONOMICA – CHEMICA – PHYSICA – MATHEMATICA | TURKU 2021

UNIVERSITY OF TURKU

SYNTHESIS OF ^{18}F-LABELLED RADIOPHARMACEUTICALS FOR CNS IMAGING

From Radiosynthesis Development to GMP Production

Salla Lahdenpohja

TURUN YLIOPISTON JULKAISUJA – ANNALES UNIVERSITATIS TURKUENSIS
SARJA – SER. AI OSA – TOM. 641 | ASTRONOMICA – CHEMICA – PHYSICA – MATHEMATICA | TURKU 2021

University of Turku

Faculty of Science
Department of Chemistry
Turku PET Centre
Radiochemistry
Doctoral Programme in Physical and Chemical Sciences

Supervised by

Adj. Prof. Anna Kirjavainen, PhD
Turku PET Centre and Department of Chemistry
University of Turku
Turku, Finland

Professor Olof Solin, PhD
Turku PET Centre and Department of Chemistry
University of Turku
Turku, Finland

Reviewed by

Assoc. Prof. Magnus Schou, PhD
Precision Medicine Diagnostic Development / AstraZeneca R&D Oncology
Department of Clinical Neuroscience
Karolinska Institutet
Stockholm, Sweden

Dr. Matthew Tredwell, PhD
Wales Research and Diagnostics PET Imaging Centre, School of Chemistry
Cardiff University
Cardiff, Wales

Opponent

Professor Raisa N. Krasikova, PhD
N.P. Bechtereva Institute of Human Brain
Russian Academy of Sciences
St. Petersburg, Russia

The originality of this thesis has been checked in accordance with the University of Turku quality assurance system using the Turnitin OriginalityCheck service.

Cover Image: Salla Lahdenpohja

ISBN 978-951-29-8342-1 (Print)
ISBN 978-951-29-8343-8 (PDF)
ISSN 0082-7002 (Print)
ISSN 2343-3175 (Online)
Painosalama Oy, Turku, Finland 2021

“One never notices what has been done;
one can only see what remains to be done”
(Marie Curie)

UNIVERSITY OF TURKU
Faculty of Science
Department of Chemistry and Turku PET Centre
Radiochemistry
SALLA LAHDENPOHJA: Synthesis of ^{18}F-labelled radiopharmaceuticals for CNS imaging: From radiosynthesis development to GMP production
Doctoral Dissertation, 139 pp.
Doctoral Programme in Physical and Chemical Sciences
January 2021

ABSTRACT

Positron emission tomography (PET) is an imaging technique that can be used to follow various biological processes, such as receptor function, in a living body. PET utilises radiopharmaceuticals, tracers containing short-lived positron-emitting radioisotopes. The aim of this thesis was to develop labelling methods using fluorine-18 and ^{18}F-labelled tracers in order to translate ^{18}F-labelling methods to clinical radiopharmaceutical production.

Traditionally, ^{18}F-fluorination has been divided into electrophilic and nucleophilic fluorination with "[^{18}F]F^{+}" and [^{18}F]fluoride ([^{18}F]F^{-}), respectively. This thesis used the recently developed approach of transition metal-mediated ^{18}F-fluorination with copper and ruthenium. In transition metal-mediated fluorination chemistry, the reactivity of electrophilic fluorination and high molar activity of nucleophilic fluorination can be combined.

The conditions for copper-mediated ^{18}F-fluorination, including [^{18}F]fluoride activation, were optimised and the method utilised for production of the norepinephrine transporter tracer [^{18}F]NS12137 and the dopamine transporter tracer [^{18}F]CFT. To evaluate the usefulness of the new methodology compared to traditional electrophilic ^{18}F-fluorination, [^{18}F]CFT was also produced via the electrophilic pathway. Ruthenium-mediated ^{18}F-fluorination was applied successfully to the production of a new cannabinoid subtype 1 receptor tracer (CB1R), [^{18}F]FPATPP. The tracer was evaluated in mice and [^{18}F]FPATPP found to be specific for CB1R with high uptake in the CB1R-rich areas in the brain. These studies showed the suitability of transition metal-mediated ^{18}F-fluorination in the development of PET tracers. Another CB1R tracer, [^{18}F]FMPEP-d_2, was translated to clinical production according to good manufacturing practices (GMP) utilising an in-house built synthesis device. The production was followed for 5 years.

KEYWORDS: fluorine-18, radiochemistry, radiofluorination, transition metal mediated fluorination, PET, copper-mediated, ruthenium-mediated, GMP

TURUN YLIOPISTO
Matemaattis-luonnontieteellinen tiedekunta
Kemian laitos ja valtakunnallinen PET-keskus
Radiokemia
SALLA LAHDENPOHJA: Keskushermostoon sitoutuvien ^{18}F-leimattujen radiolääkkeiden synteesi: Radiosynteesin kehityksestä GMP-tuotantoon
Väitöskirja, 139 s.
Fysikaalisten ja kemiallisten tieteiden tohtoriohjelma
Tammikuu 2021

TIIVISTELMÄ

Positroniemissiotomografia (PET) on kuvantamistekniikka, jolla voidaan seurata biologisia prosesseja, kuten reseptorien toimintaa, elävässä kohteessa. PET-kuvantamisessa käytetään lyhytikäisillä positronisäteilevillä radionuklideilla leimattuja radiolääkkeitä, merkkiaineita. Väitöskirjatutkimuksen tavoitteena oli kehittää ^{18}F-leimausmenetelmiä ja ^{18}F-leimattuja merkkiaineita sekä siirtää menetelmät kliiniseen radiolääketuotantoon.

^{18}F-fluorileimausreaktiot jaetaan elektrofiiliseen fluoraukseen ”[^{18}F]F^{+}”:lla ja nukleofiiliseen fluoraukseen [^{18}F]fluoridilla ([^{18}F]F^{-}). Tässä väitöskirjatutkimuksessa sovellettiin uutta siirtymämetallivälitteistä ^{18}F-leimausta käyttäen hyväksi kuparia ja ruteniumia. Siirtymämetallivälitteisessä ^{18}F-leimauskemiassa yhdistetään elektrofiilisen fluorileimauksen reaktiivisuus ja nukleofiilisella fluorileimauksella saavutettava korkea molaarinen aktiivisuus.

Työssä optimoitiin kuparivälitteisen ^{18}F-leimauksen reaktio-olosuhteet ja [^{18}F]F^{-}:n aktivointiolosuhteet. Menetelmää käytettiin noradrenaliinin kuljettajaproteiinimerkkiaineen [^{18}F]NS12137:n ja dopamiinin kuljettajaproteiinimerkkiaineen [^{18}F]CFT:n leimaussynteeseissä. Uuden kuparivälitteisen leimausmenetelmän käytettävyyttä arvioitiin vertaamalla menetelmää elektrofiiliseen ^{18}F-leimaukseen valmistamalla [^{18}F]CFT:tä myös elektrofiilisesti. Ruteniumvälitteistä leimausmenetelmää käytettiin onnistuneesti uuden kannabinoidireseptori 1 (CB1R) -merkkiaineen, [^{18}F]FPATPP:n, valmistuksessa. [^{18}F]FPATPP:n toimivuus CB1R-merkkiaineena testattiin terveillä hiirillä. Merkkiaine osoittautui spesifiseksi CB1R:lle, kertyen aivoalueille, joissa on runsaasti CB1R:ta. Osatyöt osoittavat siirtymämetallivälitteisen ^{18}F-leimauskemian sopivan uusien PET-merkkiaineiden synteesikehitykseen. Toinen CB1R-merkkiaine, [^{18}F]FMPEP-d_2, siirrettiin kliiniseen tuotantoon Hyvät tuotantotavat (Good Manufacturing Practices, GMP) -ohjeistuksien mukaisesti. Merkkiaineen tuotannossa käytettiin itserakennettua synteesilaitetta, ja tuotantoa seurattiin 5 vuoden ajan.

ASIASANAT: fluori-18, radiokemia, radiofluoraus, siirtymämetallivälitteinen fluoraus, PET, kuparivälitteinen, ruteniumvälitteinen, GMP

Table of Contents

Abbreviations

%ID/g	Injected dose per gram of tissue
18-cr-6	18-Crown-6; 1,4,7,10,13,16-hexaoxacyclooctadecane
AD	Alzheimer's disease
A_m	Molar activity
$ß^+$	Positron
BBB	Blood-brain barrier
Bl	Blocked
CB_1, CB1R	Cannabinoid receptor type 1
CB_2, CB2R	Cannabinoid receptor type 2
CNS	Central nervous system
COD	1,5-cyclooctadiene
CP	Chemical purity
CRO	Contract research organization
CT	Computed tomography
DMA	Dimethylacetamide
DMF	Dimethylformamide
DMSO	Dimethyl sulfoxide
EANM	European Association of Nuclear Medicine
EMA	European Medicines Agency
EOB	End of bombardment
EOS	End of synthesis
λ	Gamma ray
GC	Gas chromatography
GLP	Good laboratory practice
GMP	Good manufacturing practice
GPCR	G protein-coupled receptor
GRPP	Good radiopharmacy practice
HPLC	High pressure liquid chromatography
ICH	International Council for Harmonisation of Technical Requirements for Pharmaceuticals for Human Use
ICP-MS	Inductively coupled plasma mass spectrometry
(IPr)Cu^I(OTf)	(1,3-bis-(2,6-diisopropylphenyl)imidazol-2-ylidine)Cu^I(OTf)

IV	Intravenous
K_{222}	Kryptofix2.2.2, K222, 4,7,13,16,21,24-hexaoxa-1,10-diazabicyclo[8.8.8]hexacosane,
LC-MS	Liquid chromatography mass spectrometry
LG	Leaving group
MeCN	Acetonitrile
MRI	Magnetic resonance imaging
MS	Mass spectrometry
NMR	Nuclear magnetic resonance
OTf	Trifluoromethanesulfonate, triflate
OTs	4-Methylbenzenesulfonate, tosylate
PD	Parkinson's disease
PEEK	Polyether ether ketone
PET	Positron emission tomography
p.i.	Post-injection
PIC/S	Pharmaceutical Inspection Convention and Pharmaceutical Inspection Co-operation Scheme
PNS	Peripheral nervous system
PTC	Phase transfer catalyst
QC	Quality control
RAC	Radioactivity concentration
RCP	Radiochemical purity
RCY	Radiochemical yield
ROI	Region of interest
RT	Room temperature
salen	*N*,*N*′-bis(3,5-di-*tert*-butylsalicylidene)-1,2-cyclohexanediamino -ligand
SD	Standard deviation
SPE	Solid phase extraction
SUV	Standardized uptake value
$T_{½}$	Half-life
THC	Tetrahydrocannabinol
TLC	Thin-layer chromatography
UV	Ultraviolet
VOI	Volume of interest
WHO	World Health Organization
WT	Wild type

Radiopharmaceutical abbreviations

[^{11}C]CDS-MIBG	*N*-(4-(3-(3-iodobenzyl)guanidino)-4-oxobutyl)-1-[^{11}C]methyl-1,4-dihydroquinoline-3-carboxamide
[^{11}C]CFT	2β-carbomethoxy-3β-(4-fluorophenyl)[*N-methyl*-^{11}C]tropane
[^{11}C]JHU75528	[^{11}C]OMAR, 4-cyano-1-(2,4-dichlorophenyl)-5-(4-[^{11}C]methoxyphenyl)-*N*-piperidin-1-ylpyrazole-3-carboxamide
[^{11}C]MePPEP	(3*R*,5*R*)-5-(3-([^{11}C]methoxy)phenyl)-3-(((*R*)-1-phenyl-ethyl)amino)-1-(4-(trifluoromethyl)phenyl)-pyrrolidin-2-one
[^{11}C]MeNER	[^{11}C]MRB, (*S,S*)-2-(α-(2-[^{11}C]methoxyphenoxy)benzyl)morpholine
[^{11}C]SD5024	(−)-3-(4-chlorophenyl)-*N*-[(4-[*cyano*-^{11}C]cyanophenyl)-sulfonyl]-4-phenyl-4,5-dihydro-1*H*-pyrazole-1-carboxamidine
[^{18}F]AM5144	*N*-(4-[^{18}F]fluorophenyl)-5-(4-bromophenyl)-1-(2,4-dichlorophenyl)-1H-pyrazole-3-carboxamide
[^{18}F]CFT	2β-carbomethoxy-3β-(4-[^{18}F]fluorophenyl)tropane
[^{18}F]EF5	2-(2-nitro-1[*H*]-imidazol-1-yl)-*N*-(2,2,3,3,3-[^{18}F]pentafluoropropyl)-acetamide
[^{18}F]EKZ-001	[^{18}F]bavarostat, 4-(((((3*R*,5*R*,7*R*)-adamantan-1-yl)methyl)(methyl)amino)methyl)-3-[^{18}F]fluoro-*N*-hydroxybenzamide
[^{18}F]FBPA	4-borono-2-[^{18}F]fluoro-D,L-phenylalanine
[^{18}F]FDG	2-deoxy-2-[^{18}F]fluoro-D-glucose
[^{18}F]FE-PE2I	*N*-(3-iodoprop-2-enyl)-2β-carbo[^{18}F]fluoroethoxy-3β-(4'-methylphenyl)nortropane
6-[^{18}F]F-L-DOPA	L-6-[^{18}F]fluoro-3,4-dihydroxyphenylalanine
[^{18}F]FMeNER-d_2	(*S,*S)-2-(α-(2-([^{18}F]fluoromethoxy-d_2)phenoxy)benzyl)-morpholine
[^{18}F]FMPEP-d_2	(3*R*,5*R*)-5-(3-([^{18}F]fluoromethoxy-d_2)phenyl)-3-(((*R*)-1-phenyl-ethyl)amino)-1-(4-(trifluoromethyl)phenyl)-pyrrolidin-2-one
[^{18}F]FPATPP	(3*R*,5*R*)-5-(3-[^{18}F]fluorophenyl)-3-(((*R*)1-phenylethyl)amino)-1-(4-(trifluoromethyl)phenyl)-pyrrolidin-2-one
[^{18}F]HU-210F	(6a*R*,10a*R*)-3-(8-[^{18}F]fluoro-2-methyloctan-2-yl)-9-(hydroxymethyl)-6,6-dimethyl-6a,7,10,10a-tetrahydro-6*H*-benzo[*c*]chromen-1-ol
[^{18}F]MK-9470	*N*-[2-(3-cyanophenyl)-3-(4-(2-[^{18}F]fluoroethoxy)phenyl)-1-methylpropyl]-2-(5-methyl-2-pyridyloxy)-2-methylpropanamide
[^{18}F]NS12137	*exo*-3-[(6-[^{18}F]fluoro-2-pyridyl)oxy]8-azabicyclo[3.2.1]-octane
[^{18}F]SR144385	*N*-(piperidin-1-yl)-5-(4-chlorophenyl)-1-(2,4-dichloro-phenyl)-4-[^{18}F]fluoromethyl-1H-pyrazole-3-carboxamide
(–)[*5'*-^{18}F]Δ^8-THC	(6a*R*,10a*R*)-3-(5-[^{18}F]fluoropentyl)-6,6,9-trimethyl-6a,7,10,10a-tetrahydro-6*H*-benzo[*c*]chromen-1-ol
[^{18}F]paroxetine	(3*S*,4*R*)-3-((benzo[*d*][1,3]dioxol-5-yloxy)methyl)-4-(4-[^{18}F]fluoro-phenyl)piperidine
[^{18}F]MDL100907	(*S*)-(2,3-dimethoxyphenyl)(1-(4-[^{18}F]fluorophenethyl)piperidin-4-yl)methanol

List of Original Publications

This dissertation is based on the following original publications, which are referred to in the text by their Roman numerals:

I **Lahdenpohja S**, Keller T, Rajander J and Kirjavainen AK. Radiosynthesis of the norepinephrine transporter tracer [^{18}F]NS12137 via copper-mediated ^{18}F-labelling, *J Label Compd Radiopharm* 2019; 62: 259 – 264.

II **Lahdenpohja S**, Rajala N, Rajander J and Kirjavainen AK. Fast and efficient copper-mediated ^{18}F-fluorination of arylstannanes, aryl boronic acids, and aryl boronic esters without azeotropic drying, *EJNMMI Radiopharm Chem* 2019; 4: 28.

III **Lahdenpohja S***, Rajala N*, Helin J, Haaparanta-Solin M, Solin O, Lopéz-Picón F and Kirjavainen AK. Ruthenium-mediated ^{18}F-fluorination and preclinical evaluation of a new CB_1 receptor imaging agent [^{18}F]FPATPP. *ACS Chem Neurosci* 2020; 11: 2009 – 2018.

IV **Lahdenpohja S**, Keller T, Forsback S, Viljanen T, Kokkomäki E, Kivelä RV, Bergman J, Solin O, Kirjavainen AK. Automated GMP production and long-term experience in radiosynthesis of CB_1 tracer [^{18}F]FMPEP-d_2. *J Label Compd Radiopharm* 2020; 63: 408 – 418.

*Equal contribution

1 Introduction

Fluorine is the 13th most common chemical in the Earth's crust, and the first fluoride-containing mineral, fluorspar, also known as fluorite or calcium difluoride, was first found in the 14th century by Georgius Agricola. In 1810, André-Marie Ampére proposed fluorine was an element (Ampére 1816). However, elemental fluorine, F_2, is not naturally occurring and, due to its extreme reactivity, it was years before the element was isolated. In 1886, Henri Moissan was the first chemist to successfully isolate the elemental fluorine by temperature-controlled electrolysis (Moissan 1886), for which he received the Nobel Prize in Chemistry in 1906:

> "The whole world has admired the great experimental skill with which you have studied that savage beast among the elements." (Professor P. Klason in the Nobel ceremony speech, December 10, 1906)

In 2020, the beast has been tamed for more than a century and our everyday life is full of fluorine-containing molecules, including polymers, pesticides, pharmaceuticals, and radiopharmaceuticals.

Positron emission tomography (PET) is a non-invasive imaging technique that utilises radiopharmaceuticals to follow biological processes in a living body, such as blood flow, glucose metabolism, and receptor density. PET is based on the use of short-lived positron-emitting radionuclides in combination with biologically relevant molecules. For example, these molecules can mimic neurotransmitters in brain imaging or glucose when glucose metabolism is followed. The molecule of interest is labelled with a positron-emitting radionuclide to produce a radiopharmaceutical, also known as a radiotracer. The radiotracer is then administered to the subject and accumulation of the tracer followed by a PET scanner.

Since the development of PET, glucose metabolism has been the most studied field due to the increased glucose uptake in tumours. The glucose analogue tracer, 2-deoxy-2-[^{18}F]fluoro-D-glucose ([^{18}F]FDG), is the most commonly used radiotracer among PET tracers. However, [^{18}F]FDG does not provide all the answers, and the development of new radiopharmaceuticals is necessary. In the brain, PET allows the imaging of delicate processes, including neurotransmission and neuroinflammation, which are associated in neuropsychiatric and neurodegenerative diseases, such as schizophrenia,

depression, Alzheimer's disease (AD), and Parkinson's disease (PD). AD is the most common type of dementia in Western countries but its cause and prevention are still unknown. Therefore, the development of new radiotracers would allow us to understand these diseases we are facing. Furthermore, existing labelling methods need to be improved and new labelling methods developed.

This thesis consists of four individual studies (Figure 1) concerning the development and improvement of ^{18}F-labelling methods and the production of ^{18}F-radiotracers for brain imaging. Studies I – III encompass transition metal-mediated ^{18}F-fluorination reactions with copper and ruthenium to produce tracers for norepinephrine and dopamine transporter imaging and cannabinoid receptor imaging. Study IV covers process validation of a cannabinoid tracer [^{18}F]FMPEP-d_2 for clinical use and experience with its long-term production.

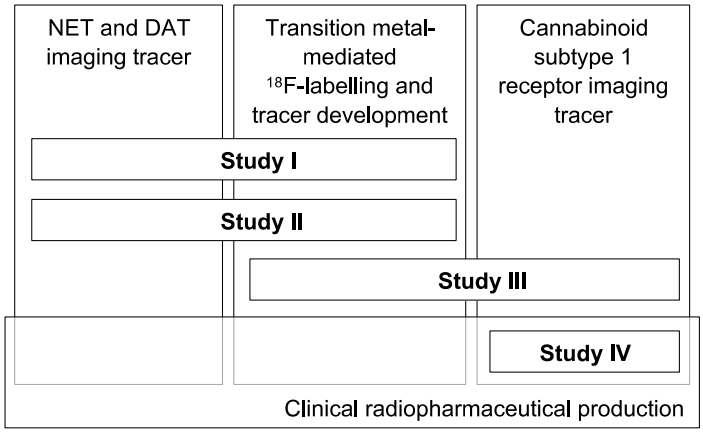

Figure 1. The relationship between studies I – IV.

2 Review of the literature

2.1 Fluorine-18 in positron emission tomography

2.1.1 PET radionuclides

In positron ($ß^+$) emission, a positron released from the nucleus of the radionuclide eventually meets an electron. In this collision, also known as annihilation, two 511 keV gamma rays (γ) are formed. These photons leave in opposite directions and are detected by a PET scanner. The radionuclides used in PET need to have specific properties to generate good images: the type of the decay, the half-life, and the energy of the positron emitted. PET radionuclides that are typically used are fluorine-18, carbon-11, nitrogen-13, oxygen-15, gallium-68, copper-64, and zirconium-89.

All PET radionuclides are positron emitters, but the decay process does not always consist only of $ß^+$-decay. Nevertheless, a high proportion of positron decay is desired because the PET scanners recognize only the γ photons formed in the annihilation process. For example, the decay of fluorine-18 consists of 96.7% $ß^+$-decay and 3.3% electron capture (EC), whereas the decay of copper-64 is only 17.5% $ß^+$-decay.

Another important property of a PET radionuclide is the energy of the positron. Positron energy determines the distance a positron can travel in the medium before annihilation. The lower the energy, the shorter the range; the higher the energy, the longer the range. PET scanners can localize only the place of annihilation, so low positron energy is desired to obtain high-resolution images. High resolution is required especially in imaging rodents and other small animals, but also in humans when imaging small targets in the brain. The maximum positron energy for fluorine-18 is 634 keV and for gallium-68 1899 keV.

Finally, the most crucial parameter from a radiochemist's point of view is the half-life of the radionuclide. The half-lives of the most common PET radionuclides vary from 2 minutes (oxygen-15) to 78 hours (zirconium-89) and define what kind of manipulations can be performed after the production of the radionuclide. The half-life needs to be long enough to enable all of the handling, including synthesis, purification, quality control (QC), and possible transportation, but short enough to enable decay in a reasonable manner and minimise the radioactivity dose. The properties of commonly used PET radionuclides are outlined in Table 1.

Table 1. Properties of common PET radionuclides (Conti & Eriksson 2016, Laboratoire National Henri Becquerel 2020).

	$T_{½}$	Decay mode [%]	$E_{max}(ß^+)$ [keV]	Maximal $ß^+$-range in water [mm]	$ß^+$-decay product
^{15}O	2.04 min	$ß^+$ 99.9 EC 0.1	1735	8.4	^{15}N
^{13}N	9.97 min	$ß^+$ 99.8 EC 0.2	1198	5.5	^{13}C
^{11}C	20.4 min	$ß^+$ 99.8 EC 0.2	961	4.2	^{11}B
^{68}Ga	67.8 min	$ß^+$ 88.9 EC 11.1	1899	9.2	^{68}Zn
^{18}F	109.8 min	$ß^+$ 96.7 EC 3.3	634	2.4	^{18}O
^{64}Cu	12.7 h	$ß^+$ 17.5 EC 44.0 $ß^-$ 38.5	653	2.5	^{64}Ni ^{64}Zn
^{89}Zr	78.4 h	$ß^+$ 22.8 EC 77.2	902	3.8	^{89}Y

2.1.2 Advantages of fluorine

Fluorine-18 has good properties for PET imaging and, as such, is among the most commonly used PET radionuclides worldwide. The clean decay process via positron emission and low $ß^+$ energy allows high-resolution imaging among commonly used PET radionuclides. High resolution enables imaging of the central nervous system (CNS) and brain. The chemistry of fluorine is not always straightforward, but the half-life of 2 hours allows multistep synthesis and complex purification processes. Nevertheless, the radiochemical properties of fluorine-18 are not the only benefits of using fluorine in radiotracers.

Naturally occurring organofluorine compounds are extremely rare and introduction of fluorine can affect pharmacological activity of the compound. From the pharmacological point of view, the use of fluorine-18 is not as straightforward as the use of carbon-11 for example. However, fluorine is widely used in pharmaceuticals and radiopharmaceuticals (Böhm et al. 2004, Purser et al. 2008, Gillis et al. 2015). The size of the fluorine atom is between that of oxygen and hydrogen (van der Waals radius H: 1.20 Å; F: 1.47 Å; O: 1.52 Å; Bondi 1964). Due to its small size, fluorine has often been used to replace hydrogen. Fluorine is the most electronegative element in the periodic table, and the C-F bond is highly polarized compared to the C-H bond (Pauling

electronegativity F: 4.0; H: 2.1; C: 2.5). Overall, fluorine substitution can have a positive effect on metabolic stability, basicity as fluorine can decrease the pKa of the compound, thus improving the membrane permeability, and binding affinity (Böhm et al. 2004).

2.1.3 Production of fluorine-18

Fluorine-18 is not a naturally occurring isotope of fluorine and is produced in a cyclotron. Various different nuclear reactions have been utilised for its production (Nickles et al. 1986); both elemental fluorine ($[^{18}F]F_2$) and ionic $[^{18}F]$fluoride can be produced in a cyclotron as presented in Table 2. For the in-target production of $[^{18}F]F_2$, a gaseous target material is needed, whereas for $[^{18}F]$fluoride production, a water target is typically used. Handling and transfer of the gaseous target material and the gaseous ^{18}F-labelling reagent is challenging. Thus, liquid targets are preferred and the most common nuclear reaction for fluorine-18 production is $^{18}O(p,n)^{18}F$ with ^{18}O-enriched water as the target material. In addition, cyclotron-produced $[^{18}F]$fluoride can be used in the production of $[^{18}F]F_2$ using a post-target production method (Bergman & Solin 1997). The original post-target production method consists of two steps: 1) synthesis of $[^{18}F]$fluoromethane from cyclotron-produced $[^{18}F]$fluoride, and 2) reforming the $[^{18}F]$fluoromethane to $[^{18}F]F_2$ with high-voltage discharge in the presence of F_2 in Ne in a discharge chamber. The post-target method has been developed further using SF_6 gas instead of F_2 (Krzyczmonik et al. 2017b) and by utilising a vacuum ultraviolet laser instead of electrical discharge (Krzyczmonik et al. 2017a).

Table 2. In-target and post-target production of fluorine-18.

In-target				
Nuclear reaction	**Target material**	**Product**	**Molar activity [GBq/µmol]**	**Ref**
$^{18}O(p,n)^{18}F$	$[^{18}O]H_2O$	$[^{18}F]F^-$	Up to 43000	(Solin et al. 1988, Füchtner et al. 2008)
	0.1 – 0.2% F_2 in $[^{18}O]O_2$	$[^{18}F]F_2$	1.3	(Nickles et al. 1984, Chirakal et al. 1995)
$^{20}Ne(d,\alpha)^{18}F$	0.1 – 0.2% F_2 in Ne	$[^{18}F]F_2$	0.13	(Blessing et al. 1986)
Post-target				
Nuclear reaction and target material	**Post-target method**	**Product**	**Molar activity [GBq/µmol]**	**Ref**
$^{18}O(p,n)^{18}F$ With $[^{18}O]H_2O$	Electrical discharge with 0.5% F_2 in Ne	$[^{18}F]F_2$	55	(Bergman & Solin 1997)
	Electrical discharge with 1% SF_6 in Xe	$[^{18}F]F_2$	1	(Krzyczmonik et al. 2017b)
	Vacuum ultraviolet laser with 0.5% F_2 in Ne	$[^{18}F]F_2$	10	(Krzyczmonik et al. 2017a)

2.2 Molar activity

Molar activity (A_m) is an important property in radiochemistry, as it represents the amount of radioactivity in relation to the molar amount of the compound. Depending on the situation, high or low A_m may be desired. High A_m is crucial when imaging low-density receptors because occupying the receptors with non-radioactive tracer is not desired. In contrast, high A_m is not necessary when imaging glucose metabolism, enzyme activity, or comparable non-easily saturable functions. With bioactive or toxic chemicals, a high A_m is again crucial to avoid pharmacological or toxic effects. The maximum theoretical A_m for a radionuclide can be calculated from Equation (1), where N_A is Avogadro's constant and $T_{½}$ is half-life.

$$A_m\ (theoretical\ maximum) = \frac{N_A \times ln2}{T_{½}} \quad (1)$$

The maximum theoretical A_m of fluorine-18 is 63 TBq/µmol. This is far from the A_m achieved in radiopharmaceutical chemistry laboratories. Typically, radiotracers are obtained with 0.1 GBq/µmol to 1 TBq/µmol A_m. Large differences in the theoretical

and achieved A_m values are due to the dilution of fluorine-18 with stable fluorine-19 during synthesis. To prevent the dilution of fluorine-18 with non-radioactive fluorine, use of fluorine-rich reagents and materials including fluorine-18 transfer lines should be avoided (Savisto et al. 2018). This is in contrast to the production of $[^{18}F]F_2$, which utilises non-radioactive F_2 (as presented in Table 2). Addition of F_2 significantly limits the achievable A_m, and ^{18}F-fluorination with in-target produced $[^{18}F]F_2$ ends up with an A_m typically under 1 GBq/μmol. With post-target produced $[^{18}F]F_2$, an A_m of 55 GBq/μmol has been achieved (Bergman & Solin 1997).

Traditionally, ^{18}F-fluorination reactions have been divided into two categories: electrophilic ^{18}F-fluorination with $[^{18}F]F_2$ and nucleophilic ^{18}F-fluorination with $[^{18}F]$fluoride. From the perspective of A_m, $[^{18}F]$fluoride seems to be overwhelmingly superior to $[^{18}F]F_2$. However, the chemistry with the relatively unreactive $[^{18}F]$fluoride is far more complex than the chemistry with the extremely reactive $[^{18}F]F_2$. These ^{18}F-labelling approaches are discussed in the following chapters.

2.3 Electrophilic ^{18}F-fluorination

2.3.1 $[^{18}F]F_2$ gas

Elemental fluorine, F_2 reacts efficiently, even violently with different electron-rich structures, such as aromatic or heteroaromatic ring structures and alkenes via electrophilic substitution or addition. F_2 is a strong oxidant, and reactions are often highly exothermic. Thus, F_2 has typically been diluted (0.1 to 5% F_2) with inert gases, such as N_2, or noble gases and reactions conducted at low temperatures. Despite these actions, multiple side products or polyfluorinated products are often formed when labelling with $[^{18}F]F_2$, leading to complex purification processes. Various leaving groups have been used to control the ^{18}F-fluorination, including trimethylsilanes, stannanes, and germanes (Coenen & Moerlein 1987). Good examples of improved regioselectivity is the production of 6-$[^{18}F]$F-L-DOPA using trimethylsilyl precursor (Diksic & Farrokhzad 1985) or trimethylstannyl precursor (Namavari et al. 1992) instead of the non-activated precursor (Firnau et al. 1984).

The most common PET radiopharmaceutical, $[^{18}F]$FDG, was originally produced via electrophilic fluorination starting from $[^{18}F]F_2$ gas (Ido et al. 1978). Thus, electrophilic ^{18}F-fluorination has been key to the progress in positron imaging as a field of interest. Although the handling of $[^{18}F]F_2$ requires extremely dedicated facilities and skilled operators, some radiopharmaceuticals, such as $[^{18}F]$EF5 (2-(2-nitro-1[*H*]-imidazol-1-yl)-*N*-(2,2,3,3,3-$[^{18}F]$pentafluoropropyl)-acetamide) (Dolbier et al. 2001) and $[^{18}F]$FBPA (4-borono-2-$[^{18}F]$fluoro-D,L-phenylalanine) (Ishiwata et al. 1991) are still produced via $[^{18}F]F_2$.

2.3.2 [^{18}F]F_2 derivatives

To dilute the extreme reactivity of [^{18}F]F_2 gas, less reactive electrophilic labelling reagents have been developed, such as derivatives of [^{18}F]F_2 (Figure 2) (Preshlock et al. 2016). Examples include [^{18}F]XeF_2 (Schrobilgen et al. 1981, Chirakal et al. 1984), [^{18}F]ClF (Lambrecht et al. 1978, Kirjavainen et al. 2013), and various [^{18}F]O-F compounds, such as trifluoromethyl [^{18}F]hypofluorite (Neirinckx et al. 1978), acetyl [^{18}F]hypofluorite (Fowler et al. 1982), and perchloryl [^{18}F]fluoride (Ehrenkaufer & MacGregor 1982, 1983), which were developed in the late 1970s and early 1980s. Shortly thereafter, ^{18}F-labelled [^{18}F]N-F reagents were developed, including *N*-[^{18}F]fluoropyridinium triflate (Oberdorfer et al. 1988a), 1-[^{18}F]fluoro-2-pyridone (Oberdorfer et al. 1988b), and *N*-[^{18}F]fluoro-*N*-alkylsulphonamides (Satyamurthy et al. 1990). The newest electrophilic labelling reagents are in the family of [^{18}F]N-F reagents: [^{18}F]*N*-fluorobenzenesulfonimide ([^{18}F]NFSi) (Teare et al. 2007) and 1-chloromethyl-4-[^{18}F]fluoro-1,4-diazoniabicyclo[2.2.2]octane *bis*(triflate) ([^{18}F]Selectfluor *bis*(triflate)) (Teare et al. 2010).

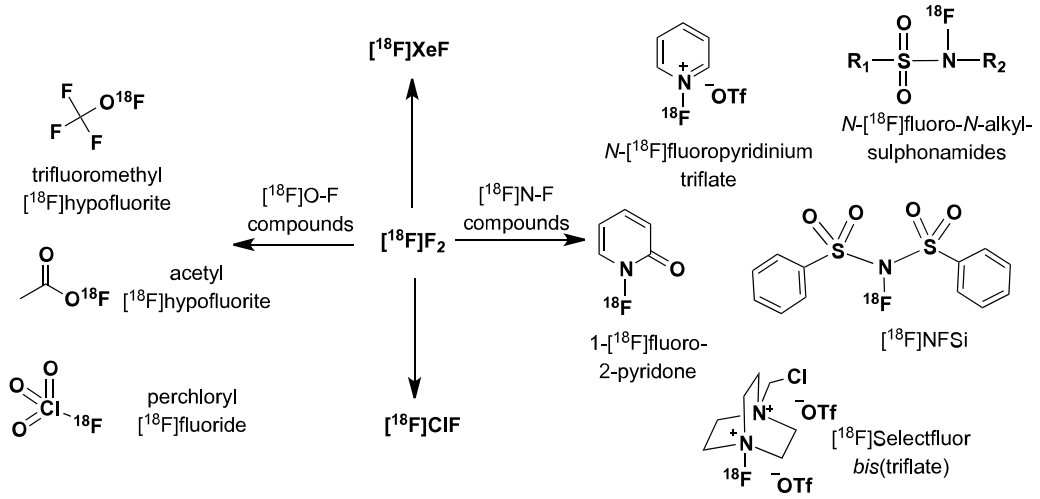

Figure 2. Electrophilic ^{18}F-labelling reagents derived from [^{18}F]F_2.

[^{18}F]O-F reagents and older [^{18}F]N-F reagents were previously utilised in fluorodemetallation reactions with mercury compounds (Visser et al. 1984), aryllithium compounds (Ehrenkaufer & MacGregor 1983), and Grignard reagents (Satyamurthy et al. 1990), but these labelling reagents have not been popular since the 1990s. The newer [^{18}F]N-F reagents [^{18}F]NFSi and [^{18}F]Selectfluor *bis*(triflate) have been used in various ^{18}F-fluorodemetallation reactions starting from arylstannane and arylboronate compounds as presented in the following chapters.

[^{18}F]NFSi

In 2007, the Gouverneur group developed an ^{18}F-labelled version of a common fluorination reagent, NFSi (Teare et al. 2007). NFSi has been used in the electrophilic fluorination of various aromatic structures since its development in 1991 (Differding & Ofner 1991, Rostami 2007). In addition, NFSi is a strong oxidant and been used in organometallic chemistry to promote reductive elimination with transition metals (Bizet 2012). The ^{18}F-labelled version of NFSi has proven to be a useful electrophilic ^{18}F-fluorination reagent (Figure 3). [^{18}F]NFSi has been used in the ^{18}F-fluorination of allylic [^{18}F]fluorides and 2-[^{18}F]fluoroketones starting from silyl precursors (Teare et al. 2007). [^{18}F]NFSi has also been used in the organo-mediated enantioselective ^{18}F-fluorination of aldehydes to produce α-[^{18}F]fluoroaldehydes (Buckingham et al. 2015) and photoactivated decatungstate catalysed ^{18}F-fluorination of deactivated C-H bonds to produce ^{18}F-labelled amino acids (Nodwell et al. 2017, 2019) and peptides (Yuan et al. 2018, 2019).

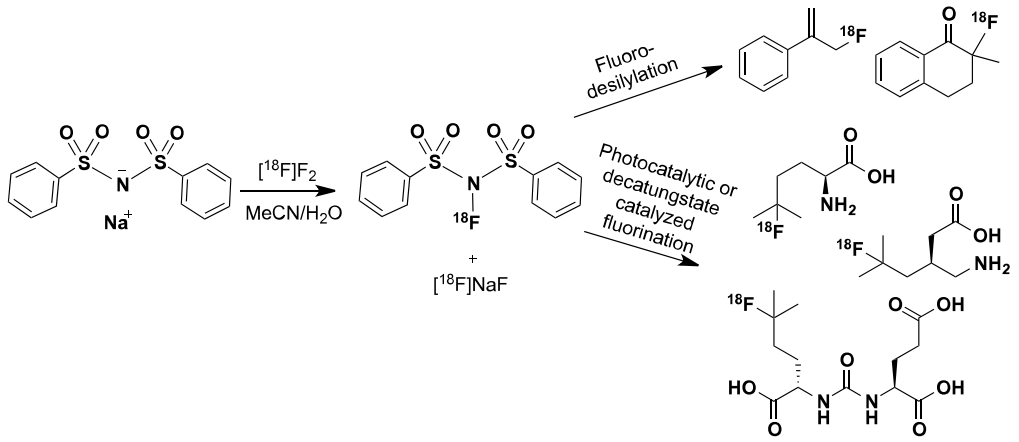

Figure 3. Synthesis of [^{18}F]NFSi and its applications.

[^{18}F]Selectfluor *bis*(triflate)

Another example of a [^{18}F]F_2 derivative is [^{18}F]Selectfluor *bis*(triflate), an analogue of a common fluorination reagent, Selectfluor™ (1-chloromethyl-4-fluoro-1,4-diazoniabicyclo[2.2.2]octane *bis*(tetrafluoroborate)). Selectfluor™ was originally developed by Banks et al. (1992) and has been widely used in selective electrophilic fluorination of electron-rich and electron-poor structures, aromatic compounds, alkenes, and steroids (Nyffeler et al. 2005). [^{18}F]Selectfluor *bis*(triflate) was developed in 2008 by Gouverneur and Solin's groups and has been applied in ^{18}F-fluorination reactions (Figure 4), such as the production of allylic [^{18}F]fluorides, 2-[^{18}F]fluoroketones from silyl precursors (Teare et al. 2010), and 6-[^{18}F]fluoro-L-DOPA from stannane precursors with AgOTf present (Teare et al. 2010, Stenhagen et al. 2013). In addition, [^{18}F]Selectfluor *bis*(triflate) has been used to produce ^{18}F-labelled di- and tri-fluoromethylarenes via a fluorodecarboxylation reaction with AgOTf present (Mizuta et al. 2013). [^{18}F]Selectfluor *bis*(triflate) has also been used in Pd-mediated ^{18}F-fluorination to produce [^{18}F]fluorosydnones, which have subsequently been used in click chemistry (Liu et al. 2016). The main limitation of Selectfluor™ is its restricted solubility (Banks et al. 1996), which has also been noted in the enantioselective ^{18}F-fluorination of aldehydes (Buckingham et al. 2015).

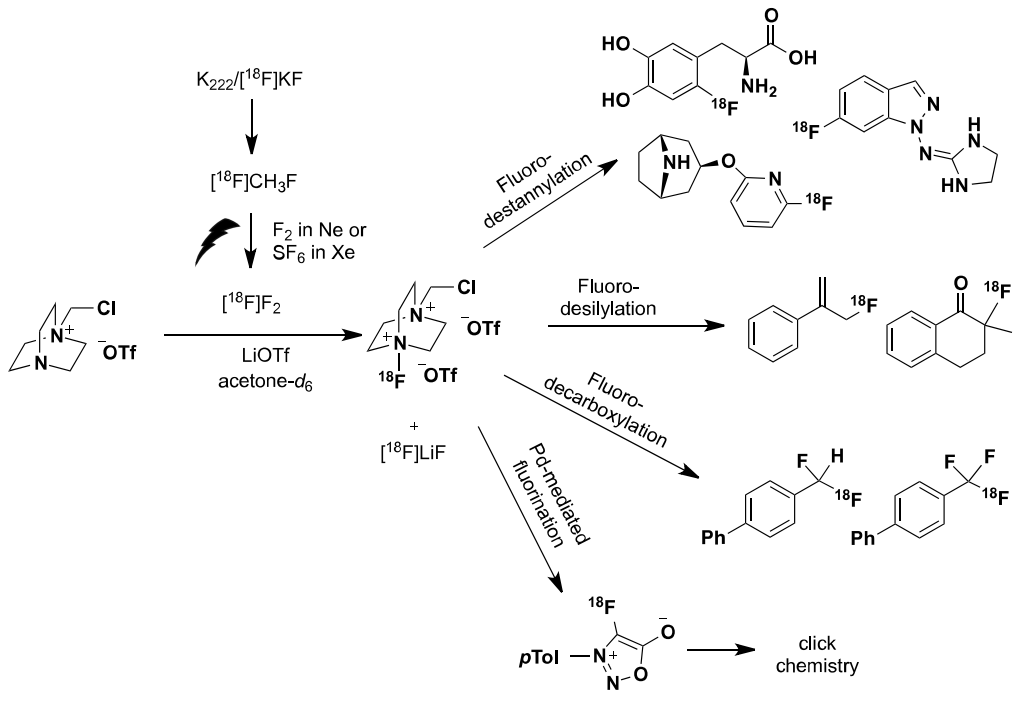

Figure 4. Synthesis of [^{18}F]Selectfluor *bis*(triflate) and its applications.

Despite the broad reactivity range of [^{18}F]Selectfluor *bis*(triflate), the low A_m is an issue. Although an F_2-free method has been utilised in the post-target production of [^{18}F]F_2 which is used in the subsequent production of [^{18}F]Selectfluor *bis*(triflate) (Krzyczmonik et al. 2017b), further improvements are still needed to increase the achievable A_m. In addition to the low A_m with [^{18}F]Selectfluor *bis*(triflate) and other similar electrophilic ^{18}F-labelling reagents, the major issue is the need for [^{18}F]F_2 in the production of these derivatives. Complex facilities are needed for handling [^{18}F]F_2; thus, nucleophilic ^{18}F-fluorination with [^{18}F]fluoride is a more popular approach.

2.4 Nucleophilic ^{18}F-fluorination

In PET, [^{18}F]fluoride is a desirable labelling precursor due to easy access with a cyclotron and the high A_m, which is typically achieved by traditional no-carrier-added nucleophilic ^{18}F-fluorination with [^{18}F]fluoride. Nucleophilic fluorination reactions are typically S_N2 type in aliphatic positions and S_NAr type in aromatic positions in which fluoride acts as a nucleophile. Fluoride is a good nucleophile; however, aqueous [^{18}F]fluoride (Figure 5) obtained from a cyclotron is rather inert due to the hydrated form. Thus, [^{18}F]fluoride needs to be activated prior to the ^{18}F-labelling reactions. A typical activation method is azeotropic distillation with acetonitrile (MeCN) (Coenen 2007).

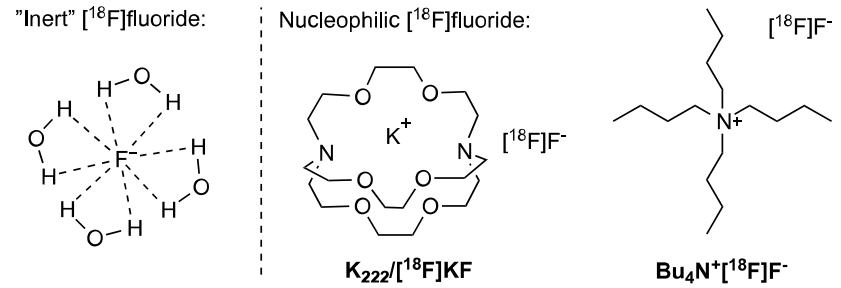

Figure 5. Inert [^{18}F]fluoride and nucleophilic [^{18}F]fluorides with PTCs cryptand and tetraalkyl ammonium salt.

Inorganic fluorides [^{18}F]KF, [^{18}F]CsF, and [^{18}F]RbF have been used in nucleophilic ^{18}F-fluorination reactions, but yields have been rather low due to poor solubility of these labelling reagents in organic solvents. Eventually, the solubility of [^{18}F]KF has been improved with phase transfer catalysts (PTCs, Figure 5), such as polyethers kryptofix-2.2.2 (K_{222}) (Coenen et al. 1985, Hamacher et al. 1986) and 18-crown-6 ether (18-cr-6) (Liotta & Harris 1974, Irie et al. 1982, 1984), and tetraalkyl ammonium salts (R_4N^+) (Gatley & Shaughnessy 1982). The reactivity of these different PTCs in

^{18}F-fluorination reactions has been shown to be similar (Liotta & Starks 1978, Korguth et al. 1988). For example, PTCs have been used successfully in the production of [^{18}F]FDG (Hamacher et al. 1986, Brodack et al. 1988). Tetraalkyl ammonium [^{18}F]fluorides exhibit better solubility, whereas [^{18}F]fluorocryptands are limited to polar aprotic solvents, such as MeCN, dimethyl sulfoxide (DMSO), and dimethylformamide (DMF), to avoid hydrogen bonding (Kilbourn & Huizenga 1990). [^{18}F]Fluoride is prone to sticking to the glass walls during processing (Block et al. 1986, Brodack et al. 1986, Nickles et al. 1986); thus, a lot of effort has been made to develop an azeotropic distillation-free method for [^{18}F]fluoride activation. Solid phase extraction (SPE) methods for [^{18}F]fluoride activation have been introduced that utilise 4-aminopyridinium resins (Mulholland et al. 1989, Toorongian et al. 1990), and cryptands (Aerts et al. 2008, Wessmann et al. 2012), tetraalkyl ammonium salts (Aerts et al. 2010), or strong bases as eluting agents (Lemaire et al. 2010).

Many review articles and books have dealt extensively with nucleophilic ^{18}F-fluorination reactions (Kilbourn & Huizenga 1990, Coenen 2007, Cai et al. 2008, Tredwell & Gouverneur 2012, Cole et al. 2014, Jacobson et al. 2015, Preshlock et al. 2016, Deng et al. 2019). S_N2 type reactions typically utilise halogens and sulfonic esters, such as 4-methylbenzenesulfonate (tosylate) and trifluoromethanesulfonate (triflate), as leaving groups. The reactivity order of these precursors is halogens < tosylate < triflate. S_NAr type reactions typically utilise various halogens, a nitro group, or trimethylammonium salts as leaving groups. In addition to a carefully selected leaving group, nucleophilic aromatic substitution reactions typically require electron-deficient aryl precursors and harsh reaction conditions. Electron deficiency is achieved with electron withdrawing groups (EWGs) in the *ortho* and *para* positions to the leaving group. To avoid harsh reaction conditions, various ^{18}F-labelled prosthetic groups have been utilised in labelling sensitive structures, such as peptides (Liu et al. 2011, Richter & Wuest 2014).

To broaden the reactivity range of [^{18}F]fluoride, various new precursor types have been introduced, including aryl iodonium salts and ylides and aryl sulphonium salts. These fluorination reactions are discussed below.

Iodonium salts, iodonium ylides, and sulfonium salts

Electron-rich [^{18}F]fluoroarenes were achieved originally by starting from [^{18}F]fluoride with a Balz–Schiemann reaction, utilising aryldiazonium [^{18}F]fluoroborate (Nozaki & Tanaka 1967). However, one major drawback of the method is the low maximal theoretical radiochemical yield (RCY) of only 25% and low A_m. Thereafter, a method utilising diaryliodoniumsalts and [^{18}F]fluoride was developed (Pike & Aigbirhio 1995, Shah et al. 1998). The method can be used to label various functionalized arenes (Chun & Pike 2013). However, the downside of using unsymmetrical diaryliodonium salts is the ^{18}F-radiofluorination of more sterically hindered (*ortho*-substituted) and more

electron-deficient arenes (Chun et al. 2010). By using (aryl)(thienyl)iodonium salts, more electron-rich [^{18}F]arenes have been obtained (Ross et al. 2007), but the stability of thienyl precursors has been questioned (Ichiishi et al. 2014). One advantage of diaryliodonium salts is that they can be used for [^{18}F]fluoride activation instead of cryptands or additional bases (Richarz et al. 2014).

The use of iodonium ylides (Satyamurthy & Barrio 2010) and spirocyclic iodonium ylides (Rotstein et al. 2014) has broadened the substrate scope of nucleophilic radiofluorination. Aryldimethyl sulfonium salts (Maeda et al. 1987), triarylsulfonium salts (Mu et al. 2012, Sander et al. 2015), and diarylsulfoxides (Chun et al. 2013) have been used in nucleophilic ^{18}F-radiolabelling, but the substrate scope has been limited to electron-deficient arenes. ^{18}F-Labelling reactions with iodonium and sulfonium salts and iodonium ylides are shown in Figure 6.

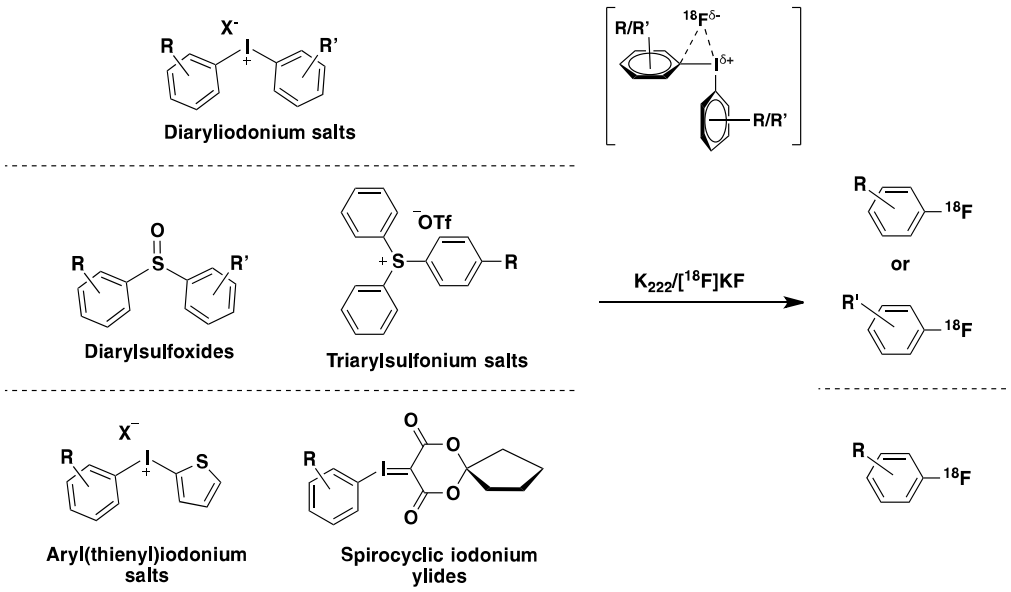

Figure 6. Nucleophilic ^{18}F-fluorination of iodonium salts, sulfonium salts, and iodonium ylides and the proposed intermediate with diaryliodonium salts. X^- = $^-$OTf, $^-$OTs, Br^-, Cl^- or TFA ion.

As noted previously, nucleophilic ^{18}F-fluorination strategies typically require multi-step synthesis, high temperature, high pressure, or other inconvenient steps, including precursor synthesis. Thus, new late stage ^{18}F-labelling strategies utilising transition metals have been developed as described in the following chapters.

2.5 Transition metal-mediated ^{18}F-fluorination

Transition metals have been used in C-F bond-forming reactions as catalysts or mediators (Watson et al. 2009, Campbell & Ritter 2015, Sather & Buchwald 2016, Boursalian & Ritter 2017). Many of the transition metal-mediated approaches have a limited substrate scope, and electron-rich aryl compounds have typically not been tolerated (Sather & Buchwald 2016). Another limitation has been the use of an electrophilic fluorine source (Campbell & Ritter 2015). Electrophilic ^{18}F-labelling reactions are constrained to low A_m and nucleophilic reactions to [^{18}F]fluoride's low reactivity, whereas high A_m and diverse reactivity have been obtained with new transition metal-mediated ^{18}F-fluorination pathways.

2.5.1 Palladium-mediated ^{18}F-fluorination

Electrophilic palladium-mediated ^{18}F-labelling reactions were introduced in 2011 by the Ritter group (Lee et al. 2011). These two-step reactions utilise two different palladium complexes, a [^{18}F]fluoride-Pd^{IV} complex and an aryl-Pd^{II} complex (Figure 7). The electrophilic [^{18}F]fluoride-Pd^{IV} complex is synthesised from conventionally processed no-carrier-added [^{18}F]fluoride with high A_m (Lee et al. 2011). In a high oxidation state, palladium can act as an oxidant and transfer [^{18}F]fluoride to the nucleophile, i.e., the aryl-Pd^{II} complex, whereas the palladium in the [^{18}F]fluoride-Pd^{IV} complex reduces to the lower Pd^{II} oxidation state. Reductive elimination of Pd^{IV} complexes to form aryl-fluoride compounds is challenging due to undesired nucleophilic attacks on the transition metal. In the Pd-mediated ^{18}F-fluorination described by Lee et al. (2011), this effect is avoided by using octahedral Pd^{IV} complex and multidentate ligands.

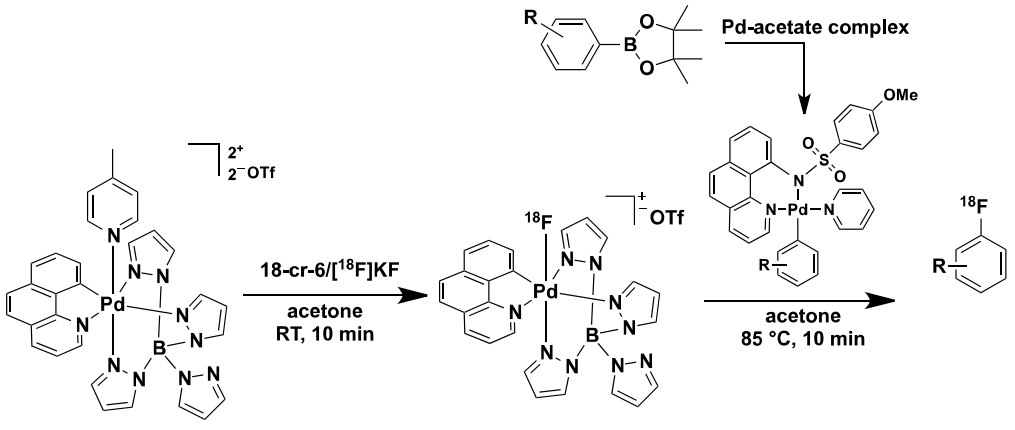

Figure 7. Palladium-mediated ^{18}F-fluorination (Lee et al. 2011).

Pd-mediated ^{18}F-fluorination reactions have shown a broad substrate scope (Lee et al. 2011), and the method has been proven to be suitable for labelling clinically interesting structures, such as [^{18}F]paroxetine, a selective serotonin reuptake inhibitor (Kamlet et al. 2013). However, a limitation is intolerability towards nucleophilic and basic functional groups, such as tertiary amines (Lee et al. 2011, Kamlet et al. 2013). The scope has been further broadened to sterically hindered aryl fluorides and alkyl fluorides using aryl silver compounds or compounds containing an activated double bond as nucleophiles instead of aryl-Pd^{II} compounds (Brandt et al. 2014).

Although the [^{18}F]fluoride-Pd^{IV} complex tolerates water, the precursor for the ^{18}F-labelling reagent is rather insensitive towards water (Lee et al. 2011). Boronic ester precursors are common precursors in radiochemistry applications and relatively easily available. However, the overall Pd-mediated ^{18}F-chemistry is complex and lacks robustness (Kamlet et al. 2013). In addition, the need for azeotropic drying of [^{18}F]fluoride in addition to two-step labelling synthesis makes palladium-mediated fluorination an unfavourable approach to clinical radiopharmaceutical production (Lee et al. 2012).

2.5.2 Nickel-mediated ^{18}F-fluorination

The next approach to transition metal-mediated ^{18}F-fluorination was the use of nickel complexes. One-step ^{18}F-labelling utilises aqueous [^{18}F]fluoride and aryl-Ni^{II} precursor in the presence of an iodine^{III} oxidant. The no-carrier-added method produces the desired [^{18}F]aryl fluorides (Figure 8) with high A_m (Lee et al. 2012). Aryl-Ni^{II} precursor and [^{18}F]fluoride form an aryl-Ni^{III} fluoride complex, which produces the [^{18}F]aryl fluoride by reductive elimination (Lee et al. 2017). Such a mechanism is enabled with suitable multidentate ligands that stabilise the high-valent nickel complex (Lee et al. 2017).

Ni-mediated ^{18}F-fluorination was originally performed in aqueous conditions at room temperature (RT) starting from brominated precursors (Lee et al. 2012). Further studies have shown a major decrease in the RCY in aqueous conditions (>1% v/v water) due to the moisture-sensitive nature of the nickel complex and the oxidizing agent (Ren et al. 2014, Zlatopolskiy et al. 2015b). Thus, microfluidic strategies have been used in [^{18}F]fluoride processing to minimise the volume of water (Hoover et al. 2016). The presence of a base was observed to be essential for the reaction (Zlatopolskiy et al. 2015b). However, traditional radiochemistry methods used for the activation of [^{18}F]fluoride usually lead to too basic conditions, which subsequently afford low yields (Ren et al. 2014). To increase the robustness, various oxidants, such as hypervalent iodine compounds have been tested in the ^{18}F-labelling, without any success (Zlatopolskiy et al. 2015b).

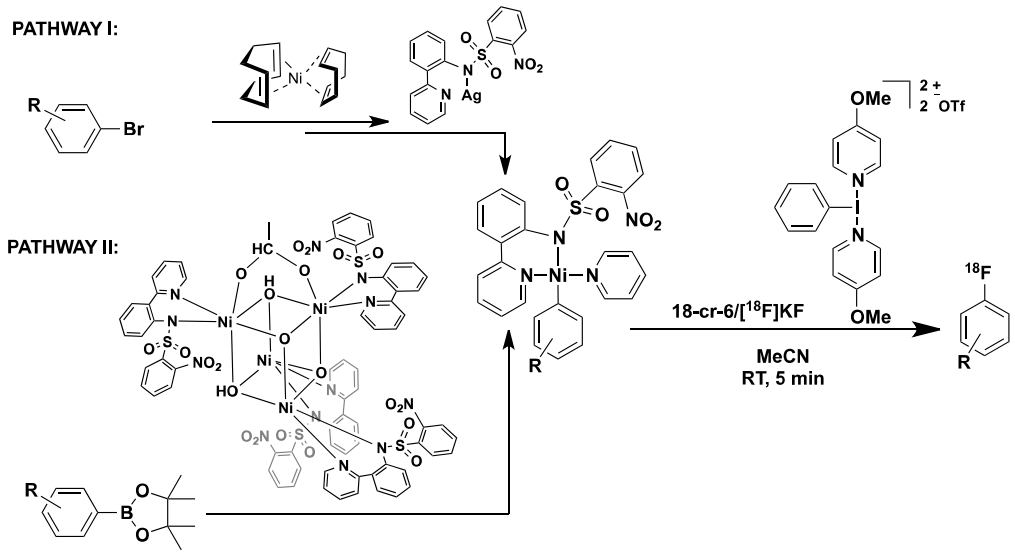

Figure 8. Ni-mediated ^{18}F-fluorination with two approaches to synthesise the Ni-aryl precursor (Lee et al. 2012, Hoover et al. 2016).

Aryl-Ni^{II} precursors have been synthesised using two different approaches (Figure 8): oxidative addition (pathway I) (Lee et al. 2012) and transmetallation (pathway II) (Hoover et al. 2016). In pathway I, oxidative addition of bis(cyclooctadiene)nickel^{0} (Ni(COD)$_2$) to arylbromide and subsequent addition of ligand results in stable aryl-Ni^{II} precursor in an inert atmosphere (Lee et al. 2012). The oxidative addition pathway is commonly used in the synthesis of aryl-Ni^{II} compounds (Semmelhack et al. 1971, Fahey & Mahan 1977, Tsou & Kochi 1979). The use of Ni^{0} limits the reactivity scope due to its strong reducing activity. An alternative method is the transmetallation pathway with organometallic precursors, such as zinc (Kurosawa et al. 1990), lithium (Chatt & Shaw 1960), and magnesium compounds (Tamao et al. 1972). These compounds limit the accessible aryl-Ni compounds by their basicity and nucleophilicity. In pathway II, aryl-Ni^{II} complexes are formed by transmetallation from arylboronic esters or arylboronic acids (Hoover et al. 2016). Transmetallation with easy access boronic acid or boronic ester precursors enabled the radiosynthesis of electron-rich [^{18}F]heteroarenes (Hoover et al. 2016).

Nickel-mediated ^{18}F-fluorination has exhibited a broad substrate scope, and various electron-rich and electron-poor [^{18}F]aryl fluorides have been produced successfully (Lee et al. 2012). In addition, the method has been used in the production of clinically interesting molecules, such as [^{18}F]5-fluorouracil (Hoover et al. 2016) and [^{18}F]MDL100907 (Ren et al. 2014). As with palladium-mediated ^{18}F-fluorination, Ni-mediated ^{18}F-fluorination is not a suitable method for ^{18}F-labelling compounds

containing highly basic functional groups (Lee et al. 2012). Overall, Ni-mediated ^{18}F-labelling is a simple method with a one-step approach at RT. However, synthesis of the aryl-nickel complexes is challenging.

2.5.3 Copper-mediated ^{18}F-fluorination

Copper-mediated radiofluorination of iodonium salts and organohalides

As presented earlier in chapter 2.4, nucleophilic ^{18}F-fluorination of aryliodonium salts typically results in ^{18}F-fluorination of the sterically more hindered arenes. Catalysing the reaction with $Cu(OTf)_2$ has led to the ^{18}F-fluorination of sterically less hindered arenes (Ichiishi et al. 2013). The mechanism has been suggested to be as follows: the Cu^{II} catalyst is reduced and undergoes ligand exchange to produce Cu^{I}-F, which is oxidized by highly electrophilic diaryliodonium salt to Cu^{III}-aryl complex. The intermediate undergoes reductive elimination to Cu^{I}-π-aryl fluoride complex and further releases aryl fluoride and Cu^{I} catalyst (Figure 9A) (Ichiishi et al. 2013).

Copper-catalysed ^{18}F-fluorination was applied to label (mesityl)(aryl)iodonium salts utilising [^{18}F]KF and $(MeCN)_4CuOTf$ (Figure 9B) (Ichiishi et al. 2014). The method has a broad substrate scope and exhibits robustness, as the synthesis can be conducted under ambient conditions (Ichiishi et al. 2014). The method has been further developed to avoid the need for PTCs and azeotropic distillation to activate aqueous [^{18}F]fluoride. The new methods utilise improved SPE elution techniques with alcohols and diminished amounts of base (Richarz et al. 2014, Zlatopolskiy et al. 2015a, Modemann et al. 2019). The labelling method has also been proven to be suitable for automation (Zischler et al. 2016). However, a weakness of the method is the iodonium precursors, the synthesis of which remains rather cumbersome (Yuan et al. 2016b).

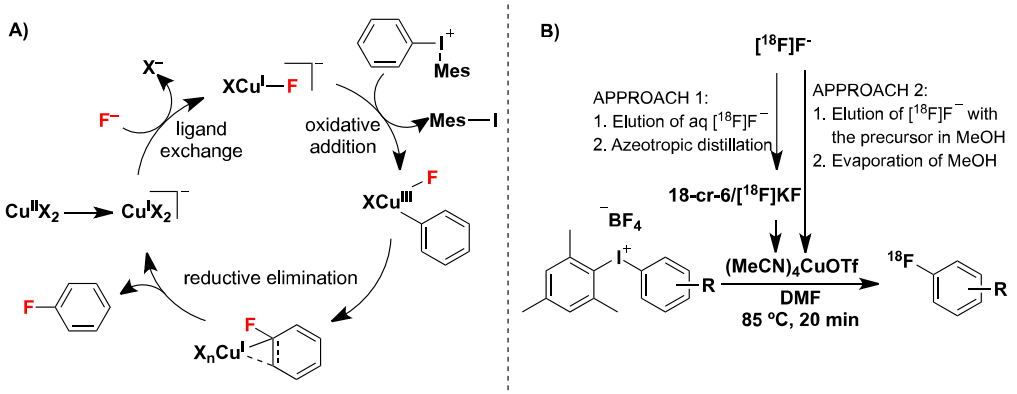

Figure 9. A) Cu^{I}/Cu^{III} catalytic cycle proposed by Ichiishi et al. (2013) and B) Cu-mediated ^{18}F-fluorination with two approaches for [^{18}F]fluoride activation.

In addition to iodonium salts, copper-mediated ^{18}F-fluorination with $(MeCN)_4CuOTf$ has been applied to label organohalides. The radiolabelling method is based on the work done with fluorine-19. Copper-catalysed fluorination of arylhalides with excess AgF has been proposed to proceed via the Cu^I/Cu^{III} catalytic cycle using $(MeCN)_4CuOTf$ or CuBr as the catalyst and aryl precursor with a directing group in the *ortho* position (Casitas et al. 2011, Mu et al. 2014). Oxidative addition of arylhalide to the Cu^I complex has been suggested to be slow (Mu et al. 2014). In the radiolabelling approach, the *N*-heterocyclic carbene (NHC) ligated Cu complex (1,3-bis-(2,6-diisopropylphenyl)imidazol-2-ylidine)Cu^I(OTf) ((IPr)Cu^I(OTf)) was used as a Cu-mediator to accelerate the oxidation step. The bulky NHC ligand also stabilises the Cu^I-F complexes against dimerization and disproportionation (Sharninghausen et al. 2020). Instead of AgF, [^{18}F]KF has been used in the radiolabelling approach, as KF has been shown to generate (NHC)Cu^I(F) complex (Dang et al. 2014). Copper-mediated ^{18}F-labelling of organohalides has exhibited a broad scope among substrates, with a directing group in the *ortho* position, and has been translated to automated production (Sharninghausen et al. 2020).

Copper-mediated radiofluorination of organoborons and organostannanes

Cu-mediated synthesis of aryl fluorides starting from organoboron and organostannane precursors were developed by several groups during the 2010s. Many of the developed methods have utilised Cu^I-mediator and a nucleophilic or electrophilic fluorine source. For example, the Hartwig group first developed a Cu-mediated fluorination method starting from aryl iodide precursors with (^{t}BuCN)$_2$Cu(OTf) and AgF (Fier & Hartwig 2012). Soon after, the same group presented a similar method with milder conditions starting from aryl boronic acid or aryl boronic ester precursors and a F^+ source, such as Selectfluor or NFSi (Fier et al. 2013). Simultaneously, the Sanford group used (^{t}BuCN)$_2$Cu(OTf) and readily available F^+ fluorinating reagents, such as *N*-fluoro-2,4,6-trimethylpyridinium triflate (NFTPT), in the fluorination of aryl stannanes and aryl trifluoroborates (Ye & Sanford 2013).

The Hartwig group proposed a method that proceeds via the cationic Cu^{III} fluoride complex to the arylboronate Cu^{III} fluoride complex and further to the aryl Cu^{III} fluoride complex via rate-limiting transmetallation, and subsequent reductive elimination forms the desired aryl fluoride (Fier et al. 2013). The formation of high-valent Cu^{III} fluoride complexes was suggested initially in Cu-mediated fluorination via a halide exchange reaction (Casitas et al. 2011). The Cu^I/Cu^{III} mechanism was supported by the Sanford group (Ye & Sanford 2013). In these reactions, electrophilic F^+ has worked as a fluorine source and an oxidant (Ye & Sanford 2013). The scope of the Cu-mediated fluorination with F^+ was broad with tolerance for electron-rich and electron-deficient substrates (Ye & Sanford 2013, Fier et al. 2013).

To avoid requiring an electrophilic F^+ source, Cu-mediated fluorination of aryltrifluoroborates and arylborons utilising nucleophilic fluoride and $Cu(OTf)_2$ was developed by the Sanford group (Ye et al. 2013). This method was proposed to proceed via $Cu^{II}(OTf)(F)$ intermediate to aryl $Cu^{II}(F)$ complex, which was further oxidized by $Cu(OTf)_2$ to aryl $Cu^{III}(OTf)(F)$ complex, and fast reductive elimination forms the aryl fluoride (Figure 10A) (Ye et al. 2013). Cu^{II}-mediators have been widely used in the Chan-Lam carbon-heteroatom bond cross-coupling reactions of arylborons (Qiao & Lam 2011), in which aryl Cu^{III} intermediate has also been suggested to be formed in a disproportionation reaction with one equivalent of Cu^{II}-mediator (King et al. 2009). The Murphy group successfully applied Cu-mediated fluorination with fluoride and $Cu(OTf)_2$ to arylstannane precursors, and their results supported the formation of Cu^{II} and Cu^{III} fluoride complexes (Gamache et al. 2016).

The Gouverneur group was the first to introduce Cu-mediated ^{18}F-labelling of aryl boronate esters using $Cu(OTf)_2(py)_4$ complex and [^{18}F]KF (Tredwell et al. 2014). This was shortly followed by Scott and Sanford's group, who utilised $Cu(OTf)_2$ complex in the presence of pyridine with aryl boronic acid precursors (Mossine et al. 2015) and aryl stannane precursors (Makaravage et al. 2016) in radiofluorination (Figure 10B). Typical radiolabelling conditions have been 20 minutes at 110 °C in DMF or dimethylacetamide (DMA) (Tredwell et al. 2014, Mossine et al. 2015, Makaravage et al. 2016). Even though the Murphy group observed significant improvements in the fluorination yields when MeCN was present (Gamache et al. 2016), no product was observed in the radiolabelling reactions carried out in MeCN (Tredwell et al. 2014, Mossine et al. 2015, Makaravage et al. 2016). However, pyridine was a critical ligand for copper in ^{18}F-radiofluorination (Tredwell et al. 2014, Mossine et al. 2015). As noted above, pyridine can be applied to the reaction in the form of $Cu(OTf)_2(py)_4$ or as a separate additive with $Cu(OTf)_2$. Low cost and good stability are benefits of using $Cu(OTf)_2$.

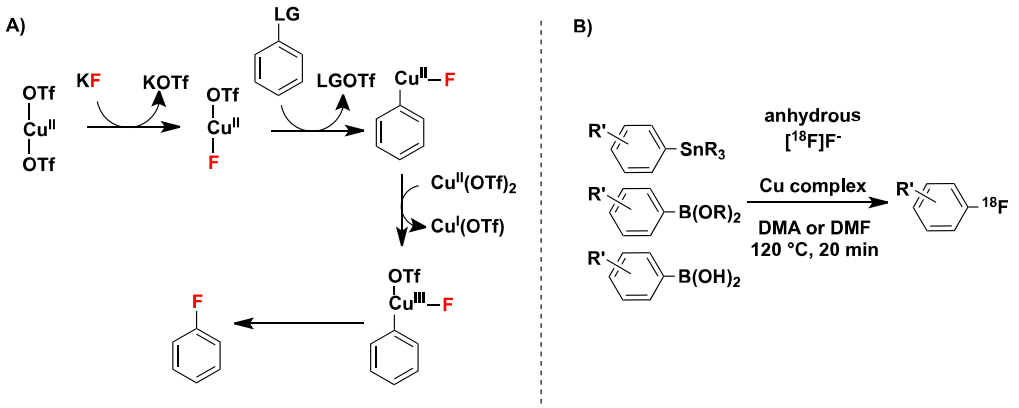

Figure 10. A) Mechanism of Cu-mediated fluorination with trifluoroborate leaving group (LG) proposed by Ye et al. (2013) and B) Cu-mediated ^{18}F-fluorination.

Since the development of Cu-mediated radiofluorination of organostannanes and organoborons, the method has been studied by several groups. Originally, [^{18}F]fluoride was activated using traditional azeotropic distillation with additional PTC and base (Tredwell et al. 2014, Mossine et al. 2015, Makaravage et al. 2016). However, the use of base has been blamed for suppressing the labelling yield; thus, a low-base approach was developed (Zlatopolskiy et al. 2015a). Similarly, when the amount of pyridine was increased over 30 equivalents compared to the copper-mediator, the reaction yield decreased, probably due to the increased basicity of the reaction solution (Antuganov et al. 2017). [^{18}F]Fluoride elution protocols have been studied to enhance the Cu-mediated radiofluorination reactions. Some of these methods still require time-consuming azeotropic distillation (Mossine et al. 2017). Cu-mediated ^{18}F-labelling has been further enhanced by developing SPE methods with different eluting agents, such as tetraethylammonium bicarbonate (Et_4NHCO_3) in alcohol (Zischler et al. 2017), pyridinium sulfonates (Antuganov et al. 2019), and dimethylaminopyridinium triflates (DMAP) (Zhang et al. 2019b).

The Neumaier group has reported that higher alcohols, such as *n*BuOH and *t*BuOH, have enhanced the Cu-mediated radiofluorination of aryl boronic acids and aryl boronic esters, but not aryl stannanes (Zischler et al. 2017, Zarrad et al. 2017). Additional alcohols have been proposed to increase [^{18}F]fluoride solvation (*i.e.*, decrease the basicity) (Kim et al. 2008a, 2008b). The enhancement has been most significant with boronic acid precursors, and alcohols have been suggested to esterify the boronic acids. Overall, in Cu-mediated radiofluorination, alcohols have been proposed to form hydrogen bonds to organoboron substrate, stabilising the rate-limiting transmetallation step (Zarrad et al. 2017).

With the above-described Cu-mediated labelling methods, a wide range of aryl [^{18}F]fluorides have been synthesised, with yields ranging from 5 to 80%. Boronic acid and boronic ester precursors have behaved similarly. Varying the alkyl substitution in the tin in organostannane precursors has had a significant effect on the radiofluorination. In prior method optimisation, -$SnMe_3$ precursors resulted in considerably higher yields than -$SnBu_3$ precursors (Makaravage et al. 2016). Lower yields with -$SnBu_3$ precursors are considered to be caused by steric hindrance on the tin centre, resulting in a slower transmetallation rate (Makaravage et al. 2016). A similar effect has been observed in hydrogenolysis with different alkyltin compounds onto metallic rhodium (Taoufik et al. 2004). After method optimisation, ^{18}F-fluorodestannylation reactions with -$SnBu_3$ precursors have, in some cases, been superior to ^{18}F-fluorodeboronation reactions (Wright et al. 2020). With both boron and stannane precursors, *ortho*-, *meta*-, and *para*-substituted arenes have been tolerated (Tredwell et al. 2014, Mossine et al. 2015, Makaravage et al. 2016). However, *ortho*-substituted arenes have shown lower RCYs with organoboron precursors. This has been speculated to be caused by steric hindrance, which affects the rate-limiting transmetallation step (Mossine et al. 2015).

Although the scope has proven to be wide, non-protected alcohol or amine substituents have not been well-tolerated (Tredwell et al. 2014). This could be explained by the competitive Cu^{II}-promoted C-O or C-N cross-coupling, Chan-Lam coupling (Qiao & Lam 2011, Huffman et al. 2011). The Gouverneur group extensively studied the effect of heterocycles and heterocyclic additives on Cu-mediated ^{18}F-labelling and noted decreased yields when the compounds contained acidic N-H protons (Taylor et al. 2017). In addition, an increased amount of Cu-mediator is needed in the reaction with compounds containing multiple basic nitrogen atoms (Taylor et al. 2017). Despite the limitations, Cu-mediated ^{18}F-fluorination is a widely used labelling method and has been adapted to production according to good manufacturing practices (GMP) (Mossine et al. 2019, 2020).

2.5.4 Ruthenium-mediated ^{18}F-fluorination

Certain transition metals, such as chromium, iron, osmium, manganese, and ruthenium, can activate otherwise inactive cyclic π-hydrocarbons by functioning as an electron-withdrawing group, favouring the subsequent nucleophilic substitution reactions (Kane-Maguire et al. 1984, Rose-Munch et al. 1998, Pike & Sweigart 1999, Pape et al. 2000, Semmelhack & Chlenov 2004). Typically, stoichiometric amounts of the transition metal activator are needed. However, catalytic approaches have also been presented with Ru as the catalyst in S_NAr reactions of inactive arenes (Otsuka et al. 2010a, 2010b, Imazaki et al. 2012, Konovalov et al. 2015, Walton & Williams 2015). In the ruthenium-catalysed fluorination of inactive chloro-, bromo-, and iodo-benzenes, the method has been proposed to proceed via a Meisenheimer complex and subsequent fluoroarene ligand exchange with the haloarene substrate (Konovalov et al. 2015). Various Ru-activators have been used, but [Ru^{II}(cyclopentadiene)] fragment has been suggested to speed up S_NAr reactions (Walton & Williams 2015).

Ru-mediated ^{18}F-deoxyfluorination reactions were introduced in 2017 by the Ritter group (Figure 11). The method utilises [^{18}F]fluoride, PhenoFluor™ reagent (*N,N′*-1,3-bis(2,6-diisopropylphenyl)chloroimidazolium chloride), and easy access phenols as starting materials (Beyzavi et al. 2017). Phenols are typically considered too inactive for nucleophilic substitution reactions. In the study by the Ritter group, the aromatic ring was activated by η^6-coordination to the ruthenium complex, such as (cyclopentadiene)Ru(COD)Cl (Beyzavi et al. 2017) or [(cyclopentadiene)Ru(naphthalene)]BF_4 (Rickmeier & Ritter 2018). PhenoFluor is used as a reaction additive, as it is known to facilitate the deoxyfluorination reaction of phenols (Neumann et al. 2016).

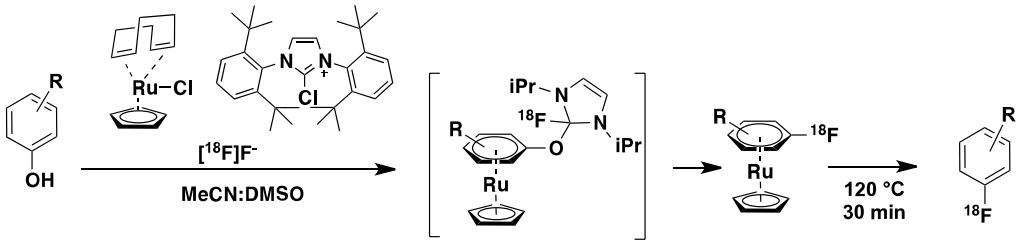

Figure 11. Ru-mediated ^{18}F-fluorination and the proposed reaction intermediate (Beyzavi et al. 2017).

The scope of the Ru-mediated ^{18}F-fluorination reaction has proven to be broad, including arenes containing very electron-rich substrates and *ortho*-substitutions (Beyzavi et al. 2017), as well as small peptides (Rickmeier & Ritter 2018). The method has been used in radiotracer production for preclinical use (Strebl et al. 2017). In addition, the Ru-mediated ^{18}F-fluorination method has been successfully converted to GMP production (Celen et al. 2020).

Notably, the Ru-mediated method does not proceed via high-valent complexes and redox chemistry, unlike Cu-mediated, Ni-mediated, or Pd-mediated ^{18}F-fluorination reactions. Another advantage of the method is that Ru complexes tolerate air and moisture (Beyzavi et al. 2017). However, as the aryl fluoride Ru-complexes are rather stable, decomplexation is the rate-limiting step and requires high temperature (Beyzavi et al. 2017).

2.5.5 Other transition metal-mediated ^{18}F-fluorinations/approaches

Pd-, Ni-, Cu-, and Ru-mediated ^{18}F-fluorination reactions have garnered a relatively large amount of attention. Nevertheless, other transition metal-mediated ^{18}F-fluorination strategies have been introduced and will be covered in the following chapters. These methods have been utilised to, for example, achieve enantioselective ^{18}F-fluorination.

Rhenium

Rhenium(I) has been applied in the ^{18}F-fluorination reactions of bipyridine and other pyridine-containing substrates, allowing bidentate ligation to Re (Figure 12) (Klenner et al. 2017, 2020). The method utilises nucleophilic tetraethylammonium [^{18}F]fluoride, and the reaction has been shown to tolerate water (Klenner et al. 2017). The electron-withdrawing effect of the Re^{I} centre has been suggested to facilitate the radiofluorination of rather inactive halogen precursors (Klenner et al. 2020).

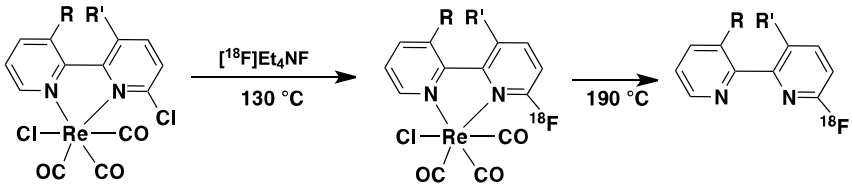

Figure 12. Re-mediated ^{18}F-fluorination (Klenner et al. 2017, 2020).

Manganese

Manganese^{III} porphyrins were originally used by the Groves group as catalysts in the oxidative fluorination of aliphatic C−H bonds with excess AgF (Liu et al. 2012). The reaction was shown to proceed via *trans*-difluoromanganese^{IV} complex (Liu et al. 2012). Hooker and Groves' group translated the method to ^{18}F-fluorination of benzylic C−H bonds using Mn(salen)OTs (*N*,*N*′-bis(3,5-di-tert-butylsalicylidene)-1,2-cyclohexanediaminomanganese^{III} tosylate) and [^{18}F]fluoride (Figure 13) (Huang et al. 2014). In ^{18}F-fluorination, the amount of [^{18}F]fluoride is very low, and the formation of *trans*-difluoromanganese^{IV} complex is highly unlikely. Thus, the reaction was suggested to proceed via ^{18}F−Mn^{IV}−OH intermediate, which then reacts with benzyl radical (Huang et al. 2014). The method has a broad scope, and various functional groups are tolerated. However, higher RCYs were achieved with substrates containing electron-donating groups (Huang et al. 2014).

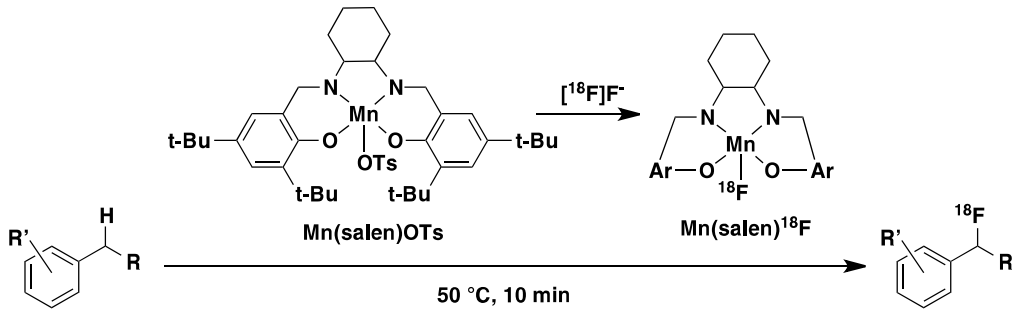

Figure 13. Mn-mediated ^{18}F-fluorination (Huang et al. 2014).

The Mn-mediated method has also been applied to direct aliphatic ^{18}F-fluorination of inactivated C-H bonds using a manganese^{III} pentafluorophenyl porphyrin tosylate (Liu et al. 2018). The method exhibits good tolerance for various functional groups containing esters and amides, and the labelling is site-selective towards the least sterically hindered position (Liu et al. 2018). Compared to the traditional nucleophilic

^{18}F-labelling reactions with [^{18}F]fluoride, Mn porphyrin-mediated labelling reactions do not need high temperatures or long reaction times, as 10 min reactions at 50 °C provide up to 80% RCY (Huang et al. 2014, Liu et al. 2018).

Cobalt

Co^{III}(salen) complex has been used as a catalyst in the enantioselective fluorination of epoxides via a ring opening reaction (Kalow & Doyle 2010). The method has been translated to ^{18}F-fluorination by the Doyle group (Figure 14) (Graham et al. 2014). Although the original Co-mediated fluorination was executed using benzoyl fluoride as the source of fluorine (Kalow & Doyle 2010), ^{18}F-labelling was performed successfully with [^{18}F]fluoride; thus, synthesis of a separate ^{18}F-fluorination reagent was avoided (Graham et al. 2014). The method has been suggested to proceed via ^{18}F−Co(salen) complex (Graham et al. 2014). Similar to Mn porphyrin-mediated ^{18}F-labelling reactions (Huang et al. 2014, Liu et al. 2018), separate drying procedures are not needed and the reaction conditions are mild: 20 min at 50 °C (Graham et al. 2014). The original ^{18}F-labelling method did not tolerate N-containing compounds. However, using a dimeric Co-catalyst allowed ^{18}F-labelling of such structures (Graham et al. 2014).

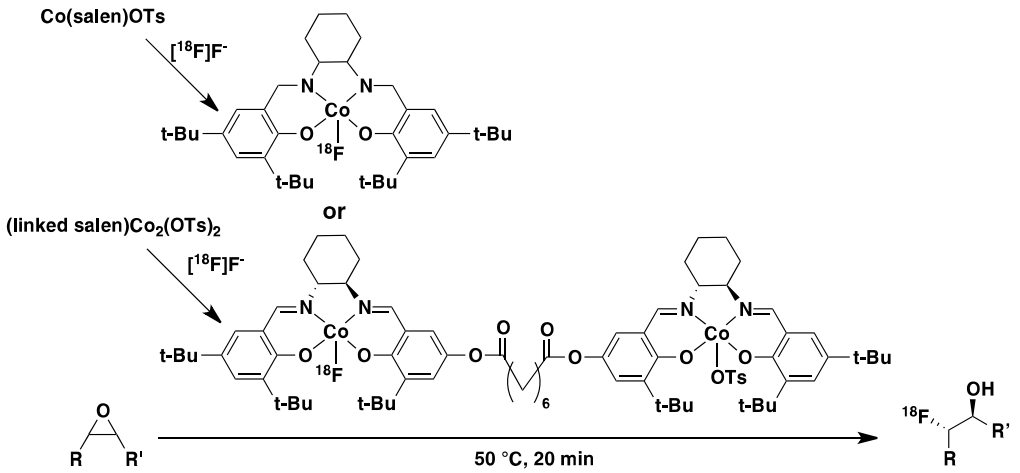

Figure 14. Co-mediated ^{18}F-fluorination (Graham et al. 2014).

Rhodium

The Szabó group utilised rhodium^{II} catalysts in the oxyfluorination and oxytrifluoromethylation reactions (Yuan et al. 2016a) to form biologically relevant

α-fluoro ether and α-trifluoromethyl ether motifs (Leroux et al. 2005). The method utilises electrophilic fluorination reagents, such as hypervalent iodine reagent fluorobenziodoxole (Yuan et al. 2016a). Other electrophilic fluorinating reagents, such as N-F compounds, result in lower yields (Yuan et al. 2016a). In addition, the reaction mechanism with hypervalent iodine reagents and N-F reagents has been shown to be different (Mai et al. 2018).

The same group translated the method to ^{18}F-oxyfluorination and utilised rhodium^{II} acetate ($Rh_2(OAc)_4$) and rhodium pivalate ($Rh_2(OPiv)_4$) as catalysts to form α-[^{18}F]fluoro ethers (Figure 15) (Cortés González et al. 2019). The two-step radiofluorination process includes synthesis of the electrophilic ^{18}F-fluorination reagent [^{18}F]fluorobenziodoxole from tetrabutylammonium [^{18}F]fluoride (Cortés González et al. 2018) and subsequent ^{18}F-oxyfluorination. The method tolerates various heterocyclic diazoketones, and electron-withdrawing and electron-donating substituents in the aromatic ring of the diazoketone (Cortés González et al. 2019). Although the method utilises electrophilic ^{18}F-fluorinating reagent, the achieved A_ms have been >200 GBq/μmol (Cortés González et al. 2019).

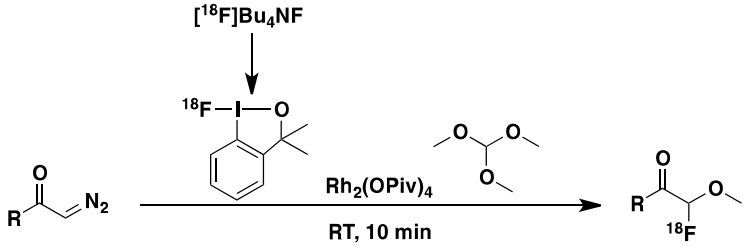

Figure 15. Rh-mediated ^{18}F-fluorination (Cortés González et al. 2019).

Silver

Silver^{I} triflate has been used in the regiospecific electrophilic fluorination of aryl boronic acids, aryl boronic esters (Furuya & Ritter 2009), and aryl stannanes (Furuya et al. 2009). With aryl boronates, the synthesis has been proposed to proceed via transmetallation and subsequent fluorination (Furuya & Ritter 2009). With aryl stannanes, the transmetallation product was observed to be the bimetallic (ArAg)·(AgOTf) complex, which then releases the corresponding aryl fluoride through oxidation and subsequent reductive elimination (Furuya et al. 2009).

AgOTf-mediated ^{18}F-fluorination method has been developed using [^{18}F]Selectfluor *bis*(triflate) as presented in chapter 2.3.2. The ^{18}F-labelling method has been further developed to avoid the need for electrophilic labelling reagents. Thus, [^{18}F]arylOCHF$_2$, [^{18}F]arylOCF$_3$, [^{18}F]arylSCF$_3$, [^{18}F]arylCF$_3$, and [^{18}F]arylCHF$_2$

compounds have been produced by halogen exchange reaction with [^{18}F]fluoride in the presence of a Ag^I source (Khotavivattana et al. 2015, Verhoog et al. 2016). Despite the method development, a downside of silver-mediated ^{18}F-fluorination has been the low A_m. With electrophilic approach, the obvious reason for low A_m is the use of F_2 in the production of the labelling reagents, and with the nucleophilic approach the reason is the use of fluorinated precursors (Teare et al. 2010, Khotavivattana et al. 2015, Verhoog et al. 2016).

2.6 CNS bound radiopharmaceuticals

PET radiopharmaceuticals have been used to study the human peripheral nervous system (PNS) and CNS. To be a suitable tracer for CNS imaging, certain prerequisites need to be fulfilled, including 1) selectivity and affinity for the receptor, 2) A_m, 3) metabolism, 4) blood-brain barrier (BBB) permeability, 5) non-specific binding, and 6) clearance rate (Ametamey et al. 2008, Waterhouse & Collier 2020).

Many receptors have low concentration in the brain; thus, one of the most important qualities of the CNS bound tracers is binding affinity. The bound-to-free *in vitro* binding ratio can be estimated by the equilibrium binding expression described by Scatchard, which can be simplified as presented below with high A_m tracers (Equation (2)) (Eckelman 1998, Gibson et al. 2000). Equation (2) and the *in vitro* binding potential (B_{max}/K_d) is not directly applicable to *in vivo* binding, as the non-specific binding is higher *in vivo* than *in vitro* (Kung & Kung 2005, Eckelman et al. 2006). B is the concentration of the bound tracer, F is the concentration of the free tracer, B_{max} is the concentration of binding sites, and K_d is the equilibrium dissociation constant.

$$\frac{B}{F} = \frac{B_{max}}{K_d} - \frac{B}{K_d} \approx \frac{B_{max}}{K_d} \tag{2}$$

The second important quality of a brain imaging tracer is high A_m (see chapter 2.2) because low A_m can lead to saturation of the binding site (Ametamey et al. 2008). Similarly, an important factor is the position of the radiolabel to avoid fast metabolism. PET cameras detect the radioactivity and do not recognize the source of radiation. Thus, radioactive metabolites interfere with PET imaging.

Without BBB permeability, a tracer cannot be used to image the CNS. A few important factors need to be taken into account when estimating the tracer's ability to cross the BBB: the molecular weight of the tracer, the tracer's ability to form hydrogen bonds, and lipophilicity. As a rule of thumb, the molecular weight should be <500 Da (Banks 2009). The higher the lipophilicity, the higher the BBB permeation. However, higher lipophilicity typically increases non-specific binding of the tracer and, thus, very

lipophilic molecules are typically not good radiopharmaceuticals (Gibson et al. 2000). Lastly, the tracer clearance from the blood should be relatively fast to enable imaging with short-lived tracers.

CNS PET has been widely utilised to image inflammation, neuropsychiatric disorders, and neurodegenerative disorders, especially AD (Frank & Hargreaves 2003, Seeman & Madras 2013, George et al. 2015, McCluskey et al. 2020). With AD, common targets have been amyloid plaques and tau proteins. Alternatively, the disease can be followed by imaging metabolic activity. A typical target for neuroinflammation imaging is the 18 kD translocator protein. Neurodegenerative and neuropsychiatric diseases are typically associated with a dysfunction of the neurotransmission systems. These systems can be followed by imaging with specific tracers. In the following chapters, the focus will be on ^{18}F-labelled norepinephrine transporter (NET) or dopamine transporter (DAT) tracers and cannabinoid receptor tracers.

2.6.1 Imaging of NET and DAT in the CNS

NET and DAT are plasma membrane proteins located on the presynaptic nerve terminals in the CNS and PNS. They belong to the family of Na^+/Cl^--dependent neurotransmitter transporters (Zahniser & Doolen 2001). DATs control the re-uptake of dopamine, and NETs the re-uptake of both norepinephrine and dopamine, from the synaptic cleft (Morón et al. 2002). Dysfunctions in the NET and DAT have been associated with various neurodegenerative diseases, including AD and PD, and neuropsychiatric diseases, such as depression (Torres et al. 2003).

NETs play a crucial role in depression; therefore, the NET is a prominent target for antidepressants, such as reboxetine. Reboxetine is a selective and specific norepinephrine reuptake inhibitor (Wong et al. 2000) that has been used as a starting point for CNS NET tracer development. Various noradrenergic ^{11}C- and ^{18}F-labelled reboxetine analogue tracers have been published (Ding et al. 2005, 2006, Zeng et al. 2009, Chen et al. 2020). Most of the NET tracers that have been developed have exhibited high non-specific binding, and only a few have proven to be suitable for *in vivo* imaging. The most promising CNS NET tracers have been [^{18}F]FMeNER-d_2 (Schou et al. 2004) and (*S*,*S*)-[^{11}C]MeNER ([^{11}C]MRB) (Wilson et al. 2003). In human studies, [^{18}F]FMeNER-d_2 has proven to be the better NET imaging tracer of the two (Moriguchi et al. 2017). PNS NET tracers typically do not penetrate the BBB. Recent developments have utilised separate chemical delivery systems to transport a PNS NET tracer, *meta*-iodobenzylguanidine, to the brain (Gourand et al. 2019). However, further evaluation is needed to prove the usefulness of this type of tracer in imaging the CNS. In rats, a novel CNS NET tracer, [^{18}F]NS12137 (Kirjavainen et al. 2018), has presented superior imaging properties, good brain uptake, fast clearance, and high specificity compared to [^{18}F]FMeNER-d_2 (López-Picón et al. 2019).

Similar to NET, dysregulation of DAT has been associated with various neurodegenerative diseases, and DAT-targeted tracers have been used for imaging in PD in particular (Vaughan & Foster 2013). Various PET tracers have been used to image DATs since the 1980s (Elsinga et al. 2006, Stehouwer & Goodman 2009). The main target of cocaine is the DAT; therefore, various cocaine analogue tracers have been developed to image DAT. These analogues are based on the phenyltropane structure. DAT-selective tracers include ^{11}C- and ^{18}F-labelled CFT (Dannals et al. 1993, Bergman et al. 1996, Haaparanta et al. 1996) and [^{18}F]FE-PE2I (Schou et al. 2009). Structures of the above-mentioned NET and DAT tracers are shown in Figure 16.

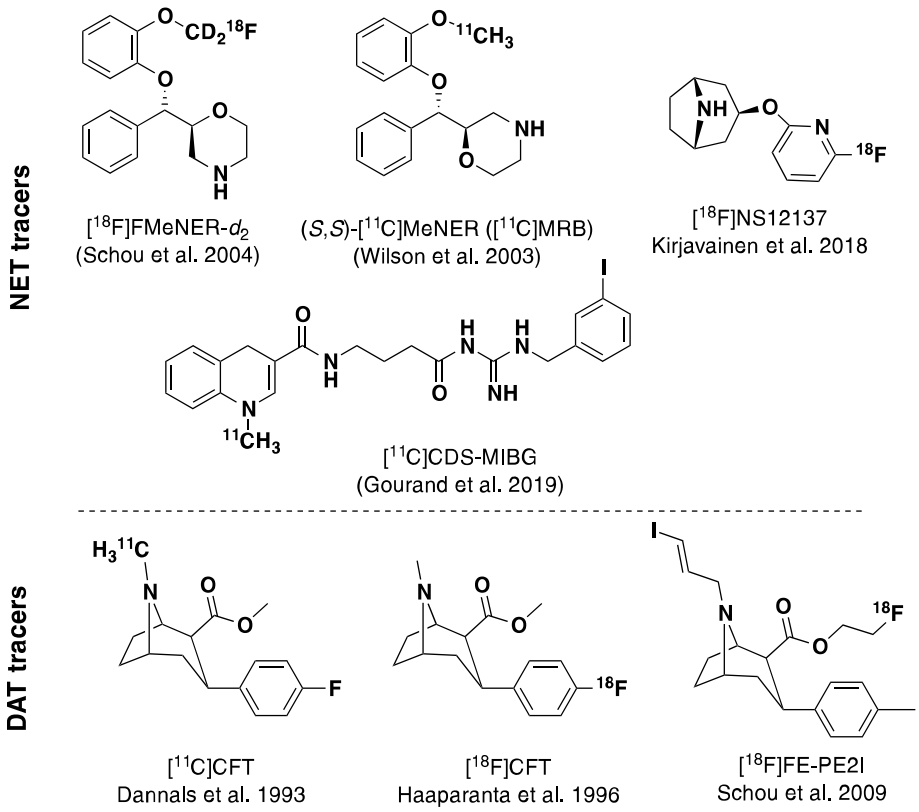

Figure 16. Examples of ^{11}C- and ^{18}F-labelled tracers for NET and DAT imaging in the CNS.

2.6.2 Imaging of cannabinoid receptors in the CNS

Cannabinoid receptors are cell membrane receptors belonging to the G protein-coupled receptor (GPCR) family, which are also known as seven-transmembrane domain receptors. Cannabinoid receptors are divided into two subclasses, cannabinoid

receptor 1 (CB1R) and cannabinoid receptor 2 (CB2R). Originally, CB1Rs were thought to be purely localized in the brain and CB2Rs in the periphery and immune system. Currently, CB1Rs are also known to be found to a lesser extent in peripheral organs, such as the lungs and liver (Howlett et al. 2002, Mechoulam & Parker 2013), and CB2Rs to a much lesser extent also in the brain (Yu et al. 2015, Jordan & Xi 2019). High levels of CB1Rs are found in the sensory, cognition, and motor regions in the brain and play a crucial role in various physiological and pathological conditions, including brain development, memory, motivation, and inflammation (Howlett et al. 2002, Mechoulam & Parker 2013). Thus, dysfunction of CB1Rs is involved in various neuropsychiatric and neurodegenerative conditions, such as schizophrenia and AD (Fattore 2015, Sloan et al. 2019).

Different ^{11}C- and ^{18}F-labelled tracers have been used to selectively image CB1Rs (Horti & Laere 2008, Ahamed et al. 2013) and CB2Rs (Slavik et al. 2014, Ni et al. 2019) in vertebrate species, including humans. This thesis focusses on CB1R tracers, and examples are shown in Figure 17. The development of CB1R tracers started from (−)[5′-^{18}F]Δ^8-tetrahydrocannabinol (THC) (Charalambous et al. 1991), an analogue of Δ^9-THC, the major psychoactive compound in cannabis. SR141716A, also known as rimonabant, is a common CB1R antagonist (Rinaldi-Carmona et al. 1994). Various rimonabant analogues have been studied (Lan et al. 1999, Katoch-Rouse et al. 2003), and a few have been successfully radiolabelled with carbon-11 (Mathews et al. 2002) or fluorine-18, such as [^{18}F]SR144385 (Mathews et al. 1999) and [^{18}F]AM5144 (Li et al. 2005). However, these tracers have shown poor imaging properties. So-called second generation CB1R radiotracers have improved affinity and reduced lipophilicity (Horti & Laere 2008). These tracers include [^{11}C]JHU75528, also known as [^{11}C]OMAR (Fan et al. 2006, Horti et al. 2006), [^{18}F]MK-9470 (Burns et al. 2007), [^{11}C]MePPEP (Yasuno et al. 2008), [^{18}F]FMPEP, [^{18}F]FMPEP-d_2 (Donohue et al. 2008a), and [^{11}C]SD5024 (Donohue et al. 2008b). Recent developments include [^{18}F]HU-210F, which, however, is not selective for CB1R (Zanato et al. 2017).

All of the second generation CB1R radiotracers have been used in clinical PET imaging (Hirvonen 2015). From the ^{11}C-labelled tracers, [^{11}C]SD5024 has proven to be the most promising (Tsujikawa et al. 2014). From the 1,5-diphenylpyrrolidin-2-one-based CB1R tracers, [^{18}F]FMPEP-d_2 has proven to be superior in stability and imaging properties compared to [^{18}F]FMPEP and [^{11}C]MePPEP (Terry et al. 2010). Furthermore, deuteration of the [^{18}F]fluoromethoxy tail improves stability (Donohue et al. 2008a).

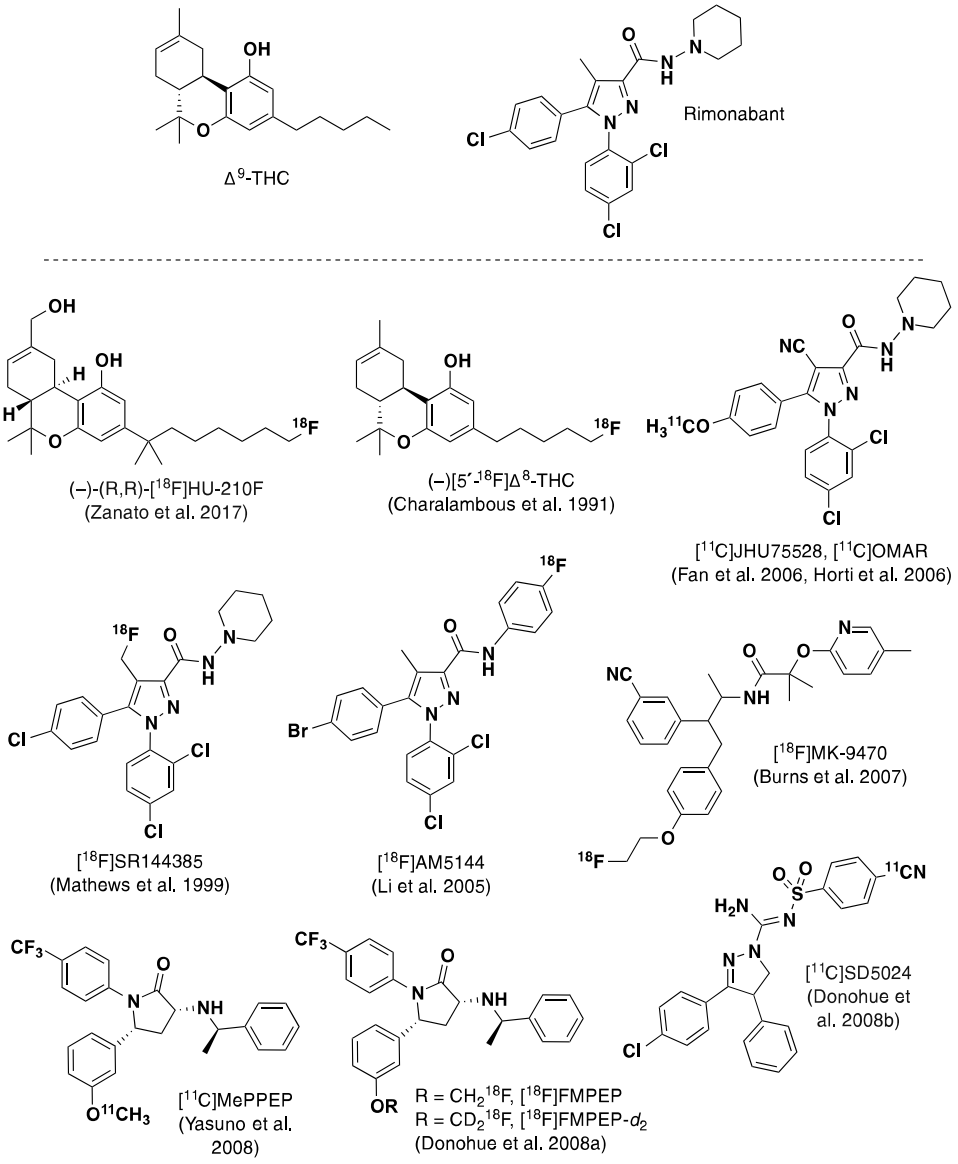

Figure 17. Examples of ^{11}C- and ^{18}F-labelled tracers for CB1R imaging in the CNS.

2.7 Clinical radiopharmaceutical production

One part of tracer and method development is translation of the method to clinical production according to GMP guidelines and national and regional regulations and guidelines. PET radiopharmaceuticals are defined as medicinal products and, thus, are legislated in directive 2001/83/EC (European Parliament and Council of the European Union 2001) in the European Union and in the Federal Food, Drug, and Cosmetic Act (Office of the Law Revision Counsel of the U.S. House of Representatives 2020) in the USA. "The rules governing medicinal products in the European Union", EudraLex volume 4, contains the guidelines for GMP production of medicinal products for human and veterinary use (European Commission 1991), whereas Annex 3 contains the guidelines for radiopharmaceutical production (European Commission 2008) and Annex 15 the guidelines for validation and qualification (European Commission 2015). In addition to regional and national regulators, various organizations have separate GMP guidelines, including European Association of Nuclear Medicine (EANM), European Medicines Agency (EMA), International Council for Harmonisation of Technical Requirements for Pharmaceuticals for Human Use (ICH), Pharmaceutical Inspection Convention and Pharmaceutical Inspection Co-operation Scheme (PIC/S), and the World Health Organization (WHO). The web of regulations for radiopharmaceutical production is broad, but Lange et al. (2015) published an overview of the European regulations and guidelines. In addition to clinical safety, radiopharmaceuticals are radioactive substances and, as such, are regulated in the radiation safety legislation and guidelines. All of these regulations set a starting point for production facilities, storage systems, and personnel.

Translation of a production method to clinical radiopharmaceutical production requires a validated synthesis procedure and validated analytical methods using qualified synthesis and analytical devices. Before synthesis procedure validation, in addition to the radiochemical synthesis procedure, the purification method and the formulation method that allows the intravenous administration of the radiopharmaceutical in humans need to be developed. Before analytical methods validation, the analytical methods need to be developed. EANM has published practice-oriented guidelines for radiopharmaceutical production, such as Good Radiopharmacy Practice (GRPP) guidelines (Elsinga et al. 2010, Aerts et al. 2014) and validation and qualification guidelines (Todde et al. 2017). Guidelines for validation of analytical procedures have been published by the ICH (International Council for Harmonisation of Technical Requirements for Pharmaceuticals for Human Use 2005), and practice-oriented guidelines by EANM (Gillings et al. 2020).

3 Aims of the study

The aim of this thesis work was to explore and develop ^{18}F-fluorination methods utilising transition metal-mediated ^{18}F-fluorination with copper and ruthenium and nucleophilic ^{18}F-fluoroalkylation.

The following aims were set:

I – II To investigate and improve copper-mediated ^{18}F-fluorination using two different [^{18}F]fluoride drying approaches:

- I Azeotropic distillation with subsequent synthesis of [^{18}F]NS12137 and [^{18}F]CFT.
- II Solid phase extraction with subsequent synthesis of certain model molecules, as well as [^{18}F]NS12137 and [^{18}F]CFT.

III To utilise ruthenium-mediated ^{18}F-fluorination in the production of a new CB_1 receptor imaging agent, [^{18}F]FPATPP, and evaluate its utility as a PET imaging agent in mice.

IV To develop an automated synthesis procedure for the production of [^{18}F]FMPEP-d_2 according to GMP and follow the long-term GMP production of the tracer.

4 Materials and Methods

4.1 General

All of the specific details concerning the reagents and chemicals, materials, and instrumentation used in the production of radiotracers, as well as specific synthesis details and preclinical evaluation details, are described in the original papers (I – IV).

4.2 Production and activation of [^{18}F]fluoride (I – IV)

4.2.1 Production of [^{18}F]fluoride (I – IV)

[^{18}F]Fluoride was produced with a CC-18/9 cyclotron (Efremov Institute of Electrophysical Apparatuses, St. Petersburg, Russia; studies I, III, and IV) or a TR-19 cyclotron (Advanced Cyclotron Systems, Inc., Richmond, British Columbia, Canada; studies I – IV).

With the CC-18/9 cyclotron, oxygen-18-enriched water (2.2 mL, 98%, Rotem Industries Ltd, Medical Imaging, Dimona, Israel) was irradiated with 17 MeV protons and 40 μA beam current in an in-house constructed niobium target equipped with a 25-μm-thick stainless steel window (AISI 321, Goodfellow Cambridge Ltd., Huntingdon, England). The irradiated target water was trapped in a carbonated QMA cartridge preconditioned with 10 mL of ultrapure (18 MΩ) water. [^{18}F]Fluoride was eluted from the cartridge with potassium carbonate solution (1.5 mL, 3 mg/mL) and transferred to the synthesis device via polyether ether ketone (PEEK) tubing (studies I, III, IV). The line was flushed three times with MeCN (1 mL/portion).

With the TR-19 cyclotron, oxygen-18-enriched water (3.7 mL) was irradiated with 17 MeV protons and 40 μA beam current in an niobium target equipped with a 25-μm-thick Havar foil (Advanced Cyclotron Systems Inc.). Aqueous [^{18}F]fluoride was transferred straight to the synthesis device via polypropylene/polyethylene tubing (studies II and III) or first trapped in a QMA cartridge and eluted as [^{18}F]KF solution and transferred to the synthesis device via PEEK tubing (studies I, III, and IV).

4.2.2 [^{18}F]Fluoride activation (I – IV)

Two different [^{18}F]fluoride activation approaches were utilised: 1) azeotropic distillation with MeCN and 2) solid phase extraction. Azeotropic distillation was utilised in studies I, III, and IV and the SPE method in studies II and III.

Azeotropic distillation (I, III, IV)

In the azeotropic distillation method, K_{222} was added to the aqueous [^{18}F]KF solution and the solution dried by azeotropic distillation with MeCN at 120 °C under He flow and reduced pressure. Two additional portions of MeCN (1 mL/portion) were added and the solvent evaporated to dryness to form dry K_{222}/[^{18}F]KF complex.

Solid phase extraction (II, III)

In the SPE approach, the aqueous [^{18}F]fluoride was trapped in a pre-activated SPE cartridge. The cartridge was washed with suitable organic solvent prior to [^{18}F]fluoride elution with appropriate eluting agent. [^{18}F]Fluoride recovery was maximized by loading and washing the cartridges from the female Luer side and eluting from the male Luer side (Figure 18).

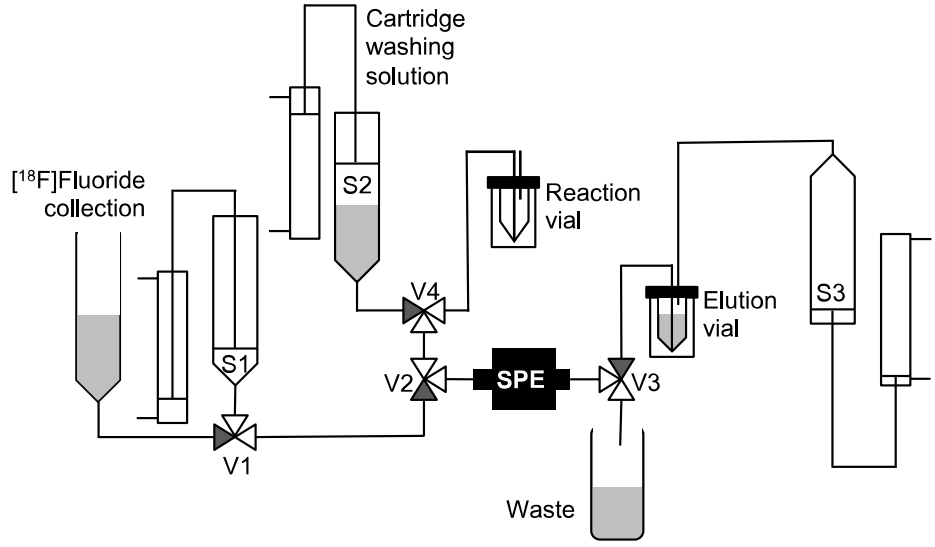

Figure 18. Technical diagram of the solid phase extraction device used for [^{18}F]fluoride activation and solvent exchange.

In study II, the elution conditions were optimised and we evaluated 10 mg QMA (Waters Corporation, Milford, MA, USA), 130 mg QMA (Waters Corp.), 46 mg

carbonated QMA (Waters Corp.), and 45 mg PS-HCO_3 (Synthra, Hamburg, Germany) cartridges. The cartridges were preconditioned with 1) water, 2) 0.5 M LiOTf and water, or 3) Na_2SO_4 and water. After trapping [^{18}F]fluoride, the cartridge was washed with DMA and [^{18}F]fluoride subsequently eluted into the reaction vessel with copper complex ($Cu(OTf)_2(py)_4$ or $Cu(OTf)_2$) and an additional eluting agent (LiOTf). The amount of copper complex varied from 12 to 96 μmol. As a control, elution was performed using only LiOTf as an eluting agent. Elution speed varied from slow (approx. 0.5 mL/min) to fast (approx. 5 mL/min).

In study III, aqueous [^{18}F]fluoride was trapped in a PS-HCO_3 cartridge (Synthra) pre-conditioned with potassium oxalate (10 mg/mL) and water. The cartridge was washed with MeCN, and [^{18}F]fluoride was eluted with a mixture containing the precursor, Ru-complex, and imidazolium chloride. The cartridge was then rinsed with DMSO and MeCN. In the base-added SPE method, K_2CO_3 (2 eq.) was added to the DMSO used for cartridge rinsing.

The terms elution efficiency and [^{18}F]fluoride recovery are used when discussing the capability of the cartridge to trap [^{18}F]fluoride and the eluting agent to elute [^{18}F]fluoride; elution efficiency discloses the efficiency of the eluting agent to elute [^{18}F]fluoride from the cartridge, and [^{18}F]fluoride recovery provides information about the ability of the cartridge to trap [^{18}F]fluoride and the eluting agent's ability to elute it. Elution efficiency is calculated by dividing the eluted radioactivity by the radioactivity of the cartridge before elution (eluted radioactivity + leftover radioactivity in the cartridge). [^{18}F]Fluoride recovery is calculated by dividing the eluted radioactivity by the radioactivity loaded into the cartridge (eluted radioactivity + leftover radioactivity in the cartridge + radioactivity in the waste after loading and washing the cartridge).

4.3 Chromatographic methods (I – IV)

4.3.1 HPLC methods (I – IV)

Synthesised radiotracers were purified and analysed by radioHPLC. The HPLC methods used in studies I – IV are specified in Table 3. Semi-preparative radioHPLC purifications were performed using a Jasco PU-2089 HPLC pump (Jasco, Inc., Easton, Maryland, USA) or a Merck-Hitachi L-6200 HPLC pump (Merck AG, Darmstadt, Germany). Purification was followed with a miniature Geiger-Müller tube placed at the column outlet. Analytical radioHPLC runs were performed with VWR Hitachi L-2000 series HPLC pumps (VWR Hitachi, VWR International GmbH, Darmstadt, Germany) and followed with a VWR Hitachi L-2400 UV-absorption detector and a 2×2-inch NaI radioactivity detector.

Table 3. Semi-preparative and analytical HPLC methods.

Study	Compound	Column	Method	Flow [ml/min]	λ [nm]
I, II	[^{18}F]NS12137 intermediate (analytical)	Luna C5, 5 µm, 4.6 × 150 mm	A: 0.1% TFA B: 0.1% TFA in MeCN 0-3 min 80% A 3-3.1 min 80-40% A 3.1-15 min 40% A	1.5	230
I, II	[^{18}F]NS12137 (preparative)	Gemini C18, 5 µm, 10 × 250 mm	A: 7 mM KH_2PO_4 B: MeCN 0-5 min 100% A 5-5.1 min 100-92% A 5.1-36 min 92% A	5.0	-
I, II	[^{18}F]NS12137 (analytical)	Gemini C18, 110 Å, 5 µm 4.6 × 250 mm	A: 7 mM KH_2PO_4 B: MeCN 0-5 min 100% A 5-5.1 min 100-92% A 5.1-20 min 92% A	1.5	230
II	[^{18}F]CFT (preparative)	Gemini NX C18 110 Å, 5 µm 10 × 250 mm	A: 7 mM KH_2PO_4 B: MeCN 0-5 min 100% A 5-20 min 100 to 20% A	5.0	-
II	[^{18}F]CFT (analytical)	Gemini C18 110 Å, 5 µm 4.6 × 250 mm	A: 7 mM KH_2PO_4 B: MeCN 0-8 min 100% A 8-16 min 100-50% A 16-22 min 50% A	1.5	215
III, IV	[^{18}F]FPATPP [^{18}F]FMPEP-d_2 (preparative)	Luna C18(2), 10 µm 10 × 250 mm	57/43 1% TFA/MeCN + ascorbic acid (500 mg/L)	8.0	-
III	[^{18}F]FPATPP (analytical)	Luna C5, 5 µm 4.6 × 150 mm	55/45 0.1% TFA/MeCN	0.95	254
IV	[^{18}F]FMPEP-d_2 (analytical)	Luna C18(2), 3 µm, 4.6 × 100 mm	55/45 0.1% TFA/MeCN	0.95	254

4.3.2 GC methods (IV)

Semi-preparative gas chromatography (GC) was used for the purification of [^{18}F]bromofluoromethane-d_2 in study IV. The GC system was an integral part of the [^{18}F]FMPEP-d_2 synthesis device. An on-line installed GC column was conditioned at 170 °C prior to the synthesis and maintained at 90 °C during the separation. Helium was used as a carrier gas. The GC column was in-house-filled with Haysep Q or Porapak Q polymer adsorbent (Supelco, Inc., Bellefonte, PA, USA).

An Agilent 7820A gas chromatograph equipped with a flame ionization detector (Agilent Technologies, Santa Clara, CA, USA) was used for residual solvent analysis in [^{18}F]FMPEP-d_2 QC with Agilent standard parameters according to USP method 467 (United States Pharmacopoeia 2020).

4.3.3 ICP-MS (I – III)

Inductively coupled plasma mass spectrometry (ICP-MS, Elan DRC Plus; PerkinElmer Inc., Waltham, MA, USA) was used to analyse the residual Cu, Sn, and Ru from the end-product fractions. The instrument was calibrated with commercial multi-element standards.

4.3.4 SPE methods (I – IV)

In addition to the activation of [^{18}F]fluoride, SPE was used for solvent exchange during tracer production. The cartridges were loaded and washed from the female Luer side and eluted from the male Luer side as presented in Figure 18.

In studies I and II, a tC18 Sep-Pak cartridge (Waters Corp.) was used for the solvent exchange from DMA to THF. The cartridge was preconditioned with ethanol (5 mL) and water (10 mL). Tracer was eluted with THF (1 mL). Here, incorporation of [^{18}F]fluoride was calculated as [^{18}F]fluoride recovery as presented in section 4.2.2.

In studies III and IV, a C18 Plus Light Sep-Pak cartridge (Waters Corp.) was used for formulation of the tracer for injection. The cartridge was preconditioned with ethanol (7 mL) and water (10 mL) and, after loading, was washed with water (20 mL, study III) or 100 mg/mL ascorbic acid (20 mL, study IV). In study III, the tracer was eluted with ethanol (300 µL), followed by 9 mg/mL NaCl (2.7 mL); in study IV, the tracer was eluted with ethanol (1 mL).

4.4 Copper-mediated ^{18}F-labelling (I, II)

4.4.1 Synthesis of model molecules (II)

As a proof of concept, the following model molecules were produced with [^{18}F]fluoride activated using the SPE approach: 1-[^{18}F]fluoro-4-iodobenzene, 4-[^{18}F]fluorobiphenyl, 4-[^{18}F]fluorophenol, [^{18}F]fluorobenzene, 4-[^{18}F]fluorobenzonitrile, 1-[^{18}F]fluoro-4-nitrobenzene, 3-[^{18}F]fluoropyridine, 2-[^{18}F]fluoronaphthalene, and 4-[^{18}F]fluoroindole. [^{18}F]Fluoride was eluted from the anion exchange cartridge with copper complex using optimised conditions straight into the reaction vial containing the boronic acid or boronic ester precursor. Reactions were heated at 120 °C for 5 – 15 minutes. The radiolabelling reactions were followed by radioHPLC.

4.4.2 [^{18}F]NS12137 (I, II)

Two approaches were used in the copper-mediated ^{18}F-labelling of [^{18}F]NS12137 as presented in Figure 19. With the azeotropic distillation approach (study I), $Cu(OTf)_2(py)_4$ in MeCN or DMA was added to the reaction vessel containing the dry K_{222}/[^{18}F]KF complex. The reaction was mixed at RT prior to addition of the NS12137 stannyl precursor. The reaction was heated at 70 – 120 °C for up to 20 min and followed by radioHPLC. During the radiofluorination optimisation study, the *tert*-butoxycarbonyl protection was not removed.

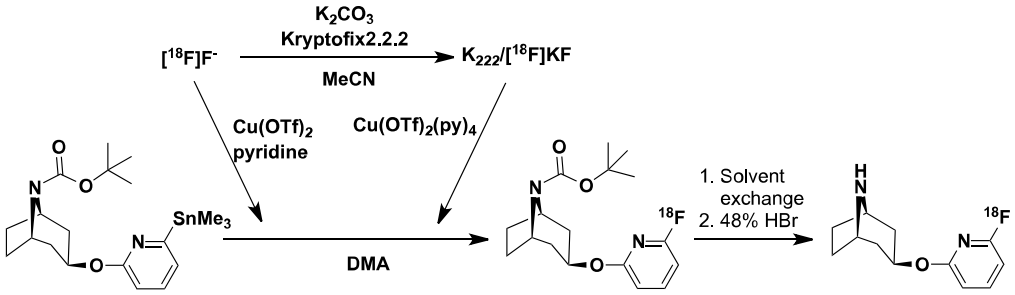

Figure 19. Cu-mediated synthesis of [^{18}F]NS12137.

Using the SPE approach (study II), [^{18}F]fluoride was eluted with copper complex straight into the reaction vial containing the precursor and the reaction heated at 120 °C for 5 to 15 minutes. The radiolabelling reactions were followed by radioHPLC. With both approaches, solvent was exchanged and subsequently evaporated to dryness prior to deprotection with HBr at RT or 80 °C. After deprotection, the reaction mixture was diluted and purified by semi-preparative HPLC.

4.4.3 Synthesis of [^{18}F]CFT (II, unpublished)

Three approaches were utilised for the production of [^{18}F]CFT (Figure 20). With the azeotropic distillation approach (unpublished), $Cu(OTf)_2(py)_4$ in DMA was added to the reaction vessel containing the dry K_{222}/[^{18}F]KF complex. The reaction was mixed at RT. Stannyl precursor was added and the mixture heated at 120 – 160 °C for up to 40 min.

In the SPE approach (study II), [^{18}F]fluoride was eluted with copper complex straight into the reaction vial containing the precursor and the reaction heated at 120 °C for up to 15 minutes. Reactions were followed by radioHPLC. After the reaction, the reaction mixture was diluted and purified by semi-preparative HPLC.

In the third approach, [^{18}F]CFT was produced with [^{18}F]Selectfluor *bis*(triflate) at RT or by heating at 40 – 80 °C for up to 40 min (unpublished). [^{18}F]Selectfluor *bis*(triflate) was produced from post-target-produced [^{18}F]F_2 as previously reported (Teare et al. 2010).

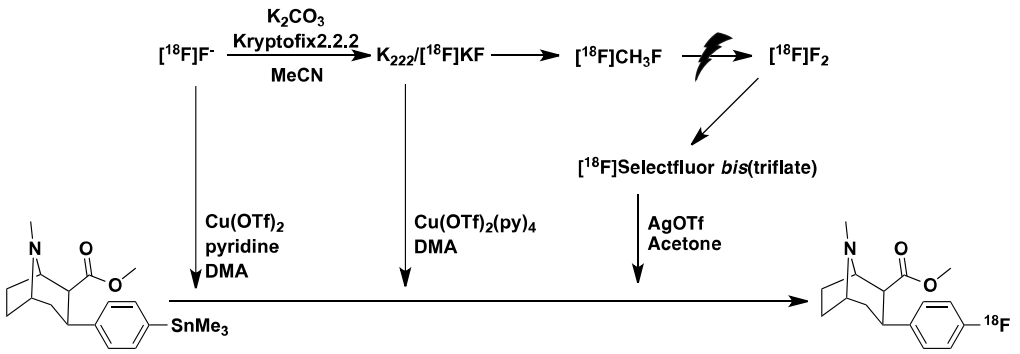

Figure 20. Synthesis of [^{18}F]CFT using Cu-mediated or AgOTf-mediated pathways.

4.5 Ruthenium-mediated ^{18}F-labelling (III)

4.5.1 Synthesis of reference standard for [^{18}F]FPATPP

Reference standard (3*R*,5*R*)-5-(3-fluorophenyl)-3-[(*R*)-1-phenylethylamino]-1-(4-trifluoromethylphenyl)-pyrrolidin-2-one was synthesised following the original precursor synthesis of FMPEP (Donohue et al. 2008a).

4.5.2 Synthesis of [^{18}F]FPATPP

A previously published Ru-mediated ^{18}F-labelling protocol was followed and further optimised in the synthesis of [^{18}F]FPATPP (Figure 21) (Beyzavi et al. 2017, Rickmeier & Ritter 2018). Before the radiosynthesis, phenol precursor and ruthenium complex (3.5 eq) were mixed at 80 °C for 30 minutes. 1,3-Bis(2,6-diisopropylphenyl)-imidazolium chloride was added to the mixture to produce the precursor mixture.

In the azeotropic distillation pathway, the reaction vessel containing dry K_{222}/[^{18}F]KF complex was allowed to cool before adding the precursor mixture. In the SPE pathway, [^{18}F]fluoride was eluted into the reaction vessel with the precursor mixture. The reaction mixture was heated at 100 °C, 130 °C, or 160 °C for 30 min. The reaction was followed by radioHPLC. For preclinical evaluation, [^{18}F]FPATPP was purified by semi-preparative HPLC and formulated for injection.

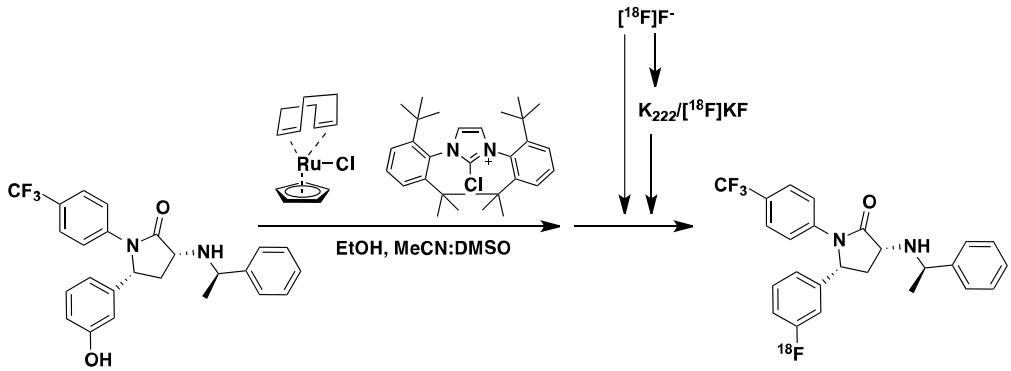

Figure 21. Ru-mediated synthesis of [^{18}F]FPATPP.

4.5.3 Preclinical evaluation of [^{18}F]FPATPP and [^{18}F]FMPEP-d_2 (III, unpublished)

Healthy wild-type (WT) mice were used for preclinical evaluation of [^{18}F]FPATPP and [^{18}F]FMPEP-d_2 as specified in Table 4. The experiments were conducted under the guidelines of the International Council of Laboratory Animal Science, and the study was approved by the Finnish National Animal Experiment Board.

Table 4. Animals used for preclinical evaluation of [^{18}F]FPATPP and [^{18}F]FMPEP-d_2 in study III.

Tracer	n	Age [mo]	Gender	Weight [g]	Study	Time points [min]
[^{18}F]FPATPP	12	2	m	25 ± 1	*Ex vivo* autoradiography, biodistribution and metabolite analysis Blocking	30 (n=4) 60 (n=2) 120 (n=6, 1 bl*)
[^{18}F]FPATPP	6	4 – 5	4 m 2 f	32 ± 4	*In vivo* PET *Ex vivo* autoradiography and biodistribution Blocking (n=3, 1 f)	120
[^{18}F]FMPEP-d_2	7	3 – 4	m	33 ± 5	*Ex vivo* biodistribution	30 (n=3) 60 (n=4)
[^{18}F]FMPEP-d_2	12	1.5 – 6	7 m, 5 f	27 ± 7	*Ex vivo* biodistribution	120 (n=12)

*unpublished; bl, blocking

In vivo brain imaging (III)

In vivo experiments were performed using an Inveon Multimodality PET/CT (computed tomography) scanner (Siemens Medical Solutions USA, Knoxville, TN) for anaesthetized (2.5% isoflurane/oxygen) mice. The 120-min dynamic PET scans were initiated simultaneously with tracer injection into the mouse tail vein (injected dose 4.0 ± 0.4 MBq; injected mass 56 ± 25 ng). CT data were used for attenuation correction of the PET images. PET images were co-registered to their corresponding CT images aligned with the average mouse CT template or MRI template. Volumes of interest (VOIs) were the whole brain, neocortex, and hippocampus, and the standardized uptake values (SUVs) were obtained from the VOIs.

Ex vivo brain autoradiography and biodistribution (III)

[^{18}F]FPATPP (injected dose 7.0 ± 3.0 MBq; injected mass 160 ± 60 ng) was used for *ex vivo* brain autoradiography and biodistribution studies. [^{18}F]FMPEP-d_2 (injected dose 2.1 ± 1.0 MBq; injected mass 2.5 ± 1.3 ng) was used for the *ex vivo* biodistribution study. Mice were sacrificed 30, 60, or 120 min post-injection (p.i.) by cardiac puncture in deep anaesthesia.

For biodistribution, organs of interest were dissected and measured using a 2480 Wizard Gamma Counter (Wallac PerkinElmer, Turku, Finland). For autoradiography, frozen brain slices (20 µm) were exposed on an imaging plate for 2 half-lives. The plates were scanned by a Fuji BAS5000 phosphoimager (FUJIFILM Life Science, Stamford, Connecticut, USA). The Aida 4 program (Raytest Isotopenmessgeräte GmbH, Straubenhardt, Germany) was used to analyse the images. Regions of interest (ROIs) were drawn in the parietotemporal cortex, striatum, frontal cortex, hippocampus, cerebellar grey matter, globus pallidus, and thalamus. The thalamus was used as a reference region when quantifying the autoradiography.

Specificity study (III)

A blocking study with rimonabant was conducted to demonstrate the specificity of [^{18}F]FPATPP for CB1Rs. Rimonabant is a CB1R antagonist. Mice (n=3) were given rimonabant (2 mg/kg in 10% EtOH in Kleptose β-cyclodextrin) in the tail vein 10 min prior to the tracer injection. Control mice (n=3) were given vehicle (10% EtOH in Kleptose β-cyclodextrin).

Metabolite analysis (III, unpublished)

Extracted brain and plasma samples were applied to HPTLC silica gel 60 RP-18 plates and the plates developed in 40/60 1% TFA/MeCN. The TLC plates were exposed on imaging plates for 2 half-lives and the imaging plates scanned using the Fuji BAS5000

phosphoimager (FUJIFILM Life Science). Images were analysed using Aida 4 (Raytest Isotopenmessgeräte GmbH).

4.6 GMP production of [^{18}F]FMPEP-d_2 (IV)

4.6.1 [^{18}F]FMPEP-d_2 synthesis

[^{18}F]FMPEP-d_2 was synthesised in two steps (Figure 22) using a fully automated in-house-built synthesis device. The device consists of PEEK tubing, pneumatic and electric multi-port valves, a Teflon membrane pump, heaters, a GC column, an injector for HPLC, and a semi-preparative HPLC column. A separate sterile filtration unit was attached to the synthesis device. These devices were controlled by an in-house-built control system. The synthesis procedure was adapted from the original publication by Donohue et al. (2008a). Compared to the original process, the reaction conditions and purification processes were optimised. The step-by-step synthesis procedure is included in paper IV.

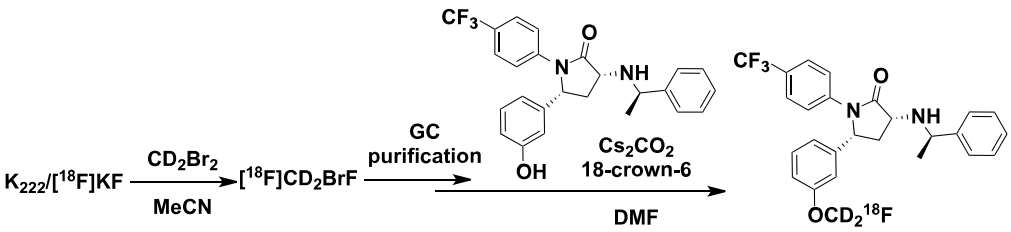

Figure 22. Nucleophilic synthesis of [^{18}F]FMPEP-d_2.

Aqueous [^{18}F]fluoride was activated by azeotropic distillation with MeCN. Deuterated dibromomethane in MeCN was added to dry K_{222}/[^{18}F]KF complex. The reaction mixture was heated at 90 °C for 5 min and the resulting [^{18}F]bromofluoromethane-d_2 purified by online GC. Subsequent nucleophilic ^{18}F-fluoroalkylation reaction was carried out at 80 or 110 °C for 5 or 10 min. [^{18}F]FMPEP-d_2 was diluted and purified by semi-preparative HPLC prior to formulation for injection.

4.6.2 [^{18}F]FMPEP-d_2 quality control

QC tests were performed for [^{18}F]FMPEP-d_2 following the EudraLex GMP guidelines and are specified in Table 10. Details for HPLC are in section 4.3.1 and details for GC analysis are in section 4.3.2. Bacterial endotoxins and sterility were analysed by a contract research organization (CRO).

Table 5. Quality control tests for [^{18}F]FMPEP-d_2 and the batch category in which each test is performed.

Test	Test method	Acceptance criteria	Validation	QC	Clinical
Appearance	Visual check	A clear and colourless solution, free of particles	x	x	x
Radiochemical identity	HPLC	R_t([^{18}F]FMPEP-d_2) = R_t(FMPEP) ± 0.5 min	x	x	x
Radioactivity	Dose calibrator	The injection contains ≥90.0% and ≤110.0% of the declared fluorine-18 radioactivity at the date and time stated on the delivery sheet	x	x	x
Radiochemical purity (RCP)	HPLC	The fluorine-18 radioactivity in the form [^{18}F]FMPEP-d_2 is ≥95.0%	x	x	x
Radionuclidic identity	Dose calibrator	Half-life of 105–115 min	x		
Radionuclidic purity	HPGe detector	≥99.9% of the radioactivity corresponds to fluorine-18	x		
Chemical purity (CP)	HPLC	The combined mass of FMPEP-d_2 and any relevant organic (UV-absorbing) impurities are ≤10.0 µg/max injected dose (max V_{INJ})	x	x	x
Residual solvents	GC	MeCN ≤410 ppm* DMF ≤880 ppm*	x		
Content of ethanol	GC	The end product contains ≤10%*	x		
pH	pH strip	4.0 – 7.5	x	x	x
Bacterial endotoxins	Ph. Eur.	<17.5 IU/mL	x	x	
Sterility	Ph. Eur.	Sterile	x	x	
Shelf life	CP, RCP and pH	-	x		
Sterile filter integrity	Pressure hold test	Relative pressure decrease (RPD) <10%	x	x	x

*International Council for Harmonisation of Technical Requirements for Pharmaceuticals for Human Use (2016)
Validation refers to process validation batches, QC refers to separate batches for quality control, and clinical refers to batches for clinical use.

4.6.3 Validation of the analytical methods

The analytical HPLC method and analytical GC method were validated in accordance with the guidelines of Turku PET Centre and the International Council for Harmonisation of Technical Requirements for Pharmaceuticals for Human Use (ICH Q2(R1) 2005). The HPLC method was used for identity, radiochemical purity (RCP), and chemical purity (CP) determination, and the GC method for residual solvent

analysis. Radiochemical identity was determined by the external reference standard. Validated parameters for RCP determination were specificity and limit of detection. Validated parameters for CP determination were specificity, linearity, repeatability, accuracy, range, and robustness. For the GC method, the specificity and limit of detection were validated.

4.6.4 Validation of the synthesis procedure

Process validation was conducted to confirm the reliability and reproductivity of the [^{18}F]FMPEP-d_2 synthesis process. Validation was executed according to the Turku PET Centre Validation Master Plan and EudraLex GMP guidelines (European Commission 2008, 2015). Three consecutive batches of [^{18}F]FMPEP-d_2 were produced according to the approved synthesis method and the batches analysed using the validated analytical methods. QC tests (see section 4.6.2) were performed for the end product at the end of synthesis (EOS). For shelf-life determination, radioHPLC analysis and pH measurements were performed at EOS + 60 min, EOS + 120 min, and EOS + 180 min.

In addition to the three consecutive batches, a batch of [^{18}F]FMPEP-d_2 was produced without sterile filtration for bioburden verification. Sterility and endotoxins were tested from process validation batches by a CRO.

4.7 Statistical analyses (I – IV)

In studies I – IV, all values were expressed as mean ± standard deviation (SD) when $n \geq 2$. Statistical analyses were performed using GraphPad Prism 6.0 (GraphPad Software, San Diego, CA USA). Differences were considered to be significant when $p<0.05$. In study III, statistical analyses of the *ex vivo* brain autoradiography were performed using the Mann-Whitney U test.

5 Results

5.1 Copper-mediated ^{18}F-labelling (I, II)

5.1.1 Activation of [^{18}F]fluoride with copper (II)

Activation of aqueous [^{18}F]fluoride was effective with various SPE cartridges. [^{18}F]Fluoride was satisfactorily eluted from these cartridges using $Cu(OTf)_2$ or $Cu(OTf)_2(py)_4$ and additional LiOTf as the eluting agent. Results from the [^{18}F]fluoride elution study are shown in Figure 23. As seen in Figure 23A, addition of LiOTf to the preconditioning and elution steps had a prominent effect on [^{18}F]fluoride recovery when using $Cu(OTf)_2(py)_4$ as the eluting agent. Addition of LiOTf enhanced the [^{18}F]fluoride recovery from 40.1 ± 0.0% to 60.3 ± 2.7% with 130 mg QMA cartridges and from 25.3 ± 5.3% to 42.7 ± 4.4% with 46 mg carbonated QMA cartridges. When Na_2SO_4 was used as the preconditioning agent instead of LiOTf, [^{18}F]fluoride recovery decreased drastically from 41.8 ± 5.2% to 0.6 ± 0.1% with the 46 mg carbonated QMA cartridge. Using only LiOTf as eluting agent did not elute [^{18}F]fluoride from the cartridge.

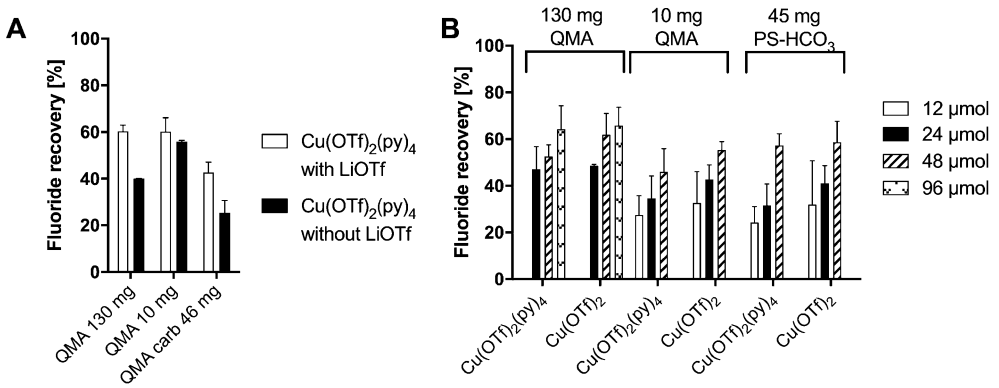

Figure 23. A) Effect of LiOTf and B) the amount of copper complex on [^{18}F]fluoride recovery.

Varying the amount of eluting agent, $Cu(OTf)_2(py)_4$ or $Cu(OTf)_2$, resulted in notable differences in the [^{18}F]fluoride recovery (Figure 23B). The highest [^{18}F]fluoride recovery, 65.8 ± 7.9%, was obtained with the 130 mg QMA cartridge using 96 µmol of $Cu(OTf)_2$, and the lowest, 24.2 ± 6.8%, with the PS-HCO_3 cartridge with 12 µmol of $Cu(OTf)_2(py)_4$. The 130 mg QMA cartridge with LiOTf preconditioning and $Cu(OTf)_2$ (48 µmol) elution was determined to be optimal and used in the subsequent ^{18}F-labelling tests.

5.1.2 Synthesis of model molecules (II)

Results from the ^{18}F-labelling reactions of model molecules when [^{18}F]fluoride was activated using the optimised SPE approach are shown in Table 6.

Table 6. Results from Cu-mediated ^{18}F-labelling of the model molecules (n=3).

	Leaving group on the precursor	RCY* after a 5 min reaction [%]	RCY* after a 15 min reaction [%]
1-[^{18}F]fluoro-4-iodobenzene	boronic acid	33.0 ± 7.6	45.7 ± 8.5
4-[^{18}F]fluorobiphenyl	boronic acid	51.1 ± 6.7	59.4 ± 6.7
4-[^{18}F]fluorophenol	boronic acid	20.0 ± 3.8	36.6 ± 15
[^{18}F]fluorobenzene	boronic acid	58.0 ± 8.1	63.5 ± 8.4
4-[^{18}F]fluorobenzonitrile	boronic acid	80.9 ± 4.0	86.5 ± 3.3
1-[^{18}F]fluoro-4-nitrobenzene	boronic acid	60.9 ± 12	76.5 ± 14
3-[^{18}F]fluoropyridine,	boronic acid	<15 (n=2)	-
2-[^{18}F]fluoronaphthalene	boronic acid	80.6 ± 10	82.4 ± 1.7
4-[^{18}F]fluoroindole	boronic ester	90.5 ± 2.1	91.6 ± 0.5

*Based on the HPLC analysis of the crude reaction mixture.

5.1.3 Synthesis of [^{18}F]NS12137 (I, II)

[^{18}F]NS12137 radiofluorination conditions were optimised in study I. Varying the reaction solvent, the molar amount of precursor and copper complex, or temperature had a significant effect on the reaction yield. However, varying the amount of base or changing the pre-reaction mixing times and solvents did not have a significant effect on the RCY.

Almost no reaction occurred when the reaction was carried out in MeCN. Changing the reaction solvent from MeCN to DMA increased the RCY (based on HPLC) from 0.5% to >85%. Increasing the amount of precursor from 2 µmol to 8 µmol while maintaining the amount of Cu complex at 3 equivalents increased the RCY (based on

HPLC) from 8% to 76%. Further increasing the molar amount of reagent did not have a significant effect on the reaction yield. Increasing the temperature from RT to 70 °C, and further to 120 °C, increased the RCY (based on HPLC) after 5 min of reaction from 2.9 ± 0.1% to 18.2 ± 1.6%, and then to 90.7 ± 3.3%, respectively. At 120 °C with 8 µmol of precursor (optimised conditions), 90% RCY was achieved after 1 min of reaction in DMA, and a longer reaction time (>5 min) increased the formation of side products according to radioHPLC (Figure 24A).

The optimised radiofluorination reaction conditions were used to produce [^{18}F]NS12137 with deprotection and semi-preparative HPLC purification steps. These results are shown in Table 7. The radioHPLC chromatograms of the reaction mixture after the radiofluorination reaction, the reaction mixture after deprotection, and the purified product are presented in Figure 24B.

Table 7. Results from the production of [^{18}F]NS12137.

	Azeotropic distillation approach (I)	**SPE approach (II)**
Reaction time [min]	2	5
RCY of the [^{18}F]NS12137 intermediate (based on HPLC) [%]	89.2 ± 1.3	96.3 ± 2.0
Incorporation of [^{18}F]fluoride according to SPE* [%]	23.7 ± 2.2	38 (n=1)
RCY [%]	15.1 ± 0.5	16.5 (n=1)
RCP [%]	97.5 ± 0.5	100 (n=1)
A_m [GBq/µmol]	300	-
Activity yield [GBq]	1.4 ± 0.2	0.3 (n=1)
Synthesis time [min]	100 ± 11	98 (n=1)
Amount of residual copper according to the ICP-MS analysis [µg]	< 0.25	3.9 (n=1)

*Radioactivity of the reaction vial before SPE was compared to the radioactivity eluted from the SPE cartridge

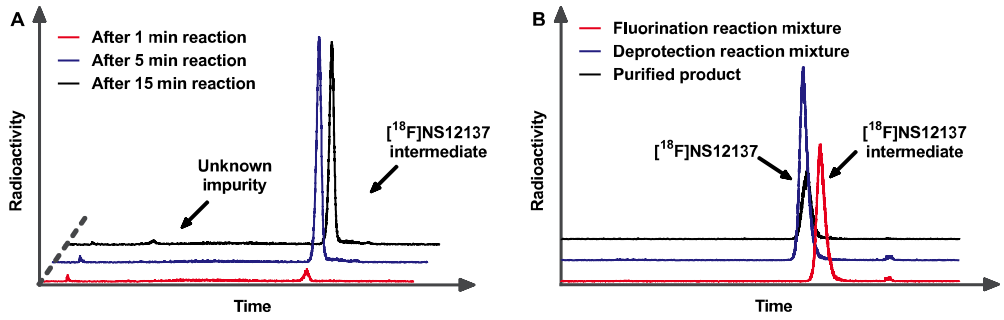

Figure 24. A) HPLC chromatograms of reaction solution after a 1-min, 5-min and 15-min reaction at 120 °C (approach I) and B) reaction solution after the ^{18}F-fluorination reaction (approach I), reaction solution after HBr deprotection, and purified product.

5.1.4 Synthesis of [^{18}F]CFT (II, unpublished)

Results from [^{18}F]CFT synthesis with Cu-mediated ^{18}F-labelling using the azeotropic distillation and SPE approaches, and electrophilic ^{18}F-labelling with [^{18}F]Selectfluor *bis*(triflate) are shown in Table 8.

Table 8. Results from the synthesis of [^{18}F]CFT.

	Azeotropic distillation approach (unpublished)		**SPE approach (II)**	**Electrophilic approach (unpublished)**		
Reaction time [min]	5		15	20		
Reaction solvent	DMA		DMA	acetone-d_6		MeCN
Reaction temperature [°C]	120	140	120	r.t.	40	80
RCY (based on HPLC) [%]	19	33	6.9	8	10	<1
RCY [%]	-		5.3	-		
RCP [%]	-		98.1	-		
A_m [GBq/µmol]	600*		-	16		
Activity yield [GBq]	-		0.2	-		
Synthesis time [min]	-		64	-		
Amount of residual copper according to the ICP-MS analysis [µg]	-		46.0	-		

*calculation was based on the amount of radioactivity eluted from the analytical HPLC column and the limit of detection value of the CFT reference (0.1 µg/mL)

5.2 Ruthenium-mediated ^{18}F-labelling (III)

5.2.1 Synthesis of [^{18}F]FPATPP

[^{18}F]FPATPP was successfully synthesised starting from a commercial phenol precursor using the SPE method or azeotropic distillation for the activation of aqueous [^{18}F]fluoride. The effect of the [^{18}F]fluoride activation method, reaction temperature, and the presence of base on the RCY were studied and the results shown in Figure 25.

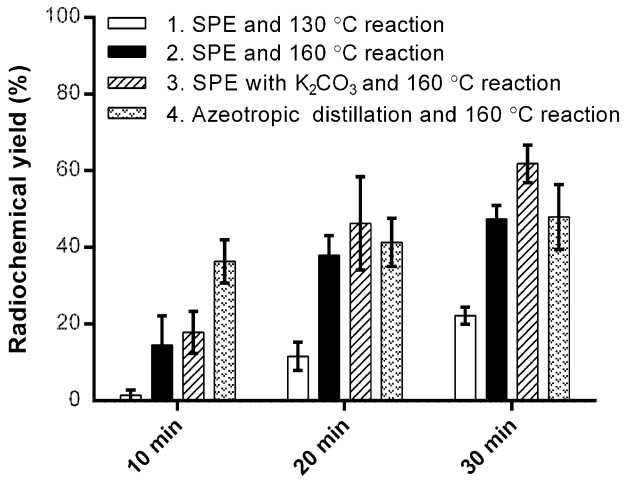

Figure 25. Results from the optimisation of [^{18}F]FPATPP reaction conditions.

With the SPE method, the elution efficiency was 93 ± 5% (III) and [^{18}F]fluoride recovery 80 ± 9% (unpublished). The reaction temperature significantly affected the RCY; no reaction occurred at 100 °C, and increasing the temperature from 130 to 160 °C increased the RCY (based on HPLC) after a 30-min reaction from 20.9 ± 0.3% to 47.4 ± 3.5%. At 100 °C and 130 °C, the main radioactive impurity was most likely [^{18}F]F-aryl ruthenium complex (Figure 26A-B). With the azeotropic distillation method, the RCY (based on HPLC) after 10 min at 160 °C was 36.3 ± 5.6%, which is considerably higher than the RCY with the SPE method after a 10-min reaction.

With the base-added SPE method, the RCY (based on HPLC) was 17.9 ± 5.5% after a 10-min reaction and 61.8 ± 4.9% (n=3) after a 30-min reaction at 160 °C. When [^{18}F]fluoride was activated via azeotropic distillation with MeCN or with the base-added SPE method, the formation of the proposed [^{18}F]F-aryl ruthenium complex was not observed (Figure 26C-D). For preclinical studies, [^{18}F]FPATPP was produced under the optimised conditions (30 min at 160 °C), and the results from these syntheses are shown in Table 9.

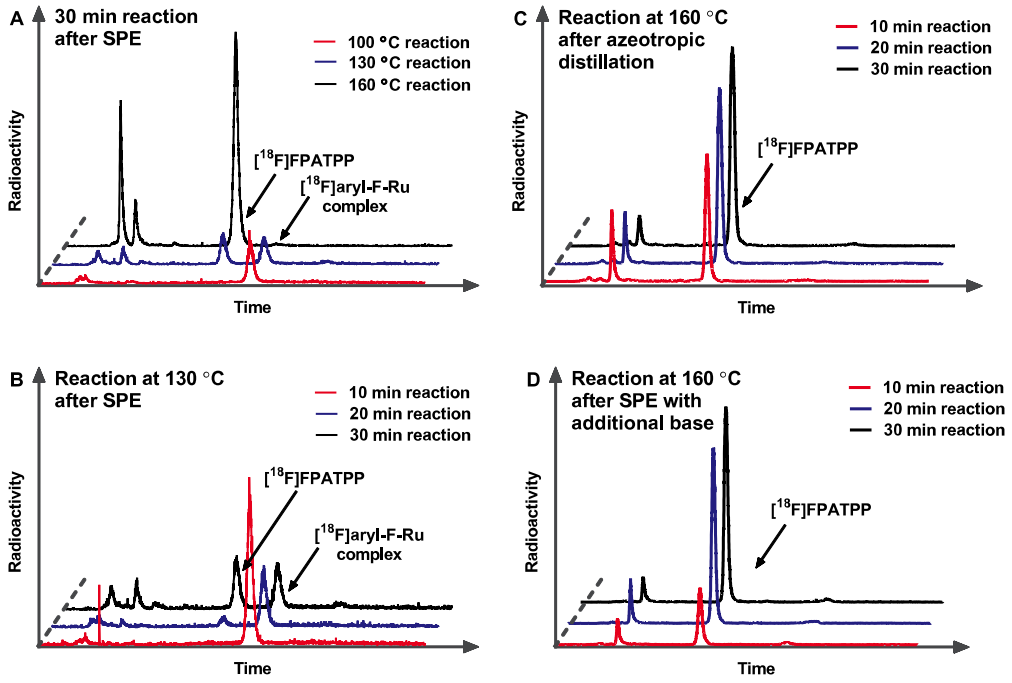

Figure 26. A) HPLC chromatograms of the radiofluorination reaction solutions A) after a 30-min reaction at 100 °C, 130 °C, and 160 °C; B) after a 10-min, 20-min, and 30-min reaction at 130 °C; C) after a 10-min, 20-min, and 30-min reaction at 160 °C after azeotropic distillation; and D) after a 10-min, 20-min, and 30-min reaction at 160 °C after using the SPE method with additional base.

Table 9. Results from the [^{18}F]FPATPP production for preclinical studies.

Starting activity	10.7 ± 3.3 GBq
Elution efficiency	93 ± 2%
[^{18}F]fluoride recovery (unpublished)	51 ± 6%
RCY (decay-corrected to EOB)	16.7 ± 5.7%
RCP at EOS	99.9 ± 0.1%
RCP at EOS + 5h (unpublished)	98.8 ± 0.6% (n=2)
A_m (decay-corrected to EOS)	>95 GBq/µmol (n=1)
Activity yield	1.0 ± 0.4 GBq
Synthesis time	87 ± 5 min
Amount of residual ruthenium	7.8 ± 1.8 µg/mL
End product volume	3 mL

5.2.2 Preclinical evaluation of [^{18}F]FPATPP

In vivo brain imaging

Maximal [^{18}F]FPATPP uptake was reached 30 min p.i., followed by clear washout (Figure 27). From 30 min to 120 min, the whole brain SUV decreased from 1.9 to 1.3. Blocking with rimonabant reduced the binding of [^{18}F]FPATPP by 58% for the whole brain.

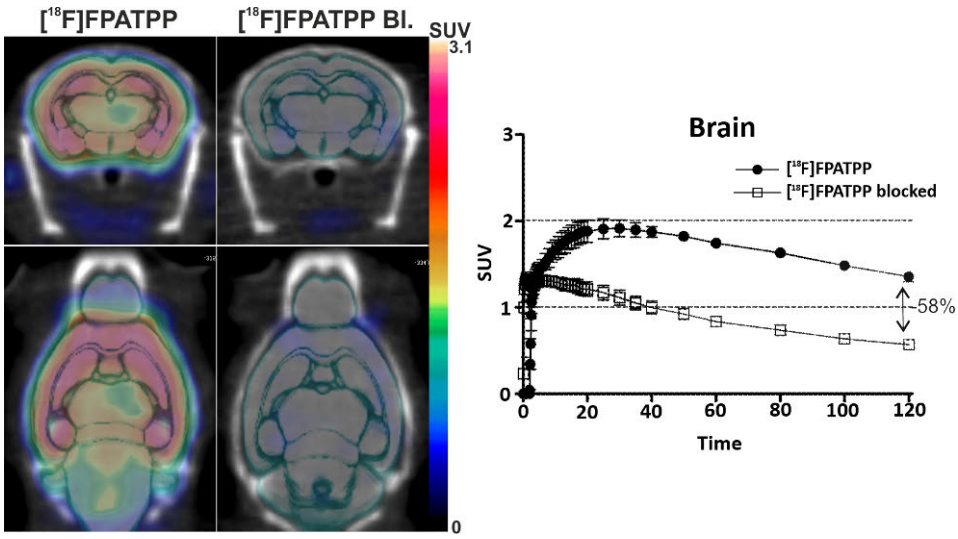

Figure 27. Left, PET/CT images (90 – 120 min) of [^{18}F]FPATPP in an adult mouse brain with vehicle or 2 mg/kg rimonabant overlaid with the MRI template. Right, time-activity curve for the whole brain at baseline or with rimonabant blocking and their percentage difference 120 min post-injection.

Ex vivo brain autoradiography

[^{18}F]FPATPP exhibited specific binding to the parietotemporal cortex, striatum, frontal cortex, hippocampus, cortex and cerebellar grey matter, and globus pallidus (Figure 28); region-to-thalamus ratios were 2.3, 2.8, 2.5, 2.6, 3.7, and 4.9, respectively ($p < 0.001$). Blocking with 2 mg/kg rimonabant significantly reduced the binding of [^{18}F]FPATPP and reduced the region-to-thalamus ratios close to 1.

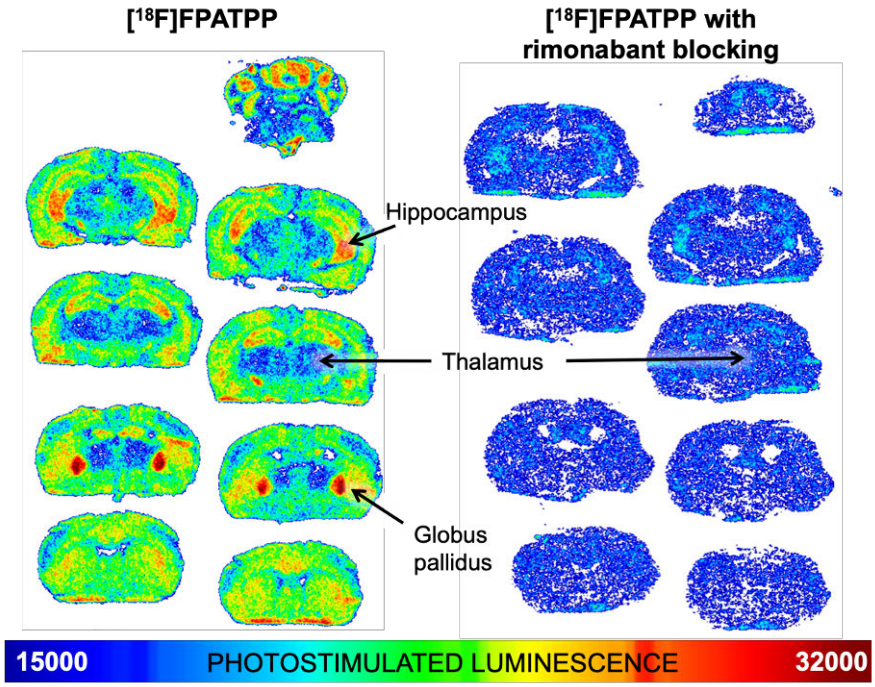

Figure 28. Representative *ex vivo* brain autoradiographic images of [^{18}F]FPATPP binding at 120 min post-injection. Images on the right are from a mouse pre-treated with 2 mg/kg rimonabant.

Ex vivo biodistribution

In the *ex vivo* biodistribution study, [^{18}F]FPATPP presented high accumulation in the whole brain 30 min p.i. with fast washout (Figure 29). Whole brain uptake was 9.8 ± 3.2%ID/g 30 min p.i. and 4.9 ± 0.9%ID/g 120 min p.i. Rimonabant pre-treatment reduced the brain uptake to 1.6 ± 0.1%ID/g 120 min p.i. Accumulation in the bone was low, only 0.4 ± 0.1%ID/g 120 min p.i. In the collateral *ex vivo* biodistribution study with [^{18}F]FMPEP-d_2, the whole brain uptake was lower and no clear washout was observed. In addition, bone uptake was 2.7 ± 0.5%ID/g 120 min p.i.

Metabolite analysis (III, unpublished)

Metabolism of [^{18}F]FPATPP was slow. Two polar radioactive metabolites were observed in the plasma and one in the cortex 120 min p.i. The amount of [^{18}F]FPATPP 120 min p.i. was 21.3 ± 3.5% in the plasma and 75.0 ± 4.3% in the cortex. Rimonabant blocking reduced [^{18}F]FPATPP binding in the cortex to 25.4% 120 min p.i. (n=1, unpublished).

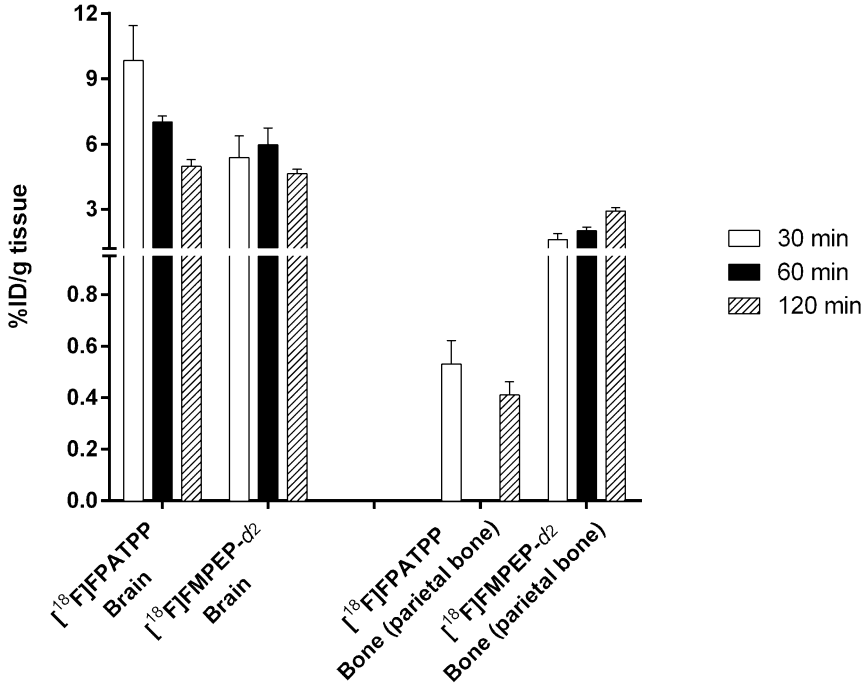

Figure 29. *Ex vivo* biodistribution of [^{18}F]FPATPP and [^{18}F]FMPEP-d_2 in the brain and parietal bone.

5.3 GMP production of [^{18}F]FMPEP-d_2 (IV)

5.3.1 [^{18}F]FMPEP-d_2 synthesis and quality control

The original [^{18}F]FMPEP-d_2 synthesis procedure by Donohue et al. (2008a) was followed with small modifications to the reaction and purification conditions. [^{18}F]Bromofluoromethane-d_2 was produced successfully in a 5-min reaction at 90 °C and purified by GC at 90 °C. The GC purification method proved to be robust and reproducible when the GC column was preconditioned before tracer production at 170 °C. The subsequent nucleophilic ^{18}F-fluoroalkylation reaction was carried out at 80 to 110 °C in 5 to 10 min. [^{18}F]FMPEP-d_2 was purified by semi-preparative HPLC in 15 min. The total synthesis time was 83 ± 7 minutes. Between 2013 and 2018, 223 batches of [^{18}F]FMPEP-d_2 were produced with a 91% success rate, 16 ± 6% decay-corrected RCY, and 600 ± 300 GBq/µmol A_m at the EOS. Yearly results are given in Table 10. The shelf-life of [^{18}F]FMPEP-d_2 was originally determined to be 180 min (validation result: RCP 97.9 ± 1.1% at EOS + 180 min, n=3), but after a short period of time, the shelf-life was decreased to 120 min (results after the original validation

process: RCP 96.3 ± 1.8% at EOS + 180 min, RCP 96.8 ± 1.2% at EOS + 120 min, n=3) at RT.

Table 10. Summary of [^{18}F]FMPEP-d_2 production during 2013-2018.

Year	Total / for clinical use / rejected	Success rate [%]	RCP [%]	Radioactivity at EOS [GBq]	A_m at EOS [GBq/μmol]
2013	46 / 6 / 0	100	99.1 ± 0.7	0.8 ± 0.4	430 ± 260
2014	38 / 27 / 5	87	98.5 ± 0.8	0.8 ± 0.4	410 ± 250
2015	35 / 28 / 3	91	98.2 ± 1.0	1.1 ± 0.4	730 ± 290
2016	37 / 34 / 2	95	97.9 ± 0.8	1.2 ± 0.3	790 ± 220
2017	27 / 21 / 6	78	98.1 ± 1.0	0.9 ± 0.3	540 ± 190
2018	40 / 33 / 3	93	98.5 ± 0.8	1.1 ± 0.3	660 ± 350
Total	223 / 149 / 19	91	98.3 ± 0.9	1.1 ± 0.4	600 ± 300

RCP, radioactivity, and A_m values were calculated from the batches produced for clinical use; thus, the rejected batches are not included in the calculations.

In the production of [^{18}F]FMPEP-d_2, both occasional and continuous problems have been encountered. Occasional problems include radiolysis when the radioactivity concentration (RAC) is >150 MBq/mL (Figure 30A). When the RAC increases, the RCP decreases; whereas the A_m increases with increasing RAC (Figure 30B). Ascorbic acid was added to the HPLC eluent and HPLC fraction dilution solutions to prevent radiolytic dissociation. In addition, the amount of starting activity was decreased to avoid radiolytic dissociation.

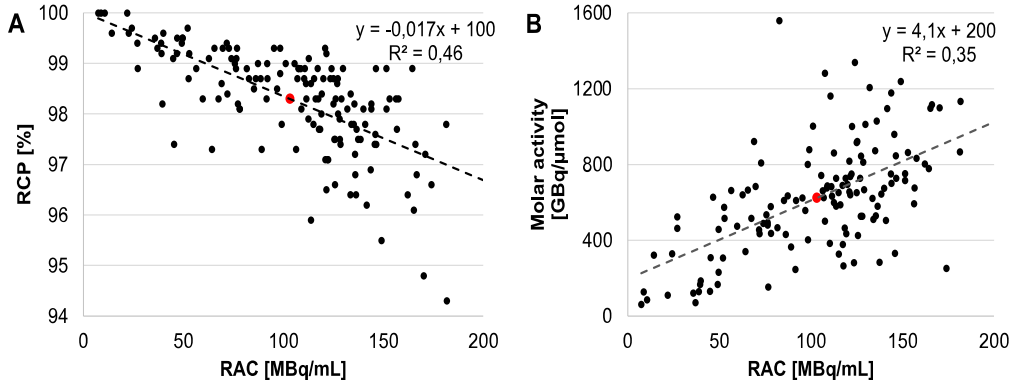

Figure 30. A) Radiochemical purity (RCP) as a function of radioactivity concentration (RAC) at EOS and B) molar activity as a function of RAC at EOS. Average RCP and A_m values are marked by a red dot in both graphs.

Continuous problems include the lipophilicity of FMPEP. The use of a hydrophilic polyethersulfone membrane filter for sterile filtration and two-component polypropylene or polyethylene syringes for radiopharmaceutical administration diminished the adherence of [^{18}F]FMPEP-d_2 to the filter and syringe materials compared to different membranes and three-component syringes.

As seen in Table 10, in 2017 there was an unusually high number of rejections, as more than 20% of all syntheses were rejected. Originally, the cause was thought to be a non-functional heating unit that resulted in incomplete radiofluorination. The radiofluorination reaction temperature was increased (80 °C to 110 °C) and time prolonged (5 to 10 min) and the synthesis device modified to solve the problem. However, these changes did not improve the RCY or RCP. Eventually, the cause was found to be invalid DMF. The use of old DMF had a detrimental effect on the radiofluorination yield and RCP.

5.3.2 Method validation

Qualification of the synthesis device and validation of the synthesis process, as well as validation of the analytical HPLC and GC methods, were successful. Successful validation confirmed that the synthesis process and analytical methods were appropriate for [^{18}F]FMPEP-d_2 production and QC. After validation, three major controlled changes were made to the synthesis process: 1) decreasing the shelf-life from 180 min to 120 min to fulfil the specifications until the end of shelf-life, 2) changing the GC column stationary phase, and 3) changing the heating unit from an electric heater to oil bath and simultaneously changing the reaction temperature and time. Changes were carried out and documented according to GMP guidelines.

6 Discussion

When working with short-living fluorine-18, late-stage fluorination is the preferred approach to minimise the time needed for the radiosynthesis and to avoid purification steps between multiple reactions. One of the most novel approaches to late-stage ^{18}F-fluorination is transition metal-mediated ^{18}F-labelling. These reactions have been gaining in popularity since the first publications in the beginning of the 2010s. Copper-mediated ^{18}F-labelling reactions have been widely investigated, and studies I and II are continuing the trend. Although ruthenium-mediated ^{18}F-labelling is still a relatively unfamiliar ^{18}F-labelling approach, it has been shown to be a robust and reproducible method for tracer production. Regardless of the ^{18}F-labelling method, activation of [^{18}F]fluoride is a key step in all ^{18}F-fluorination processes.

6.1 Copper-mediated ^{18}F-labelling (I, II)

6.1.1 [^{18}F]Fluoride processing

Azeotropic distillation and SPE are both suitable [^{18}F]fluoride activation methods for subsequent copper-mediated ^{18}F-labelling of [^{18}F]NS12137 and [^{18}F]CFT. With the azeotropic distillation method, extra attention should be given to the distillation conditions to avoid the adherence of [^{18}F]fluoride in the glass vial. Although the RCY (based on HPLC) was approximately 90% with [^{18}F]NS12137 using the azeotropic distillation method, [^{18}F]fluoride incorporation was only up to 25%. Incorporation was 1.5-times higher with the SPE activation method. Even with the SPE activation method, [^{18}F]fluoride was adsorbed onto the glass vial walls during the ^{18}F-fluorination reaction. The high difference in the RCY (based on HPLC) and [^{18}F]fluoride incorporation is explained by the use of water to dilute the reaction mixture prior to SPE, which dissolves the [^{18}F]fluoride from the reaction vessel walls.

Azeotropic distillation is typically considered to be a more time-consuming method than [^{18}F]fluoride activation with SPE. However, the synthesis times observed in the [^{18}F]NS12137 production in studies I and II were similar, approximately 100 min. The synthesis procedure with the SPE activation method could be improved and made faster by automating the device.

Another disadvantage of the azeotropic distillation method is the use of Kryptofix2.2.2, which is considered toxic. To avoid the use of K_{222}, tetraalkyl ammonium compounds have been used in [^{18}F]fluoride activation, achieving high RCYs (Zhang et al. 2019a). The basic conditions achieved with azeotropic distillation have been criticised, as some reactions are base-sensitive. Azeotropic distillation-free copper-mediated ^{18}F-labelling methods have been developed, but most of these still utilise additional evaporation steps, as in the alcohol-enhanced copper-mediated radiofluorination described by Zischler et al. (2017), or unnecessary or even toxic chemicals, such as pyridinium sulphonates (Antuganov et al. 2019) or 4-dimethylaminopyridinium triflate (Zhang et al. 2019b). The advantage of the SPE activation method developed in study II is the lack of extra evaporation steps or toxic chemicals excluding the copper complex, which is necessary for the subsequent ^{18}F-labelling process. However, an advantage of azeotropic distillation is the elevated reaction vial temperature at the start of the reaction. Especially in the copper-mediated ^{18}F-labelling reactions, the reaction times are relatively short, and elevating the starting temperature of the reaction vial promotes the subsequent ^{18}F-labelling reaction.

Both $Cu(OTf)_2$ and $Cu(OTf)_2(py)_4$ were used successfully in the activation of [^{18}F]fluoride with SPE. With most cartridges, $Cu(OTf)_2$ was a more efficient eluting agent than $Cu(OTf)_2(py)_4$. In study II, we suggested that pyridine coordination to copper causes steric hindrance in [^{18}F]fluoride coordination. Using large amounts of copper complex diminished the difference between the two different complexes. In addition, [^{18}F]fluoride recovery increased with an increased amount of copper complex (12 µmol < 24 µmol < 48 µmol < 96 µmol). However, the highest amount of copper was not considered to be optimal due to high cost and to avoid possible purification problems.

Our results support the reaction mechanism previously proposed by Zarrad et al. (2017) in which [^{18}F]fluoride is eluted from the anion exchange cartridge as a Cu(OTf)[^{18}F]F or Cu(OTf)[^{18}F]F(py)$_4$ complex (Figure 31). Using aqueous LiOTf to precondition the cartridge and adding LiOTf to the elution solution enhances the anion exchange in the cartridge.

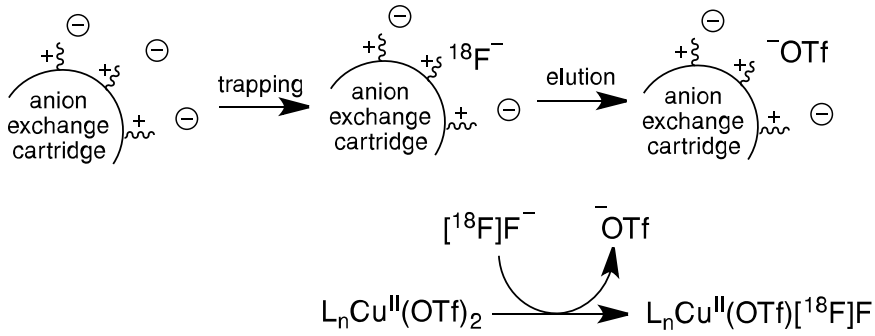

Figure 31. Proposed mechanism for [^{18}F]fluoride activation using the SPE method.

6.1.2 ^{18}F-Radiolabelling

Model molecules 1-[^{18}F]fluoro-4-iodobenzene, 4-[^{18}F]fluorobiphenyl, 4-[^{18}F]fluorophenol, [^{18}F]fluorobenzene, 4-[^{18}F]fluorobenzonitrile, 1-[^{18}F]fluoro-4-nitrobenzene, 2-[^{18}F]fluoronaphthalene, and 4-[^{18}F]fluoroindole, and the tracer molecules [^{18}F]NS12137 and [^{18}F]CFT were successfully produced by copper-mediated fluorination with moderate to excellent yields. 3-[^{18}F]Fluoropyridine was produced with less than 15% RCY. The low yield is probably due to the coordination of nitrogen in the precursor molecule to copper instead of pyridine. Low yield may be avoided by changing the order in which reagents are added. In this study, [^{18}F]fluoride was eluted with $Cu(OTf)_2$ complex into the vessel containing the precursor and pyridine. Pyridine may stabilise the Cu intermediate as MeCN does with fluorine-19 (Gamache et al. 2016) and, as such, may be crucial to producing the $Cu(py)_4(OTf)(F)$ intermediate before addition of the precursor. An alternative reason for the low yield with 3-[^{18}F]fluoropyridine could be the stability of the boronic acid precursor, 3-pyridinylboronic acid, as some heteroaromatic boronic acids are unstable under aerobic conditions (Hall 2005). However, the mechanism of Cu-mediated ^{18}F-labelling should be studied further.

Copper-mediated ^{18}F-labelling reactions have generally been carried out in 20 min. However, in studies I and II, 5-min reaction times were found to be sufficient. In most cases, increasing the reaction time from 5 to 15 min had only a minor effect on the RCY. In addition, in the synthesis of [^{18}F]NS12137 in study I, longer reaction times were observed to slightly decrease the RCY and increase the amount of side products, which suggests that [^{18}F]NS12137 starts to slowly decompose at high temperatures.

Regardless of the [^{18}F]fluoride activation method used and the amount of copper in the [^{18}F]fluoride elution step, the copper was efficiently removed in the purification steps with both [^{18}F]NS12137 and [^{18}F]CFT. According to ICH guidelines, the daily parenteral administration limit for copper is 340 µg (International Council for

Harmonisation of Technical Requirements for Pharmaceuticals for Human Use 2019), and both [^{18}F]NS12137 and [^{18}F]CFT were well under the limit.

To compare the effectiveness of copper-mediated radiofluorination to traditional electrophilic fluorination, [^{18}F]CFT was produced via electrophilic ^{18}F-fluorination with [^{18}F]Selectfluor *bis*(triflate). Although the yield was comparable to the yield achieved with the SPE approach, the A_m was considerably lower with the electrophilic approach, as expected. Similarly, [^{18}F]NS12137 has been produced via electrophilic ^{18}F-fluorination with considerably lower A_m (Kirjavainen et al. 2018) than via copper-mediated ^{18}F-fluorination.

6.2 Ruthenium-mediated ^{18}F-labelling (III)

6.2.1 ^{18}F-radiolabelling

Production of [^{18}F]FPATPP was successful via ruthenium-mediated labelling with both [^{18}F]fluoride activation methods, azeotropic distillation and SPE. During optimisation of the SPE method, the elution efficiency and [^{18}F]fluoride recovery were at similar levels (93% vs. 80%), but when [^{18}F]FPATPP was produced for preclinical use, these values were very different (93% vs. 51%). Preclinical batches were made with high starting activities (>7 GBq). Extending irradiation times increases the formation of cationic impurities from the metallic target foil and the target chamber material. Poor [^{18}F]fluoride recovery with larger starting activities could be caused by these cationic impurities.

With SPE, RCY (based on HPLC) was acceptable after a 30-min reaction, whereas activation of [^{18}F]fluoride via azeotropic distillation led to a good RCY (based on HPLC) after a 10-min reaction. The differences in the RCY between these two methods were no longer present after 30 minutes. Although, base-free ^{18}F-fluorination approaches are sometimes desired due to the use of base-sensitive precursors, the addition of base enhanced the reaction in Ru-mediated labelling. In addition, as seen in Figure 26A-D, the proposed [^{18}F]F-aryl ruthenium complex is not observed when K_2CO_3 is present in the radiofluorination reaction mixture.

Ruthenium-mediated radiofluorination has been proven a robust and reproducible method although the conditions are extreme. As such, ruthenium-mediated production of [^{18}F]FPATPP is not ready for translation to clinical production due to the high ruthenium content in the purified product (7.8 ± 1.8 µg/mL). According to the European pharmacopoeia and ICH Q3D(R1) guidelines, the maximum daily exposure of parenteral ruthenium is 10 µg/day (European Pharmacopoeia 2013, International Council for Harmonisation of Technical Requirements for Pharmaceuticals for Human Use 2019).

6.2.2 Preclinical evaluation

[^{18}F]FPATPP is an analogue of a known CB1R imaging tracer, [^{18}F]FMPEP-d_2. The binding properties of [^{18}F]FPATPP were compared to a mouse study with [^{18}F]FMPEP-d_2 (Donohue et al. 2008a) and a rat study with [^{18}F]MK-9470 (Casteels et al. 2012). According to the *in vivo* study, [^{18}F]FPATPP uptake was similar to [^{18}F]FMPEP-d_2 and considerably faster than [^{18}F]MK-9470. Thus, unlike with [^{18}F]FMPEP-d_2 and [^{18}F]MK-9470, the washout began immediately after the peak uptake.

Ex vivo autoradiography showed [^{18}F]FPATPP binding to CB1R-rich areas in the mouse brain. An exceptional property of [^{18}F]FPATPP is the ability to distinguish different hippocampal and cortical layers. Similar resolution has not been detected with [^{18}F]FMPEP-d_2 or [^{18}F]MK-9470. [^{18}F]FPATPP binding was quantified by comparing the CB1R-rich areas to the thalamus; we observed significant binding ($P<0.001$). According to the low bone accumulation observed in the *ex vivo* biodistribution study, [^{18}F]FPATPP does not seem to be prone to undergoing defluorination, unlike [^{18}F]FMPEP-d_2. Although [^{18}F]FMPEP-d_2 exhibited higher metabolic stability in the brain (86% vs. 75% of unchanged tracer) (Takkinen et al. 2018), the higher brain uptake and lower defluorination with [^{18}F]FPATPP are advantages for imaging.

Specificity study

The specificity of [^{18}F]FPATPP for CB1Rs was studied with rimonabant blocking. Rimonabant has been shown to be specific and selective for CB1Rs over CB2R (Rinaldi-Carmona et al. 1994). In addition, CB2R expression in the CNS is very low (Howlett et al. 2002), so rimonabant is suitable for demonstrating the specificity for CB1R. *In vivo* PET imaging, *ex vivo* autoradiography and biodistribution studies, and metabolism studies showed blocking of [^{18}F]FPATPP binding. In previous *in vitro* studies, [^{18}F]FMPEP-d_2, the close analogue of [^{18}F]FPATPP, was specific and selective for CB1Rs over CB2R (Donohue et al. 2008a). Thus, [^{18}F]FPATPP is specific and selective for CB1R.

6.2.3 Comparison of cannabinoid tracers [^{18}F]FPATPP and [^{18}F]FMPEP-d_2 (III, IV)

As already described in chapter 6.2.2, [^{18}F]FPATPP exhibited improved uptake and washout kinetics compared to [^{18}F]FMPEP-d_2; thus, [^{18}F]FPATPP could be a superior tracer in clinical imaging. In addition, unlike [^{18}F]FPATPP, [^{18}F]FMPEP-d_2 is prone to defluorination and [^{18}F]fluoride accumulation in parietal bone (Figure 29). The RCP, shelf-life, and radioactivity concentration for both of these tracers are provided in

Table 11. With [^{18}F]FMPEP-d_2, RCP decreases as a function of the RAC (Figure 30). [^{18}F]FPATPP exhibited better stability towards radiolysis.

Table 11. Radiochemical data for [^{18}F]FPATPP and [^{18}F]FMPEP-d_2.

	[^{18}F]FPATPP	[^{18}F]FMPEP-d_2
RCP at EOS [%]	99.9 ± 0.1 (range 99.8 – 100.0, n=5)	98.3 ± 1.0 (range 94.3 – 100.0, n=149)
RAC [MBq/mL]	200 – 450	20 – 200
Shelf-life [min]	300	120
RCP at the end of shelf-life [%]	98.8 ± 0.6% (n=2)	96.8 ± 1.2 (range 95.4 – 97.8, n=3)

6.3 Future aspects with transition metal-mediated ^{18}F-labelling (I – III)

Discussion concerning the toxicity of chemicals used in the radiosynthesis of clinical tracers has been going on for years. Tin-containing compounds have traditionally been used as precursors in electrophilic ^{18}F-labelling reactions. However, the use of tin has been criticised as one more weakness of the electrophilic ^{18}F-labelling approach. As demonstrated in study I, the tin residue in the purified product fraction is minimal compared to the maximal parenteral dose according to the ICH guidelines (Table 12). Similarly, copper can be removed from the product fraction via traditional chromatographic methods with excellent purification factor. For palladium, nickel, and ruthenium, the maximal parenteral doses per day are considerably lower than for copper or tin (International Council for Harmonisation of Technical Requirements for Pharmaceuticals for Human Use 2019). In study III with [^{18}F]FPATPP, a high amount of ruthenium was observed in the end product fraction although the product was purified with HPLC and passed through an SPE cartridge during formulation. Celen et al. (2020) reported successful removal of ruthenium from the product fraction with similar chromatographic methods: two SPE cartridges, HPLC, and sterile filter. Similarly, palladium and nickel have successfully been removed from the product fractions by HPLC and typically multiple SPE cartridges (Lee et al. 2011, Hoover et al. 2016).

Table 12. Metal residues in the products achieved with transition metal-mediated ^{18}F-fluorination.

Metal	Maximal parenteral dose according to ICH* [µg/day]	Metal residue [µg/mL]	Tracers	Purification method	Reference
Palladium	10	0.005	[^{18}F]fluoro-deoxyestrone	Filtration and HPLC	(Lee et al. 2011)
Nickel	22	< 0.1	[^{18}F]5-fluorouracil	HPLC and SPE	(Hoover et al. 2016)
Copper	340	< 0.25 – 3.9 µg** 46 µg**	[^{18}F]NS12137 [^{18}F]CFT	SPE and HPLC HPLC	Study I – II Study II
Tin	640	< 0.25 µg**	[^{18}F]NS12137	HPLC	Study I
Ruthenium	10	< 0.015	[^{18}F]EKZ-001	HPLC and SPE	(Celen et al. 2020)
		< 10	[^{18}F]FPATPP	HPLC and SPE	Study III

*ICH Q3D(R1) 2019
** 5 – 10 mL volume

As discussed above, copper can be removed sufficiently by simple chromatographic methods. The copper-mediated ^{18}F-fluorination method is a simple labelling approach with wide substrate scope, mild reaction conditions, and readily available chemicals. Thus, the method would easily be translated to clinical production. For example, in the production of [^{18}F]NS12137, considerably milder reaction conditions are needed for the copper-mediated approach (5 min, 120 °C, studies I – II) than for the nucleophilic approach (15 min, 185 °C, López-Picón et al. 2019).

Radiofluorination processes utilising ruthenium, palladium, and nickel require a more careful design of the purification system, but metal residues can be minimised with multiple SPE systems. As palladium and nickel-mediated labelling reactions have turned out to be unsuitable for clinical production due to complex precursor synthesis (Lee et al. 2011, 2012, Hoover et al. 2016), ruthenium-mediated ^{18}F-fluorination is a desirable method with easy access phenol precursors. Ru-mediated ^{18}F-labelling proved to be a robust ^{18}F-fluorination method, but the reaction conditions are extreme. Unlike in the original studies with ruthenium (Beyzavi et al. 2017), study III demonstrated that 130 °C is not hot enough of a reaction temperature for the decomplexation and 160 °C was needed. Despite the robustness, the harshness of the reaction conditions in Ru-mediated ^{18}F-labelling are close to traditional nucleophilic reaction conditions. In addition, premixing of the precursor and Ru complex is needed, which is an extra step compared to the copper-mediated ^{18}F-labelling chemistry. Thus, from the current developments in transition metal-mediated ^{18}F-fluorination, copper-mediated ^{18}F-labelling is the most obvious labelling method to choose when proceeding to clinical radiopharmaceutical production with aromatic structures.

6.4 GMP production of [^{18}F]FMPEP-d_2 (IV)

Modifications to the original synthesis process by Donohue et al. (2008a) shortened the synthesis time significantly. One major improvement was purification of [^{18}F]dibromomethane-d_2 via GC instead of SPE cartridges. The GC method is robust and reproducible when the GC column is appropriately preconditioned before every synthesis. Overall, the production of [^{18}F]FMPEP-d_2 has been robust and reproducible with a 91% success rate. The greatest cause for rejection has been resolved and the validity of DMF is monitored.

[^{18}F]FMPEP-d_2 is prone to undergoing defluorination via radiolytic dissociation. Previous studies have shown that changing the [^{18}F]fluoromethoxy tail to deuterated [^{18}F]fluoromethoxy makes the structure more stable (Donohue et al. 2008a, Terry et al. 2010). Radiolytic dissociation has been successfully reduced by adding ascorbic acid to critical steps in the synthesis process. A RAC of 50 MBq/mL was considered a limit when radiolysis is observed, but issues with too low RCP have started with an RAC of 150 MBq/mL. To avoid high RACs and subsequent radiolysis, the amount of starting activity was decreased. However, as the real reason for incomplete radiofluorination reactions was invalid DMF, whether invalid DMF enhanced the radiolysis and complicated the semi-preparative purification, causing low RCP of the final product, can be discussed.

Lipophilicity of [^{18}F]FMPEP-d_2 has been a problem, especially with syringes used for radiopharmaceutical administration; therefore, these syringes have been switched to lubricant-free syringes. In addition, sterile filters were changed to filters with hydrophilic membranes. Both of these actions diminished the tracer adherence to consumable materials. Despite the high lipophilicity of [^{18}F]FMPEP-d_2, it did not get stuck in the device to a significant degree.

7 Conclusions

In studies I and II, copper-mediated ^{18}F-fluorination was found to be suitable for the production of various model molecules, [^{18}F]NS12137, and [^{18}F]CFT with moderate to good yields. Both [^{18}F]fluoride activation methods, azeotropic distillation and SPE, work with subsequent copper-mediated ^{18}F-fluorination starting from boronic acid precursors, boronic ester precursors, or stannylated precursors. Reaction conditions were optimised and 5 min reactions found to be satisfactory for most of the studied compounds. Using the SPE approach, [^{18}F]NS12137 was produced with up to 16% RCY and [^{18}F]CFT with up to 5% RCY. Copper-mediated labelling via SPE was simple, straightforward, and more effective than using azeotropic distillation and, thus, is a more reasonable choice for translation to clinical production in the future.

In study III, ruthenium-mediated ^{18}F-labelling was successfully implemented into the production of [^{18}F]FPATPP, a new imaging agent for CB1R imaging. Ruthenium-mediated ^{18}F-labelling proved to be a robust and reproducible radiofluorination method. However, the high amount of ruthenium in the purified product is a disadvantage. Preclinical evaluation with [^{18}F]FPATPP showed specific binding to CB1Rs, high brain uptake, fast washout, and low defluorination.

In study IV, the synthesis device for [^{18}F]FMPEP-d_2 was built and the device and analytical methods validated successfully for clinical radiopharmaceutical production. Clinical production was followed for 5 years and [^{18}F]FMPEP-d_2 produced with 16% RCY and A_m of 600 GBq/μmol. With more than 220 syntheses over the 5-year period, the success rate was 91%.

Acknowledgements

This work was carried out at the Radiopharmaceutical Chemistry Laboratory and at the MediCity Research Laboratory of the Turku PET Centre, University of Turku and the Department of Chemistry, University of Turku. This work was financially supported by The Finnish Concordia Fund, Kemian Päivien Säätiö, The Emil Aaltonen Foundation, and the Orion Research Foundation sr. Doctoral Programme in Physical and Chemical Sciences, University of Turku Foundation, Finnish Society of Nuclear Medicine, and the Scandinavian Society of Clinical Physiology and Nuclear Medicine are acknowledged for travel grants.

I owe my deepest gratitude to my supervisors, Adjunct Professor Anna Kirjavainen and Professor Olof Solin. You both showed me the way in the fascinating world of radiopharmaceutical chemistry. The last few years have been full of ups and downs, and without the never-ending optimism I would have been lost in the downs. Working under your guidance was easy and I could always count on your help.

I wish to express my gratitude to Associate Professor Magnus Schou and Doctor Matthew Tredwell for reviewing my thesis and offering constructive comments and criticism, which highly improved my thesis.

I thank all of my co-authors; you have shared your expertise in chemistry, radiochemistry, and preclinical studies with me, resulting in our articles. In particular, I want to thank Noora Rajala – you have been there in the lab and listened to the craziest research ideas and helped me make them come true.

I am grateful to Thomas Keller, Ania Krzyczmonik, Sarita Forsback, Olli Eskola, Tapio Viljanen, Jörgen Bergman for sharing your knowledge in radiochemistry with me. I also want to thank my other fellow radiochemists Nina Sarja, Semi Helin, Anu Airaksinen, Paula Lehtiniemi, Cheng-Bin Yim, Ari Hietanen, Henna Koivikko, and Saara Wahlroos. I wish to thank the technical staff of the radiochemistry laboratory, especially Jani Uotinen for practical help in the laboratory, and Nina Laurén for all the chemicals that needed to be ordered. Riikka Purtanen, Enni Saksa, Heidi Sundström, Hanna-Maarit Seikkula, Juha Seikkula, Leena Tokoi-Eklund, Melina Väkiparta, Margit Åhman-Kantola, and Marja-Liisa Pakkanen – this journey would have been completely different without your company in the lab and coffee breaks. Not to mention, I'm sorry for the mess I always left behind.

As no radiochemistry work would have been done without radioactivity, special thanks are given to the cyclotron staff, Johan Rajander, Mikael Bergelin, Per-Olof Eriksson, Stefan Johansson, and Jan-Olof Lill. I'm thankful to Francisco López-Picón, Jatta Helin, Merja Haaparanta-Solin, Richard Aarnio, Aake Honkaniemi, and Marko Vehmanen for their help and expertise in preclinical studies. For technical support, I thank Esa Kokkomäki, Timo Saarinen, and Simo Vauhkala, you were always there when the devices stopped working or the tools were lost. In the GMP issues, pharmacist and QA Riikka Kivelä provided me with very valuable supervision – thank you. During this thesis work, I've also needed the expertise of Adj. Prof. Ari Lehtonen in materials chemistry and Prof. Pasi Virta in organic chemistry, thank you. Marko Pilkkakangas is acknowledged for linguistic assistance. During the past years, I have been honoured to supervise bachelor's and master's theses. Thus, I want to thank Krista, Pietari, Joonas and Juho, guiding you taught me a lot, too.

I am lucky to have so many friends inside and outside the Turku PET centre who have supported me during these years. Ania and Thomas, besides your help in the lab, I'm extremely grateful for the cakes, dinners, parties and the company outside the lab! These parties would have been nothing without you, Kumail and Amy, Kamil and Suvi, Vilma, Miikka, Priyanka, Sina and Katri, thank you for all the unforgettable moments.

I wish to thank my friends who I've met during my studies, Laura, Tuuli, Ville, Eemi, Mikaela, and Hellen. I moved to Turku 10 years ago and you helped make this city (where they talk in a weird dialect!) my home. I especially want to thank Isabella. We started our chemistry studies at the same time and oh what fun we have had during the past years! What would I have become without my friends since primary school – thank you Saija, Eveliina, and Siina. And I'm sorry if I didn't thank YOU, please fix my mistake by placing your name in the following sentence: I thank you, _____ for being awesome!

I'm grateful for my new family in Turku, Minna, Leo and Aino, thank you for the Sunday dinners – and everything else. I want to thank my family, mom, dad, and Tuukka, for supporting me through all my studies. Although living far away, I've always been able to count on you. And finally, I thank you my love, Aleksi. You have been there since the beginning of my journey as a chemist, during the worst and the best days. Who knows, if I hadn't met you, would I even be here defending my thesis?

Turku, January 2021

Salla Lahdenpohja

List of References

Aerts J, Ballinger JR, Behe M, Decristoforo C, Elsinga PH, Faivre-Chauvet A, Mindt TL, Kolenc Peitl P, Todde SC and Koziorowski J: Guidance on current good radiopharmacy practice for the small-scale preparation of radiopharmaceuticals using automated modules: a European perspective. *J Label Compd Radiopharm*. **2014**, 57: 615–620.

Aerts J, Lemaire C, Lignon S, Luxen A, Morelle J-L, Philippart G and Voccia S: Method for the elution of ^{18}F-fluoride trapped on an anion-exchange phase in a form suitable for efficient radiolabeling without any evaporation step. US20110006011A1, **2008**.

Aerts J, Voccia S, Lemaire C, Giacomelli F, Goblet D, Thonon D, Plenevaux A, Warnock G and Luxen A: Fast production of highly concentrated reactive [^{18}F]fluoride for aliphatic and aromatic nucleophilic radiolabelling. *Tetrahedron Lett*. **2010**, 51: 64–66.

Ahamed M, Verbruggen A and Bormans G: Synthetic strategies for radioligands for *in vivo* imaging of brain cannabinoid type-1 receptors. *J Label Compd Radiopharm*. **2013**, 56: 207–214.

Ametamey SM, Honer M and Schubiger PA: Molecular imaging with PET. *Chem Rev*. **2008**, 108: 1501–1516.

Ampére A-M: Suite d'une classification naturelle pour les corps simples. In *Annales de chimie et de physique 2: 1–5*; **1816**.

Antuganov D, Zykov M, Timofeev V, Timofeeva K, Antuganova Y, Orlovskaya V, Fedorova O and Krasikova R: Copper-mediated radiofluorination of aryl pinacolboronate esters: A straightforward protocol by using pyridinium sulfonates. *Eur J Org Chem*. **2019**, 2019: 918–922.

Antuganov D, Zykov M, Timofeeva K, Antuganova Y, Orlovskaya V and Krasikova R: Effect of pyridine addition on the efficiency of copper-mediated radiofluorination of aryl pinacol boronates. *ChemistrySelect*. **2017**, 2: 7909–7912.

Banks RE, Besheesh MK, Mohialdin-Khaffaf SN and Sharif I: *N*-Halogeno compounds. Part 18. 1-Alkyl-4-fluoro-1,4-diazoniabicyclo[2.2.2]octane salts: user-friendly site-selective electrophilic fluorinating agents of the *N*-fluoroammonium class. *J Chem Soc Perkin Trans 1*. **1996**, 1996: 2069–2076.

Banks RE, Mohialdin-Khaffaf SN, Lal GS, Sharif I and Syvret RG: 1-Alkyl-4-fluoro-1,4-diazoniabicyclo[2.2.2]octane salts: a novel family of electrophilic fluorinating agents. *J Chem Soc, Chem Commun*. **1992**, 1992: 595–596.

Banks WA: Characteristics of compounds that cross the blood-brain barrier. *BMC Neurol*. **2009**, 9: S3.

Bergman J, Haaparanta-Solin M and Solin O: A novel radioisotope labelled compound, a mixture comprising said compound and a method for its preparation. Finnish Patent 96603, WO 96/20940, **1996**.

Bergman J and Solin O: Fluorine-18-labeled fluorine gas for synthesis of tracer molecules. *Nucl Med Biol*. **1997**, 24: 677–683.

Beyzavi MH, Mandal D, Strebl MG, Neumann CN, D'Amato EM, Chen J, Hooker JM and Ritter T: ^{18}F-Deoxyfluorination of phenols via Ru π-complexes. *ACS Cent Sci*. **2017**, 3: 944–948.

Bizet V: *N*-Fluorobenzenesulfonimide. *Synlett*. **2012**, 23: 2719–2720.

Blessing G, Coenen HH, Franken K and Qaim SM: Production of [^{18}F]F_2, $H^{18}F$ and $^{18}F_{aq}^-$ using the ^{20}Ne(d,α)^{18}F process. *Int J Radiat Appl Instrumentation Part A Appl Radiat Isot*. **1986**, 37: 1135–1139.

Block D, Klatte B, Knöchel A, Beckmann R and Holm U: N.C.A. [^{18}F]-labelling of aliphatic compounds in high yields via aminopolyether - supported nucleophilic substitution. *J Label Compd Radiopharm*. **1986**, 23: 467–477.

Böhm H-J, Banner D, Bendels S, Kansy M, Kuhn B, Müller K, Obst-Sander U and Stahl M: Fluorine in medicinal chemistry. *ChemBioChem*. **2004**, 5: 637–643.

Bondi A: Van der Waals volumes and radii. *J Phys Chem*. **1964**, 68: 441–451.

Boursalian GB and Ritter T: Nickel-mediated fluorination for preparing aryl fluorides. In *Fluorination*; Hu J, Umemoto T, Eds.; Springer: Singapore, **2017**; pp 1–11.

Brandt JR, Lee E, Boursalian GB and Ritter T: Mechanism of electrophilic fluorination with Pd(IV): fluoride capture and subsequent oxidative fluoride transfer. *Chem Sci*. **2014**, 5: 169–179.

Brodack JW, Dence CS, Kilbourn MR and Welch MJ: Robotic production of 2-deoxy-2[^{18}F]fluoro-D-glucose: A routine method of synthesis using tetrabutylammonium [^{18}F]fluoride. *Int J Radiat Appl Instrumentation Part A Appl Radiat Isot*. **1988**, 39: 699–703.

Brodack JW, Kilbourn MR, Welch MJ and Katzenellenbogen JA: NCA 16α-[^{18}F]fluoroestradiol-17β: The effect of reaction vessel on fluorine-18 resolubilization, product yield, and effective specific activity. *Int J Radiat Appl Instrumentation Part A Appl Radiat Isot*. **1986**, 37: 217–221.

Buckingham F, Kirjavainen AK, Forsback S, Krzyczmonik A, Keller T, Newington IM, Glaser M, Luthra SK, Solin O and Gouverneur V: Organomediated enantioselective ^{18}F-fluorination for PET applications. *Angew Chem*. **2015**, 127: 13564–13567.

Burns HD, Laere K Van, Sanabria-Bohórquez S, Hamill TG, Bormans G, Eng W, Gibson R, Ryan C, Connolly B, Patel S, Krause S, Vanko A, Hecken A Van, Dupont P, Lepeleire I De, Rothenberg P, Stoch SA, Cote J, Hagmann WK, Jewell JP, Lin LS, Liu P, Goulet MT, Gottesdiener K, Wagner JA, de Hoon J, Mortelmans L, Fong TM and Hargreaves RJ: [^{18}F]MK-9470, a positron emission tomography (PET) tracer for in vivo human PET brain imaging of the cannabinoid-1 receptor. *Proc Natl Acad Sci USA*. **2007**, 104: 9800–9805.

Cai L, Lu S and Pike VW: Chemistry with [^{18}F]fluoride ion. *Eur J Org Chem*. **2008**, 2008: 2853–2873.

Campbell MG and Ritter T: Modern carbon–fluorine bond forming reactions for aryl fluoride synthesis. *Chem Rev*. **2015**, 115: 612–633.

Casitas A, Canta M, Solà M, Costas M and Ribas X: Nucleophilic aryl fluorination and aryl halide exchange mediated by a Cu^{I}/Cu^{III} catalytic cycle. *J Am Chem Soc*. **2011**, 133: 19386–19392.

Casteels C, Koole M, Celen S, Bormans G and Laere K Van: Preclinical evaluation and quantification of [^{18}F]MK-9470 as a radioligand for PET imaging of the type 1 cannabinoid receptor in rat brain. *Eur J Nucl Med Mol Imaging*. **2012**, 39: 1467–1477.

Celen S, Rokka J, Gilbert TM, Koole M, Vermeulen I, Serdons K, Schroeder FA, Wagner FF, Bleeser T, Hightower BG, Hu J, Rahal D, Beyzavi MH, Vanduffel W, Van Laere K, Kranz JE, Hooker JM, Bormans G and Cawthorne CJ: Translation of HDAC6 PET imaging using [^{18}F]EKZ-001–cGMP production and measurement of HDAC6 target occupancy in nonhuman primates. *ACS Chem Neurosci*. **2020**, 11: 1093–1101.

Charalambous A, Marciniak G, Shiue C-Y, Dewey SL, Schlyer DJ, Wolf AP and Makriyannis A: PET studies in the primate brain and biodistribution in mice using (−)-5′-^{18}F-Δ^8-THC. *Pharmacol Biochem Behav*. **1991**, 40: 503–507.

Chatt J and Shaw BL: 345. Alkyls and aryls of transition metals. Part III. Nickel(II) derivatives. *J Chem Soc*. **1960**, No. 0: 1718–1729.

Chen X, Kudo T, Lapa C, Buck A and Higuchi T: Recent advances in radiotracers targeting norepinephrine transporter: structural development and radiolabeling improvements. *J Neural Transm*. **2020**, 127: 851–873.

Chirakal R, Adams RM, Firnau G, Schrobilgen GJ, Coates G and Garnett ES: Electrophilic ^{18}F from a siemens 11 MeV proton-only cyclotron. *Nucl Med Biol*. **1995**, 22: 111–116.

Chirakal R, Firnau G, Schrobilgen GJ, Mckay J and Garnett ES: The synthesis of [^{18}F]Xenon difluoride from [^{18}F]fluoride gas. *Int J Appl Radiat Isot*. **1984**, 35: 401–404.

Chun J-H, Lu S, Lee Y-S and Pike VW: Fast and high-yield microreactor syntheses of ortho-substituted [^{18}F]fluoroarenes from reactions of [^{18}F]fluoride ion with diaryliodonium salts. *J Org Chem*. **2010**, 75: 3332–3338.

Chun J-H, Morse CL, Chin FT and Pike VW: No-carrier-added [^{18}F]fluoroarenes from the radiofluorination of diaryl sulfoxides. *Chem. Commun.* **2013**, 49: 2151–2153.

Chun J-H and Pike VW: Single-step syntheses of no-carrier-added functionalized [^{18}F]fluoroarenes as labeling synthons from diaryliodonium salts. *Org Biomol Chem*. **2013**, 11: 6300–6306.

Coenen HH: Fluorine-18 labeling methods: Features and possibilities of basic reactions. In *PET Chemistry - The Driving Force in Molecular Imaging*; Schubiger PA, Lehmann L, Friebe M, Eds.; Springer, Berlin, Heidelberg, **2007**; pp 15–50.

Coenen HH and Moerlein SM: Regiospecific aromatic fluorodemetallation of group IVb metalloarenes using elemental fluorine or acetyl hypofluorite. *J Fluorine Chem*. **1987**, 36: 63–75.

Coenen HH, Colosimo M, Schüller M and Stöckin G: Mild and effective aliphatic and aromatic n.c.a. ^{18}F-fluorination using crown ether. *J Nucl Med*. **1985**, 26: P37.

Cole EL, Stewart MN, Littich R, Hoareau R and Scott PJH: Radiosyntheses using fluorine-18: The art and science of late stage fluorination. *Curr Top Med Chem*. **2014**, 14: 875–900.

Conti M and Eriksson L: Physics of pure and non-pure positron emitters for PET: a review and a discussion. *EJNMMI Phys*. **2016**, 3: 1–8.

Cortés González MA, Jiang X, Nordeman P, Antoni G and Szabó KJ: Rhodium-mediated ^{18}F-oxyfluorination of diazoketones using a fluorine-18-containing hypervalent iodine reagent. *Chem Commun*. **2019**, 55: 13358–13361.

Cortés González MA, Nordeman P, Bermejo Gómez A, Meyer DN, Antoni G, Schou M and Szabó KJ: [^{18}F]fluoro-benziodoxole: a no-carrier-added electrophilic fluorinating reagent. Rapid, simple radiosynthesis, purification and application for fluorine-18 labelling. *Chem Commun*. **2018**, 54: 4286–4289.

Dang H, Mailig M and Lalic G: Mild copper-catalyzed fluorination of alkyl triflates with potassium fluoride. *Angew Chemie Int Ed*. **2014**, 53: 6473–6476.

Dannals RF, Neumeyer JL, Milius RA, Ravert HT, Wilson AA and Wagner Jr. HN: Synthesis of a radiotracer for studying dopamine uptake sites *in vivo* using PET: 2β-carbomethoxy-3β-(4-fluorophenyl)-[N-^{11}C-methyl]tropane ([^{11}C]CFT or [^{11}C]WIN-35,428). *J Label Compd Radiopharm*. **1993**, 33: 147–152.

Deng X, Rong J, Wang L, Vasdev N, Zhang L, Josephson L and Liang SH: Chemistry for positron emission tomography: recent advances in ^{11}C-, ^{18}F-, ^{13}N-, and ^{15}O-labeling reactions. *Angew Chemie Int Ed*. **2019**, 58: 2580–2605.

Differding E and Ofner H: *N*-Fluorobenzenesulfonimide: a practical reagent for electrophilic fluorinations. *Synlett*. **1991**, 1991: 187–189.

Diksic M and Farrokhzad S: New synthesis of fluorine-18-labeled 6-fluoro-L-dopa by cleaving the carbon-silicon bond with fluorine. *J Nucl Med*. **1985**, 26: 1314–1318.

Ding Y-S, Lin K-S and Logan J: PET imaging of norepinephrine transporters. *Curr Pharm Des*. **2006**, 12: 3831–3845.

Ding Y-S, Lin K-S, Logan J, Benveniste H and Carter P: Comparative evaluation of positron emission tomography radiotracers for imaging the norepinephrine transporter: (*S,S*) and (*R,R*) enantiomers of reboxetine analogs ([^{11}C]methylreboxetine, 3-Cl-[^{11}C]methylreboxetine and [^{18}F]fluororeboxetine), (*R*)-[^{11}C]nisoxetine, [^{11}C]oxaprotiline and [^{11}C]lortalamine. *J Neurochem*. **2005**, 94: 337–351.

Dolbier WR, Li A-R, Koch CJ, Shiue C-Y and Kachur A V: [^{18}F]-EF5, a marker for PET detection of hypoxia: synthesis of precursor and a new fluorination procedure. *Appl Radiat Isot*. **2001**, 54: 73–80.

Donohue SR, Krushinski JH, Pike VW, Chernet E, Phebus L, Chesterfield AK, Felder CC, Halldin C and Schaus JM: Synthesis, *ex vivo* evaluation, and radiolabeling of potent 1,5-diphenylpyrrolidin-2-one cannabinoid subtype-1 receptor ligands as candidates for *in*

vivo imaging. *J Med Chem*. **2008a**, 51: 5833–5842.

Donohue SR, Pike VW, Finnema SJ, Truong P, Andersson J, Gulyás B and Halldin C: Discovery and labeling of high-affinity 3,4-diarylpyrazolines as candidate radioligands for *in vivo* imaging of cannabinoid subtype-1 (CB_1) Receptors. *J Med Chem*. **2008b**, 51: 5608–5616.

Eckelman WC: Sensitivity of new radiopharmaceuticals. *Nucl Med Biol*. **1998**, 25: 169–173.

Eckelman WC, Kilbourn MR and Mathis CA: Discussion of targeting proteins *in vivo*: *in vitro* guidelines. *Nucl Med Biol*. **2006**, 33: 449–451.

Ehrenkaufer RE and MacGregor RR: Synthesis of [^{18}F]perchloryl fluoride and its reactions with functionalized aryl lithiums. *Int J Appl Radiat Isot*. **1983**, 34: 613–615.

Ehrenkaufer RE and MacGregor RR: ^{18}F-perchloryl fluoride: synthesis and reactions. *J Label Compd Radiopharm*. **1982**, 19: 1637–1638.

Elsinga P, Hatano K and Ishiwata K: PET tracers for imaging of the dopaminergic system. *Curr Med Chem*. **2006**, 13: 2139–2153.

Elsinga P, Todde S, Penuelas I, Meyer G, Farstad B, Faivre-Chauvet A, Mikolajczak R, Westera G, Gmeiner-Stopar T, Decristoforo C and EANM TRC of the: Guidance on current good radiopharmacy practice (cGRPP) for the small-scale preparation of radiopharmaceuticals. *Eur J Nucl Med Mol Imaging*. **2010**, 37: 1049–1062.

European Commission: EudraLex - Volume 4: Guidelines of Good Manufacturing Practice (GMP) for Medicinal Products for Human and Veterinary Use (91/356/EEC, 2003/94/EC, 91/412/EEC). https://ec.europa.eu/health/documents/eudralex/vol-4_en (Accessed Aug 1st, 2020).

European Commission: EudraLex - Volume 4: Guidelines of Good Manufacturing Practice (GMP) for Medicinal Products for Human and Veterinary Use. Annex 3: Manufacture of Radiopharmaceuticals. https://ec.europa.eu/health/documents/eudralex/vol-4_en (Accessed Aug 1st, 2020).

European Commission: EudraLex - Volume 4: Guidelines of Good Manufacturing Practice (GMP) for medicinal products for human and veterinary use. Annex 15: Qualification and validation. https://ec.europa.eu/health/documents/eudralex/vol-4_en (Accessed Aug 1st, 2020).

European Parliament and Council of the European Union: Directive 2001/83/EC of the European Parliament and of the Council of 6 November 2001 on the Community code relating to medicinal products for human use. https://ec.europa.eu/health/sites/health/files/files/eudralex/vol-1/dir_2001_83_consol_2012/dir_2001_83_cons_2012_en.pdf (Accessed Aug 1st, 2020).

European Pharmacopoeia: *5.20. Metal catalyst or metal reagent residues*, 9th ed.; Strasbourg, **2013**.

Fahey DR and Mahan JE: Oxidative additions of aryl, vinyl, and acyl halides to triethylphosphinenickel(0) complexes. *J Am Chem Soc*. **1977**, 99: 2501–2508.

Fan H, Ravert HT, Holt DP, Dannals RF and Horti AG: Synthesis of 1-(2,4-dichlorophenyl)-4-cyano-5-(4-[^{11}C]methoxyphenyl)-*N*-(piperidin-1-yl)-1*H*-pyrazole-3-carboxamide ([^{11}C]JHU75528) and 1-(2-bromophenyl)-4-cyano-5-(4-[^{11}C]methoxy-phenyl)-*N*-(piperidin-1-yl)-1*H*-pyrazole-3-carboxamide ([^{11}C]JHU75575) as potential radioligands for PET imaging of cerebral cannabinoid receptor. *J Label Compd Radiopharm*. **2006**, 49: 1021–1036.

Fattore L: Cannabinoids in Neurologic and Mental Disease; Fattore L, Ed.; Elsevier Inc: San Diego, United States, **2015**; pp 1–452.

Fier PS and Hartwig JF: Copper-mediated fluorination of aryl iodides. *J Am Chem Soc*. **2012**, 134: 10795–10798.

Fier PS, Luo J and Hartwig JF: Copper-mediated fluorination of arylboronate esters. Identification of a copper(III)fluoride complex. *J Am Chem Soc*. **2013**, 135: 2552–2559.

Firnau G, Chirakal R and Garnett ES: Aromatic radiofluorination with [^{18}F]fluorine gas: 6-[^{18}F]fluoro-L-dopa. *J Nucl Med*. **1984**, 25: 1228–1233.

Fowler JS, Shiue C-Y, Wolf AP, Salvadori PA and MacGregor RR: Synthesis of ^{18}F-labeled acetyl hypofluorite for radiotracer synthesis. *J Label Compd Radiopharm*. **1982**, 19: 1634–1635.

Frank R and Hargreaves R: Clinical biomarkers in drug discovery and development. *Nat Rev Drug Discovery*. **2003**, 2: 566–580.

Füchtner F, Preusche S, Mäding P, Zessin J and Steinbach J: Factors affecting the specific activity of [^{18}F]fluoride from a [^{18}O]water target. *Nuklearmedizin*. **2008**, 47: 116–119.

Furuya T and Ritter T: Fluorination of boronic acids mediated by silver(I) triflate. *Org Lett*. **2009**, 11: 2860–2863.

Furuya T, Strom AE and Ritter T: Silver-mediated fluorination of functionalized aryl stannanes. *J Am Chem Soc*. **2009**, 131: 1662.

Gamache RF, Waldmann C and Murphy JM: Copper-mediated oxidative fluorination of aryl stannanes with fluoride. *Org Lett*. **2016**, 18: 4522–4525.

Gatley SJ and Shaughnessy WJ: Production of ^{18}F-labeled compounds with $^{18}F^{-}$ produced with a 1-MW Research reactor. *Int J Appl Radiat Isot*. **1982**, 33: 1325–1330.

George N, Gean EG, Nandi A, Frolov B, Zaidi E, Lee H, Brašić JR and Wong DF: Advances in CNS imaging agents: focus on PET and SPECT tracers in experimental and clinical use. *CNS Drugs*. **2015**, 29: 313–330.

Gibson R, Donald Burns H, Hamill T, Eng W, Francis B and Ryan C: Non-invasive radiotracer imaging as a tool for drug development. *Curr Pharm Des*. **2000**, 6: 973–989.

Gillings N, Todde S, Behe M, Decristoforo C, Elsinga P, Ferrari V, Hjelstuen O, Peitl PK, Koziorowski J, Laverman P, Mindt TL, Ocak M and Patt M: EANM guideline on the validation of analytical methods for radiopharmaceuticals. *EJNMMI Radiopharm Chem*. **2020**, 5: 7.

Gillis EP, Eastman KJ, Hill MD, Donnelly DJ and Meanwell NA: Applications of fluorine in medicinal chemistry. *J Med Chem*. **2015**, 58: 8315–8359.

Gourand F, Patin D, Henry A, Ibazizène M, Dhilly M, Fillesoye F, Tirel O, Tintas M-L, Papamicaël C, Levacher V and Barré L: Chemical delivery system of MIBG to the central nrvous system: synthesis, ^{11}C-radiosynthesis, and *in vivo* evaluation. *ACS Med Chem Lett*. **2019**, 10: 352–357.

Graham TJA, Lambert RF, Ploessl K, Kung HF and Doyle AG: Enantioselective radiosynthesis of positron emission tomography (PET) tracers containing [^{18}F]fluorohydrins. *J Am Chem Soc*. **2014**, 136: 5291–5294.

Haaparanta M, Bergman J, Laakso A, Hietala J and Solin O: [^{18}F]CFT ([^{18}F]WIN 35,428), a radioligand to study the dopamine transporter with PET: Biodistribution in rats. *Synapse*. **1996**, 23: 321–327.

Hall DG: Structure, properties, and preparation of boronic acid derivatives. Overview of their reactions and applications. In *Boronic acids: preparation and applications in organic synthesis and medicine*; Hall DG, Ed.; WILEY-VCH Verlag GmbH & Co.KGaA: Weinheim, Germany, **2005**; p 8.

Hamacher K, Coenen HH and Stöcklin G: Efficient stereospecific synthesis of no-carrier-added 2-[^{18}F]fluoro-2-deoxy-D-glucose using aminopolyether supported nucleophilic substitution. *J Nucl Med*. **1986**, 27: 235–238.

Hirvonen J: *In vivo* imaging of the cannabinoid CB_1 receptor with positron emission tomography. *Clin Pharmacol Ther*. **2015**, 97: 565–567.

Hoover A, Lazari M, Ren H, Narayanam MK, Murphy J, van Dam M, Hooker J and Ritter T: A Transmetalation reaction enables the synthesis of [^{18}F]5-fluorouracil from [^{18}F]fluoride for human PET imaging. *Organometallics*. **2016**, 35: 1008–1014.

Horti AG, Fan H, Kuwabara H, Hilton J, Ravert HT, Holt DP, Alexander M, Kumar A, Rahmim A, Scheffel U, Wong DF and Dannals RF: ^{11}C-JHU75528: A radiotracer for PET imaging of CB_1 cannabinoid receptors. *J Nucl Med*. **2006**, 47: 1689–1696.

Horti A and Laere K: Development of radioligands for *in vivo* imaging of type 1 cannabinoid receptors (CB_1) in human brain. *Curr Pharm Des*. **2008**, 14: 3363–3383.

Howlett AC, Barth F, Bonner TI, Cabral G, Casellas P, Devane WA, Felder CC, Herkenham M, Mackie K, Martin BR, Mechoulam R and Pertwee RG: International union of pharmacology. XXVII. Classification of cannabinoid receptors. *Pharmacol Rev*. **2002**, 54: 161–202.

Huang X, Liu W, Ren H, Neelamegam R, Hooker JM and Groves JT: Late stage benzylic C–H fluorination with [^{18}F]fluoride for PET

imaging. *J Am Chem Soc*. **2014**, 136: 6842–6845.

Huffman LM, Casitas A, Font M, Canta M, Costas M, Ribas X and Stahl SS: Observation and mechanistic study of facile C-O bond formation between a well-defined aryl-copper(III) complex and oxygen nucleophiles. *Chem – A Eur J*. **2011**, 17: 10643–10650.

Ichiishi N, Brooks AF, Topczewski JJ, Rodnick ME, Sanford MS and Scott PJH: Copper-catalyzed [^{18}F]fluorination of (mesityl)(aryl)iodonium salts. *Org Lett*. **2014**, 16: 3224–3227.

Ichiishi N, Canty AJ, Yates BF and Sanford MS: Cu-catalyzed fluorination of diaryliodonium salts with KF. *Org Lett*. **2013**, 15: 5134–5137.

Ido T, Wan C-N, Casella V, Fowler JS, Wolf AP, Reivich M and Kuhl DE: Labeled 2-deoxy-D-glucose analogs. ^{18}F-labeled 2-deoxy-2-fluoro-D-glucose, 2-deoxy-2-fluoro-D-mannose and ^{14}C-2-deoxy-2-fluoro-D-glucose. *J Label Compd Radiopharm*. **1978**, 14: 175–183.

Imazaki Y, Shirakawa E, Ueno R and Hayashi T: Ruthenium-catalyzed transformation of aryl and alkenyl triflates to halides. *J Am Chem Soc*. **2012**, 134: 14760–14763.

International Council for Harmonisation of Technical Requirements for Pharmaceuticals for Human Use: Validation of analytical procedures: text and methodology Q2(R1). https://ich.org (Accessed Aug 10th, 2020).

International Council for Harmonisation of Technical Requirements for Pharmaceuticals for Human Use: Guideline for residual solvents Q3C(R6). https://ich.org (Accessed Aug 10th, 2020).

International Council for Harmonisation of Technical Requirements for Pharmaceuticals for Human Use: Guideline for elemental impurities Q3D(R1). https://ich.org (Accessed Aug 10th, 2020).

Irie T, Fukushi K, Ido T, Nozaki T and Kasida Y: ^{18}F-fluorination by crown ether-metal fluoride: II. Non-carrier-added labeling method. *Int J Appl Radiat Isot*. **1984**, 35: 517–520.

Irie T, Fukushi K, Ido T, Nozaki T and Kasida Y: ^{18}F-Fluorination by crown ether—metal fluoride: (I) On labeling ^{18}F-21-fluoroprogesterone. *Int J Appl Radiat Isot*. **1982**, 33: 1449–1452.

Ishiwata K, Ido T, Mejia AA, Ichihashi M and Mishima Y: Synthesis and radiation dosimetry of 4-borono-2-[^{18}F]fluoro-D,L-phenylalanine: A target compound for PET and boron neutron capture therapy. *Int J Radiat Appl Instrumentation Part A Appl Radiat Isot*. **1991**, 42: 325–328.

Jacobson O, Kiesewetter DO and Chen X: Fluorine-18 radiochemistry, labeling strategies and synthetic routes. *Bioconjugate Chem*. **2015**, 26: 1–18.

Jordan CJ and Xi Z-X: Progress in brain cannabinoid CB_2 receptor research: From genes to behavior. *Neurosci Biobehav Rev*. **2019**, 98: 208–220.

Kalow JA and Doyle AG: Enantioselective ring opening of epoxides by fluoride anion promoted by a cooperative dual-catalyst system. *J Am Chem Soc*. **2010**, 132: 3268–3269.

Kamlet AS, Neumann CN, Lee E, Carlin SM, Moseley CK, Stephenson N, Hooker JM and Ritter T: Application of palladium-mediated ^{18}F-fluorination to PET radiotracer development: overcoming hurdles to translation. *PLoS One*. **2013**, 8: e59187.

Kane-Maguire LAP, Honig ED and Sweigart DA: Nucleophilic addition to coordinated cyclic π-hydrocarbons: mechanistic and synthetic studies. *Chem Rev*. **1984**, 84: 525–543.

Katoch-Rouse R, Pavlova OA, Caulder T, Hoffman AF, Mukhin AG and Horti AG: Synthesis, structure−activity relationship, and evaluation of SR141716 analogues: development of central cannabinoid receptor ligands with lower lipophilicity. *J Med Chem*. **2003**, 46: 642–645.

Khotavivattana T, Verhoog S, Tredwell M, Pfeifer L, Calderwood S, Wheelhouse K, Lee Collier T and Gouverneur V: ^{18}F-labeling of aryl-SCF_3, -OCF_3 and -$OCHF_2$ with [^{18}F]fluoride. *Angew Chemie Int Ed*. **2015**, 54: 9991–9995.

Kilbourn MR and Huizenga JR: *Fluorine-18 Labeling of Radiopharmaceuticals*; Nuclear science series; National Academy Press, **1990**.

Kim DW, Jeong H-J, Lim ST and Sohn M-H: Tetrabutylammonium tetra(*tert*-butyl alcohol)-coordinated fluoride as a facile

fluoride source. *Angew Chemie Int Ed*. **2008a**, 47: 8404–8406.

Kim DW, Jeong, Lim ST, Sohn M-H, Katzenellenbogen JA and Chi DY: Facile nucleophilic fluorination reactions using *tert*-alcohols as a reaction medium: Significantly enhanced reactivity of alkali metal fluorides and improved selectivity. *J Org Chem*. **2008b**, 73: 957–962.

King AE, Brunold TC and Stahl SS: Mechanistic study of copper-catalyzed aerobic oxidative coupling of arylboronic esters and methanol: insights into an organometallic oxidase reaction. *J Am Chem Soc*. **2009**, 131: 5044–5045.

Kirjavainen AK, Forsback S, Grönroos TJ, Haavisto L, Haaparanta M and Solin O: Electrophilic addition of chlorine monofluoride for PET tracers. *Mol Imaging Biol*. **2013**, 15: 131–135.

Kirjavainen AK, Forsback S, López-Picón FR, Marjamäki P, Takkinen J, Haaparanta-Solin M, Peters D and Solin O: ^{18}F-labeled norepinephrine transporter tracer [^{18}F]NS12137: radiosynthesis and preclinical evaluation. *Nucl Med Biol*. **2018**, 56: 39–46.

Klenner MA, Pascali G, Zhang B, Sia TR, Spare LK, Krause-Heuer AM, Aldrich-Wright JR, Greguric I, Guastella AJ, Massi M and Fraser BH: A Fluorine-18 radiolabeling method enabled by rhenium(I) complexation circumvents the requirement of anhydrous conditions. *Chem – A Eur J*. **2017**, 23: 6499–6503.

Klenner MA, Zhang B, Ciancaleoni G, Howard JK, Maynard-Casely HE, Clegg JK, Massi M, Fraser BH and Pascali G: Rhenium(I) complexation–dissociation strategy for synthesising fluorine-18 labelled pyridine bidentate radiotracers. *RSC Adv*. **2020**, 10: 8853–8865.

Konovalov AI, Gorbacheva EO, Miloserdov FM and Grushin VV: Ruthenium-catalyzed nucleophilic fluorination of halobenzenes. *Chem Commun*. **2015**, 51: 13527–13530.

Korguth M, Degrado T, Holden J and Gatley S: Effects of reaction conditions on rates of incorporation of no-carrier added F-18 fluoride into several organic compounds. *J Label Compd Radiopharm*. **1988**, 25: 369–381.

Krzyczmonik A, Keller T, Kirjavainen AK, Forsback S and Solin O: Vacuum ultraviolet photon–mediated production of [^{18}F]F_2. *J Label Compd Radiopharm*. **2017a**, 60: 186–193.

Krzyczmonik A, Keller T, Kirjavainen AK, Lahdenpohja S, Forsback S and Solin O: Use of SF_6 for the production of electrophilic ^{18}F-fluorination reagents. *J Fluorine Chem*. **2017b**, 204: 90–97.

Kung M-P and Kung HF: Mass effect of injected dose in small rodent imaging by SPECT and PET. *Nucl Med Biol*. **2005**, 32: 673–678.

Kurosawa H, Ohnishi H, Emoto M, Chatani N, Kawasaki Y, Murai S and Ikeda I: Preparation and reductive elimination of (eta$_3$-allyl)(aryl)nickel(II) complexes: unusually facile eta$_3$-allyl-aryl coupling on nickel having an 18-electron configuration. *Organometallics*. **1990**, 9: 3038–3042.

Laboratoire National Henri Becquerel: Atomic and Nuclear data. http://www.lnhb.fr/nuclear-data/nuclear-data-table/ (Accessed Sep 14th, 2020).

Lambrecht RM, Neirinckx R and Wolf AP: Cyclotron isotopes and radiopharmaceuticals — XXIII: Novel anhydrous ^{18}F-fluorinating intermediates. *Int J Appl Radiat Isot*. **1978**, 29: 175–183.

Lan R, Liu Q, Fan P, Lin S, Fernando SR, McCallion D, Pertwee R and Makriyannis A: Structure−activity relationships of pyrazole derivatives as cannabinoid receptor antagonists. *J Med Chem*. **1999**, 42: 769–776.

Lange R, ter Heine R, Decristoforo C, Peñuelas I, Elsinga PH, van der Westerlaken MML and Hendrikse NH: Untangling the web of European regulations for the preparation of unlicensed radiopharmaceuticals. *Nucl Med Commun*. **2015**, 36: 414–422.

Lee E, Hooker JM and Ritter T: Nickel-mediated oxidative fluorination for PET with aqueous [^{18}F]fluoride. *J Am Chem Soc*. **2012**, 134: 17456–17458.

Lee E, Kamlet AS, Powers DC, Neumann CN, Boursalian GB, Furuya T, Choi DC, Hooker JM and Ritter T: A fluoride-derived electrophilic late-stage fluorination reagent for PET imaging. *Science*. **2011**, 334: 639–642.

Lee H, Börgel J and Ritter T: Carbon–fluorine reductive elimination from nickel(III)

complexes. *Angew Chemie Int Ed*. **2017**, 56: 6966–6969.

Lemaire CF, Aerts JJ, Voccia S, Libert LC, Mercier F, Goblet D, Plenevaux AR and Luxen AJ: Fast production of highly reactive no-carrier-added [^{18}F]fluoride for the labeling of radiopharmaceuticals. *Angew Chemie Int Ed*. **2010**, 49: 3161–3164.

Leroux F, Jeschke P and Schlosser M: α-Fluorinated ethers, thioethers, and amines: anomerically biased species. *Chem Rev*. **2005**, 105: 827–856.

Li Z, Gifford A, Liu Q, Thotapally R, Ding Y-S, Makriyannis A and Gatley SJ: Candidate PET radioligands for cannabinoid CB_1 receptors: [^{18}F]AM5144 and related pyrazole compounds. *Nucl Med Biol*. **2005**, 32: 361–366.

Liotta CL and Harris HP: Chemistry of naked anions. I. Reactions of the 18-crown-6 complex of potassium fluoride with organic substrates in aprotic organic solvents. *J Am Chem Soc*. **1974**, 96: 2250–2252.

Liotta C and Starks CM: *Phase Transfer Catalysis: Principles and Techniques*, 1st ed.; Academic Press Inc: New York, **1978**.

Liu H, Audisio D, Plougastel L, Decuypere E, Buisson D-A, Koniev O, Kolodych S, Wagner A, Elhabiri M, Krzyczmonik A, Forsback S, Solin O, Gouverneur V and Taran F: Ultrafast click chemistry with fluorosydnones. *Angew Chemie Int Ed*. **2016**, 55: 12073–12077.

Liu S, Shen B, T. Chin F and Cheng Z: Recent progress in radiofluorination of peptides for PET molecular imaging. *Curr Org Synth*. **2011**, 8: 584–592.

Liu W, Huang X, Cheng M-J, Nielsen RJ, Goddard WA and Groves JT: Oxidative aliphatic C-H fluorination with fluoride ion catalyzed by a manganese porphyrin. *Science*. **2012**, 337: 1322–1325.

Liu W, Huang X, Placzek MS, Krska SW, McQuade P, Hooker JM and Groves JT: Site-selective ^{18}F-fluorination of unactivated C–H bonds mediated by a manganese porphyrin. *Chem Sci*. **2018**, 9: 1168–1172.

López-Picón FR, Kirjavainen AK, Forsback S, Takkinen JS, Peters D, Haaparanta-Solin M and Solin O: *In vivo* characterization of a novel norepinephrine transporter PET tracer [^{18}F]NS12137 in adult and immature Sprague Dawley rats. *Theranostics*. **2019**, 9: 11–19.

Maeda M, Fukumura T and Kojima M: The dimethylsulfonium moiety as a leaving group in aromatic radiofluorination using tetra-n-butylammonium [^{18}F]fluoride. *Int J Radiat Appl Instrumentation Part A Appl Radiat Isot*. **1987**, 38: 307–310.

Mai BK, Szabó KJ and Himo F: Mechanisms of Rh-catalyzed oxyfluorination and oxytrifluoromethylation of diazocarbonyl compounds with hypervalent fluoroiodine. *ACS Catal*. **2018**, 8: 4483–4492.

Makaravage KJ, Brooks AF, Mossine A V, Sanford MS and Scott PJH: Copper-mediated radiofluorination of arylstannanes with [^{18}F]KF. *Org Lett*. **2016**, 18: 5440–5443.

Mathews WB, Ravert HT, Musachio JL, Frank RA, Rinaldi-Carmona M, Barth F and Dannals RF: Synthesis of [^{18}F]SR144385: a selective radioligand for positron emission tomographic studies of brain cannabinoid receptors. *J Label Compd Radiopharm*. **1999**, 42: 589–596.

Mathews WB, Scheffel U, Rauseo PA, Ravert HT, Frank RA, Ellames GJ, Herbert JM, Barth F, Rinaldi-Carmona M and Dannals RF: Carbon-11 labeled radioligands for imaging brain cannabinoid receptors. *Nucl Med Biol*. **2002**, 29: 671–677.

McCluskey SP, Plisson C, Rabiner EA and Howes O: Advances in CNS PET: the state-of-the-art for new imaging targets for pathophysiology and drug development. *Eur J Nucl Med Mol Imaging*. **2020**, 47: 451–489.

Mechoulam R and Parker LA: The endocannabinoid system and the brain. *Annu Rev Psychol*. **2013**, 64: 21–47.

Mizuta S, Stenhagen ISR, O'Duill M, Wolstenhulme J, Kirjavainen AK, Forsback SJ, Tredwell M, Sandford G, Moore PR, Huiban M, Luthra SK, Passchier J, Solin O and Gouverneur V: Catalytic decarboxylative fluorination for the synthesis of tri- and difluoromethyl arenes. *Org Lett*. **2013**, 15: 2648–2651.

Modemann DJ, Zlatopolskiy BD, Urusova EA, Zischler J, Craig A, Ermert J, Guliyev M, Endepols H and Neumaier B: 2-[^{18}F]Fluorophenylalanine: synthesis by nucleophilic ^{18}F-fluorination and preliminary biological evaluation. *Synthesis*. **2019**, 51: 664–676.

Moissan H: Sur la décomposition de l'acide fluorhydrique par un courant électrique (On the decomposition of hydrofluoric acid by an electric current). *Comptes rendus l'Académie des Sci*. **1886**, 103: 202–205.

Moriguchi S, Kimura Y, Ichise M, Arakawa R, Takano H, Seki C, Ikoma Y, Takahata K, Nagashima T, Yamada M, Mimura M and Suhara T: PET quantification of the norepinephrine transporter in human brain with (*S,S*)-^{18}F-FMeNER-D$_2$. *J Nucl Med*. **2017**, 58: 1140–1145.

Morón JA, Brockington A, Wise RA, Rocha BA and Hope BT: Dopamine uptake through the norepinephrine transporter in brain regions with low levels of the dopamine transporter: Evidence from knock-out mouse lines. *J Neurosci*. **2002**, 22: 389–395.

Mossine AV, Tanzey SS, Brooks AF, Makaravage KJ, Ichiishi N, Miller JM, Henderson BD, Skaddan MB, Sanford MS and Scott PJH: One-pot synthesis of high molar activity 6-[^{18}F]fluoro- l -DOPA by Cu-mediated fluorination of a BPin precursor. *Org Biomol Chem*. **2019**, 17: 8701–8705.

Mossine AV, Brooks AF, Ichiishi N, Makaravage KJ, Sanford MS and Scott PJH: Development of customized [^{18}F]fluoride elution techniques for the enhancement of copper-mediated late-stage radiofluorination. *Sci Reports*. **2017**, 7: 233.

Mossine AV, Brooks AF, Makaravage KJ, Miller JM, Ichiishi N, Sanford MS and Scott PJH: Synthesis of [^{18}F]arenes via the copper-mediated [^{18}F]fluorination of boronic acids. *Org Lett*. **2015**, 17: 5780–5783.

Mossine AV, Tanzey SS, Brooks AF, Makaravage KJ, Ichiishi N, Miller JM, Henderson BD, Erhard T, Bruetting C, Skaddan MB, Sanford MS and Scott PJH: Synthesis of high-molar-activity [^{18}F]6-fluoro-L-DOPA suitable for human use via Cu-mediated fluorination of a BPin precursor. *Nat Protoc*. **2020**, 15: 1742–1759.

Mu L, Fischer CR, Holland JP, Becaud J, Schubiger PA, Schibli R, Ametamey SM, Graham K, Stellfeld T, Dinkelborg LM and Lehmann L: ^{18}F-Radiolabeling of aromatic compounds using triarylsulfonium salts. *Eur J Org Chem*. **2012**, 2012: 889–892.

Mu X, Zhang H, Chen P and Liu G: Copper-catalyzed fluorination of 2-pyridyl aryl bromides. *Chem Sci*. **2014**, 5: 275–280.

Mulholland GK, Mangner TJ, Jewett DM and Kilbourn MR: Polymer-supported nucleophilic radiolabeling reactions with [^{18}F]fluoride and [^{11}C]cyanide ion on quaternary ammonium resins. *J Label Compd Radiopharm*. **1989**, 26: 378–380.

Namavari M, Bishop A, Satyamurthy N, Bida G and Barrio JR: Regioselective radiofluorodestannylation with [^{18}F]F$_2$ and [^{18}F]CH$_3$COOF: A high yield synthesis of 6-[^{18}F]fluoro-l-dopa. *Int J Radiat Appl Instrumentation Part A Appl Radiat Isot*. **1992**, 43: 989–996.

Neirinckx RD, Lambrecht RM and Wolf AP: Cyclotron isotopes and radiopharmaceuticals — XXV An anhydrous ^{18}F-fluorinating intermediate: Trifluoromethyl hypofluorite. *Int J Appl Radiat Isot*. **1978**, 29: 323–327.

Neumann CN, Hooker JM and Ritter T: Concerted nucleophilic aromatic substitution with ^{19}F$^-$ and ^{18}F$^-$. *Nature*. **2016**, 534: 369–373.

Ni R, Mu L and Ametamey S: Positron emission tomography of type 2 cannabinoid receptors for detecting inflammation in the central nervous system. *Acta Pharmacol Sin*. **2019**, 40: 351–357.

Nickles RJ, Daube ME and Ruth TJ: An ^{18}O$_2$ target for the production of [^{18}F]F$_2$. *Int J Appl Radiat Isot*. **1984**, 35: 117–122.

Nickles RJ, Gatley SJ, Votaw JR and Kornguth ML: Production of reactive fluorine-18. *Int J Radiat Appl Instrumentation Part A Appl Radiat Isot*. **1986**, 37: 649–661.

Nodwell MB, Yang H, Merkens H, Malik N, Čolović M, Björn Wagner, Martin RE, Bénard F, Schaffer P and Britton R: ^{18}F-Branched-chain amino acids: structure–activity relationships and PET imaging potential. *J Nucl Med*. **2019**, 60: 1003–1009.

Nodwell MB, Yang H, Čolović M, Yuan Z, Merkens H, Martin RE, Bénard F, Schaffer P and Britton R: ^{18}F-Fluorination of unactivated C–H bonds in branched aliphatic amino acids: direct synthesis of oncological positron emission tomography imaging agents. *J Am Chem Soc*. **2017**, 139: 3595–3598.

Nozaki T and Tanaka Y: The preparation of ^{18}F-labelled aryl fluorides. *Int J Appl Radiat Isot*. **1967**, 18: 111–119.

Nyffeler PT, Durón SG, Burkart MD, Vincent SP and Wong C-H: Selectfluor: mechanistic insight and applications. *Angew Chemie Int Ed*. **2005**, 44: 192–212.

Oberdorfer F, Hofmann E and Maier-Borst W: Preparation of ^{18}F-labelled *N*-fluoropyridinium triflate. *J Label Compd Radiopharm*. **1988a**, 25: 999–1005.

Oberdorfer F, Hofmann E and Maier-Borst W: Preparation of a new ^{18}F-labelled precursor: 1-[^{18}F]fluoro-2-pyridone. *Int J Radiat Appl Instrumentation Part A Appl Radiat Isot*. **1988b**, 39: 685–688.

Office of the Law Revision Counsel of the U.S. House of Representatives: 21 USC Ch. 9: Federal Food, Drug, and Cosmetic Act. 2020.

Otsuka M, Endo K and Shibata T: Catalytic S_NAr reaction of non-activated fluoroarenes with amines via Ru η^6-arene complexes. *Chem Commun*. **2010a**, 46: 336–338.

Otsuka M, Yokoyama H, Endo K and Shibata T: Facile catalytic S_NAr reaction of nonactivated fluoroarenes with amines using η^6-benzene ruthenium(II) complex. *Synlett*. **2010b**, 2010: 2601–2606.

Pape AR, Kaliappan KP and Kündig EP: Transition-metal-mediated dearomatization reactions. *Chem Rev*. **2000**, 100: 2917–2940.

Pike RD and Sweigart DA: Electrophilic reactivity of coordinated cyclic π-hydrocarbons. *Coord Chem Rev*. **1999**, 187: 183–222.

Pike VW and Aigbirhio FI: Reactions of cyclotron-produced [^{18}F]fluoride with diaryliodonium salts—a novel single-step route to no-carrier-added [^{18}F]fluoroarenes. *J Chem Soc, Chem Commun*. **1995**, 1995: 2215–2216.

Preshlock S, Tredwell M and Gouverneur V: ^{18}F-Labeling of arenes and heteroarenes for applications in positron emission tomography. *Chem Rev*. **2016**, 116: 719–766.

Purser S, Moore PR, Swallow S and Gouverneur V: Fluorine in medicinal chemistry. *Chem Soc Rev*. **2008**, 37: 320–330.

Qiao JX and Lam PYS: Copper-promoted carbon-heteroatom bond cross-coupling with boronic acids and derivatives. *Synthesis*. **2011**, 2011: 829–856.

Ren H, Wey H-Y, Strebl M, Neelamegam R, Ritter T and Hooker JM: Synthesis and imaging validation of [^{18}F]MDL100907 enabled by Ni-mediated fluorination. *ACS Chem Neurosci*. **2014**, 5: 611–615.

Richarz R, Krapf P, Zarrad F, Urusova EA, Neumaier B and Zlatopolskiy BD: Neither azeotropic drying, nor base nor other additives: a minimalist approach to ^{18}F-labeling. *Org Biomol Chem*. **2014**, 12: 8094–8099.

Richter S and Wuest F: ^{18}F-Labeled peptides: the future Is bright. *Molecules*. **2014**, 19: 20536–20556.

Rickmeier J and Ritter T: Site-specific deoxyfluorination of small peptides with [^{18}F]fluoride. *Angew Chemie Int Ed*. **2018**, 57: 14207–14211.

Rinaldi-Carmona M, Barth F, Héaulme M, Shire D, Calandra B, Congy C, Martinez S, Maruani J, Néliat G, Caput D, Ferrara P, Soubrié P, Brelière JC and Fur G Le: SR141716A, a potent and selective antagonist of the brain cannabinoid receptor. *FEBS Lett*. **1994**, 350: 240–244.

Rose-Munch F, Gagliardini V, Renard C and Rose E: (η^6-Arene)tricarbonylchromium and (η^5-cyclohexadienyl) tricarbonylmanganese complexes: indirect nucleophilic substitutions. *Coord Chem Rev*. **1998**, 178–180: 249–268.

Ross TL, Ermert J, Hocke C and Coenen HH: Nucleophilic ^{18}F-fluorination of heteroaromatic iodonium salts with no-carrier-added [^{18}F]fluoride. *J Am Chem Soc*. **2007**, 129: 8018–8025.

Rostami A: *N*-Fluorobenzenesulfonimide [$(PhSO_2)_2NF$] - a neutral N-F-containing electrophilic fluorinating agent. *Synlett*. **2007**, 2007: 2924–2925.

Rotstein BH, Stephenson NA, Vasdev N and Liang SH: Spirocyclic hypervalent iodine(III)-mediated radiofluorination of non-activated and hindered aromatics. *Nat Commun*. **2014**, 5: 4365.

Sander K, Gendron T, Yiannaki E, Cybulska K, Kalber TL, Lythgoe MF and Årstad E: Sulfonium salts as leaving groups for aromatic labelling of drug-like small molecules with fluorine-18. *Sci Reports*. **2015**, 5: 9941.

Sather AC and Buchwald SL: The Evolution of Pd^0/Pd^{II}-catalyzed aromatic fluorination. *Acc Chem Res*. **2016**, 49: 2146–2157.

Satyamurthy N and Barrio JR: No-carrier-added nucleophilic ^{18}F-fluorination of aromatic compounds. WO2010/117435 A2, **2010**.

Satyamurthy N, Bida GT, Phelps ME and Barrio JR: *N*-[^{18}F]fluoro-*N*-alkylsulfonamides: Novel reagents for mild and regioselective radiofluorination. *Int J Radiat Appl Instrumentation Part A Appl Radiat Isot*. **1990**, 41: 733–738.

Savisto N, Bergman J, Aromaa J, Forsback S, Eskola O, Viljanen T, Rajander J, Johansson S, Grigg J, Luthra S and Solin O: Influence of transport line material on the molar activity of cyclotron produced [^{18}F]fluoride. *Nucl Med Biol*. **2018**, 64–65: 8–15.

Schou M, Halldin C, Sóvágó J, Pike VW, Hall H, Gulyás B, Mozley PD, Dobson D, Shchukin E, Innis RB and Farde L: PET evaluation of novel radiofluorinated reboxetine analogs as norepinephrine transporter probes in the monkey brain. *Synapse*. **2004**, 53: 57–67.

Schou M, Steiger C, Varrone A, Guilloteau D and Halldin C: Synthesis, radiolabeling and preliminary *in vivo* evaluation of [^{18}F]FE-PE2I, a new probe for the dopamine transporter. *Bioorg Med Chem Lett*. **2009**, 19: 4843–4845.

Schrobilgen GJ, Firnau G, Chirakal R and Garnett ES: Synthesis of [^{18}F]XeF_2, a novel agent for the preparation of ^{18}F-radiopharmaceuticals. *J Chem Soc, Chem Commun*. **1981**, 1981: 198.

Seeman P and Madras B: *Imaging of the human brain in health and disease*, 1st ed.; Seeman P, Madras B, Eds.; Academic Press Inc/Elsevier, **2013**.

Semmelhack MF, Helquist PM and Jones LD: Synthesis with zerovalent nickel. Coupling of aryl halides with bis(1,5-cyclooctadiene)nickel(0). *J Am Chem Soc*. **1971**, 93: 5908–5910.

Semmelhack MF and Chlenov A: (Arene)$Cr(CO)_3$ complexes: aromatic nucleophilic substitution. In *Transition metal arene π-complexes in organic synthesis and catalysis. Topics in organometallic chemistry, vol 7.*; Kündig PE, Ed.; Springer: Berlin, Heidelberg, **2004**; pp 43–69.

Shah A, W. Pike V and A. Widdowson D: The synthesis of [^{18}F]fluoroarenes from the reaction of cyclotron-produced [^{18}F]fluoride ion with diaryliodonium salts. *J Chem Soc Perkin Trans 1*. **1998**, No. 13: 2043–2046.

Sharninghausen LS, Brooks AF, Winton WP, Makaravage KJ, Scott PJH and Sanford MS: NHC-Copper mediated ligand-directed radiofluorination of aryl halides. *J Am Chem Soc*. **2020**, 142: 7362–7367.

Slavik R, Bieri D, Čermak S, Müller A, Krämer SD, Weber M, Schibli R, Ametamey SM and Mu L: Development and evaluation of novel PET tracers for imaging cannabinoid receptor type 2 in brain. *Chim Int J Chem*. **2014**, 68: 208–210.

Sloan ME, Grant CW, Gowin JL, Ramchandani VA and Le Foll B: Endocannabinoid signaling in psychiatric disorders: a review of positron emission tomography studies. *Acta Pharmacol Sin*. **2019**, 40: 342–350.

Solin O, Bergman J, Haaparanta M and Reissell A: Production of ^{18}F from water targets. Specific radioactivity and anionic contaminants. *Int J Radiat Appl Instrumentation Part A Appl Radiat Isot*. **1988**, 39: 1065–1071.

Stehouwer JS and Goodman MM: Fluorine-18 radiolabeled PET tracers for imaging monoamine transporters: dopamine, serotonin, and norepinephrine. *PET Clin*. **2009**, 4: 101–128.

Stenhagen ISR, Kirjavainen AK, Forsback SJ, Jorgensen CG, Robins EG, Luthra SK, Solin O and Gouverneur V: [^{18}F]Fluorination of an arylboronic ester using [^{18}F]selectfluor bis(triflate): application to 6-[^{18}F]fluoro-L-DOPA. *Chem Commun*. **2013**, 49: 1386–1388.

Strebl MG, Campbell AJ, Zhao W-N, Schroeder FA, Riley MM, Chindavong PS, Morin TM, Haggarty SJ, Wagner FF, Ritter T and Hooker JM: HDAC6 brain mapping with [^{18}F]bavarostat enabled by a Ru-mediated deoxyfluorination. *ACS Cent Sci*. **2017**, 3: 1006–1014.

Takkinen JS, López-Picón FR, Kirjavainen AK, Pihlaja R, Snellman A, Ishizu T, Löyttyniemi E, Solin O, Rinne JO and Haaparanta-Solin M: [^{18}F]FMPEP-d_2 PET imaging shows age- and genotype-dependent impairments in the availability of cannabinoid receptor 1 in a mouse model of Alzheimer's disease. *Neurobiol Aging*. **2018**, 69: 199–208.

Tamao K, Sumitani K and Kumada M: Selective carbon-carbon bond formation by cross-coupling of Grignard reagents with organic halides. Catalysis by nickel-phosphine complexes. *J Am Chem Soc*. **1972**, 94: 4374–4376.

Taoufik M, Cordonnier M-A, Santini CC, Basset J-M and Candy J-P: Surface organometallic chemistry on metals: controlled hydrogenolysis of Me_4Sn, Me_3SnR, Me_2SnR_2, $MeSnBu_3$ and $SnBu_4$ (R = methyl, n-butyl, tert-butyl, neopentyl, cyclohexyl) onto metallic rhodium supported on silica. *New J Chem*. **2004**, 28: 1531–1537.

Taylor NJ, Emer E, Preshlock S, Schedler M, Tredwell M, Verhoog S, Mercier J, Genicot C and Gouverneur V: Derisking the Cu-mediated ^{18}F-fluorination of heterocyclic positron emission tomography radioligands. *J Am Chem Soc*. **2017**, 139: 8267–8276.

Teare H, Robins EG, Årstad E, Luthra SK and Gouverneur V: Synthesis and reactivity of [^{18}F]-*N*-fluorobenzenesulfonimide. *Chem Commun*. **2007**, 2007: 2330–2332.

Teare H, Robins EG, Kirjavainen A, Forsback S, Sandford G, Solin O, Luthra SK and Gouverneur V: Radiosynthesis and evaluation of [^{18}F]Selectfluor *bis*(triflate). *Angew Chemie Int Ed*. **2010**, 49: 6821–6824.

Terry GE, Hirvonen J, Liow J-S, Zoghbi SS, Gladding R, Tauscher JT, Schaus JM, Phebus L, Felder CC, Morse CL, Donohue SR, Pike VW, Halldin C and Innis RB: Imaging and quantitation of cannabinoid CB_1 receptors in human and monkey brains using ^{18}F-labeled inverse agonist radioligands. *J Nucl Med*. **2010**, 51: 112–120.

Todde S, Peitl PK, Elsinga P, Koziorowski J, Ferrari V, Ocak EM, Hjelstuen O, Patt M, Mindt TL and Behe M: Guidance on validation and qualification of processes and operations involving radiopharmaceuticals. *EJNMMI Radiopharm Chem*. **2017**, 2: 8.

Toorongian SA, Mulholland GK, Jewett DM, Bachelor MA and Kilbourn MR: Routine production of 2-deoxy-2-[^{18}F]fluoro-D-glucose by direct nucleophilic exchange on a quaternary 4-aminopyridinium resin. *Int J Radiat Appl Instrumentation Part B Nucl Med Biol*. **1990**, 17: 273–279.

Torres GE, Caron MG and Gainetdinov RR: Plasma membrane monoamine transporters: structure, regulation and function. *Nat Rev Neurosci*. **2003**, 4: 13–25.

Tredwell M and Gouverneur V: ^{18}F-labeling of arenes. *Angew Chemie Int Ed*. **2012**, 51: 11426–11437.

Tredwell M, Preshlock SM, Taylor NJ, Gruber S, Huiban M, Passchier J, Mercier J, Génicot C and Gouverneur V: A General copper-mediated nucleophilic ^{18}F-fluorination of arenes. *Angew Chemie Int Ed*. **2014**, 53: 7751–7755.

Tsou TT and Kochi JK: Mechanism of oxidative addition. Reaction of nickel(0) complexes with aromatic halides. *J Am Chem Soc*. **1979**, 101: 6319–6332.

Tsujikawa T, Zoghbi SS, Hong J, Donohue SR, Jenko KJ, Gladding RL, Halldin C, Pike VW, Innis RB and Fujita M: *In vitro* and *in vivo* evaluation of ^{11}C-SD5024, a novel PET radioligand for human brain imaging of cannabinoid CB_1 receptors. *NeuroImage*. **2014**, 84: 733–741.

United States Pharmacopoeia: Residual solvents <467>. https://www.uspnf.com/ (Accessed Sep 15th, 2020).

Vaughan RA and Foster JD: Mechanisms of dopamine transporter regulation in normal and disease states. *Trends Pharmacol Sci*. **2013**, 34: 489–496.

Verhoog S, Pfeifer L, Khotavivattana T, Calderwood S, Collier TL, Wheelhouse K, Tredwell M and Gouverneur V: Silver-mediated ^{18}F-labeling of aryl-CF_3 and aryl-CHF_2 with ^{18}F-fluoride. *Synlett*. **2016**, 27: 25–28.

Visser GWM, van Halteren BW, Herscheid JDM, Brinkman GA and Hoekstra A: Reaction of acetyl hypofluorite with aromatic mercury compounds: a new selective fluorination method. *J Chem Soc, Chem Commun*. **1984**, No. 10: 655–656.

Walton JW and Williams JMJ: Catalytic S_NAr of unactivated aryl chlorides. *Chem Commun*. **2015**, 51: 2786–2789.

Waterhouse RN and Collier TL: Neuroreceptor imaging: applications, advances, and limitations. In *Molecular Imaging*; Ross B, Gambhir S, Eds.; Elsevier, **2020**; pp 1035–1059.

Watson DA, Su M, Teverovskiy G, Zhang Y, García-Fortanet J, Kinzel T and Buchwald SL: Formation of ArF from LPdAr(F): catalytic conversion of aryl triflates to aryl fluorides. *Science*. **2009**, 325: 1661–1664.

Wessmann SH, Henriksen G and Wester H-J: Cryptate mediated nucleophilic ^{18}F-

fluorination without azeotropic drying. *Nuklearmedizin*. **2012**, 51: 1–8.

Wilson AA, Patrick Johnson D, Mozley D, Hussey D, Ginovart N, Nobrega J, Garcia A, Meyer J and Houle S: Synthesis and *in vivo* evaluation of novel radiotracers for the *in vivo* imaging of the norepinephrine transporter. *Nucl Med Biol*. **2003**, 30: 85–92.

Wong EHF, Sonders MS, Amara SG, Tinholt PM, Piercey MFP, Hoffmann WP, Hyslop DK, Franklin S, Porsolt RD, Bonsignori A, Carfagna N and McArthur RA: Reboxetine: a pharmacologically potent, selective, and specific norepinephrine reuptake inhibitor. *Biol Psychiatry*. **2000**, 47: 818–829.

Wright JS, Kaur T, Preshlock S, Tanzey SS, Winton WP, Sharninghausen LS, Wiesner N, Brooks AF, Sanford MS and Scott PJH: Copper-mediated late-stage radiofluorination: five years of impact on preclinical and clinical PET imaging. *Clin Transl Imaging*. **2020**, 8: 167–206.

Yasuno F, Brown AK, Zoghbi SS, Krushinski JH, Chernet E, Tauscher J, Schaus JM, Phebus LA, Chesterfield AK, Felder CC, Gladding RL, Hong J, Halldin C, Pike VW and Innis RB: The PET radioligand [^{11}C]MePPEP binds reversibly and with high specific signal to cannabinoid CB_1 receptors in nonhuman primate brain. *Neuropsychopharmacology*. **2008**, 33: 259–269.

Ye Y and Sanford MS: Mild copper-mediated fluorination of aryl stannanes and aryl trifluoroborates. *J Am Chem Soc*. **2013**, 135: 4648–4651.

Ye Y, Schimler SD, Hanley PS and Sanford MS: $Cu(OTf)_2$-mediated fluorination of aryltrifluoroborates with potassium fluoride. *J Am Chem Soc*. **2013**, 135: 16292–16295.

Yu S-J, Reiner D, Shen H, Wu K-J, Liu Q-R and Wang Y: Time-dependent protection of CB_2 receptor agonist in stroke. *PLoS One*. **2015**, 10: e0132487.

Yuan W, Eriksson L and Szabó KJ: Rhodium-catalyzed geminal oxyfluorination and oxytrifluoro-methylation of diazocarbonyl compounds. *Angew Chemie Int Ed*. **2016a**, 55: 8410–8415.

Yuan Z, Cheng R, Chen P, Liu G and Liang SH: Efficient pathway for the preparation of aryl(isoquinoline)iodonium(III) salts and synthesis of radiofluorinated isoquinolines. *Angew Chemie Int Ed*. **2016b**, 55: 11882–11886.

Yuan Z, Nodwell MB, Yang H, Malik N, Merkens H, Bénard F, Martin RE, Schaffer P and Britton R: Site-selective, late-stage C−H ^{18}F-fluorination on unprotected peptides for positron emission tomography imaging. *Angew Chemie Int Ed*. **2018**, 57: 12733–12736.

Yuan Z, Yang H, Malik N, Čolović M, Weber DS, Wilson D, Bénard F, Martin RE, Warren JJ, Schaffer P and Britton R: Electrostatic effects accelerate decatungstate-catalyzed C–H fluorination using [^{18}F]- and [^{19}F]NFSI in small molecules and peptide mimics. *ACS Catal*. **2019**, 9: 8276–8284.

Zahniser NR and Doolen S: Chronic and acute regulation of Na^+/Cl^--dependent neurotransmitter transporters: drugs, substrates, presynaptic receptors, and signaling systems. *Pharmacol Ther*. **2001**, 92: 21–55.

Zanato C, Pelagalli A, Marwick KFM, Piras M, Dall'Angelo S, Spinaci A, Pertwee RG, Wyllie DJA, Hardingham GE and Zanda M: Synthesis, radio-synthesis and in vitro evaluation of terminally fluorinated derivatives of HU-210 and HU-211 as novel candidate PET tracers. *Org Biomol Chem*. **2017**, 15: 2086–2096.

Zarrad F, Zlatopolskiy B, Krapf P, Zischler J and Neumaier B: A Practical method for the preparation of ^{18}F-labeled aromatic amino acids from nucleophilic [^{18}F]fluoride and stannyl precursors for electrophilic radiohalogenation. *Molecules*. **2017**, 22: 2231.

Zeng F, Mun J, Jarkas N, Stehouwer JS, Voll RJ, Tamagnan GD, Howell L, Votaw JR, Kilts CD, Nemeroff CB and Goodman MM: Synthesis, radiosynthesis, and biological evaluation of carbon-11 and fluorine-18 labeled reboxetine analogues: potential positron emission tomography radioligands for *in vivo* imaging of the norepinephrine transporter. *J Med Chem*. **2009**, 52: 62–73.

Zhang B, Fraser BH, Klenner MA, Chen Z, Liang SH, Massi M, Robinson AJ and Pascali G: [^{18}F]Ethenesulfonyl fluoride as a practical radiofluoride relay reagent. *Chem – A Eur J*. **2019a**, 25: 7613–7617.

Zhang X, Basuli F and Swenson RE: An azeotropic drying-free approach for copper-mediated radiofluorination without addition of base. *J Label Compd Radiopharm*. **2019b**, 62: 139–145.

Zischler J, Kolks N, Modemann D, Neumaier B and Zlatopolskiy BD: Alcohol-enhanced Cu-mediated radiofluorination. *Chem - A Eur J*. **2017**, 23: 3251–3256.

Zischler J, Krapf P, Richarz R, Zlatopolskiy BD and Neumaier B: Automated synthesis of 4-[^{18}F]fluoroanisole, [^{18}F]DAA1106 and 4-[^{18}F]FPhe using Cu-mediated radiofluorination under "minimalist" conditions. *Appl Radiat Isot*. **2016**, 115: 133–137.

Zlatopolskiy BD, Zischler J, Krapf P, Zarrad F, Urusova EA, Kordys E, Endepols H and Neumaier B: Copper-mediated aromatic radiofluorination revisited: efficient production of PET tracers on a preparative scale. *Chem – A Eur J*. **2015a**, 21: 5972–5979.

Zlatopolskiy BD, Zischler J, Urusova EA, Endepols H, Kordys E, Frauendorf H, Mottaghy FM and Neumaier B: A Practical one-pot synthesis of positron emission tomography (PET) tracers via nickel-mediated radiofluorination. *ChemistryOpen*. **2015b**, 4: 457–462.

UNIVERSITY OF TURKU

Painosalama Oy, Turku, Finland 2021

ISBN 978-951-29-8342-1 (Print)
ISBN 978-951-29-8343-8 (PDF)
ISSN 0082-7002 (Print)
ISSN 2343-3175 (Online)